


Università degli Studi di Cagliari

PHD DEGREE

NEUROSCIENCE

Cycle XXXIII

TITLE OF THE PHD THESIS

Functional brain networks: intra and inter-subject variability in healthy individuals and patients with neurological or neuropsychiatric diseases.

Scientific Disciplinary Sector(s)
Area 06 –Medical Sciences MED/26 Neurology

PhD Student Sara Maria Pani

Supervisor Prof. Monica M.F. Puligheddu

Co-tutor Prof. Ing. Matteo Fraschini

Final exam. Academic Year 2019 – 2020
Thesis defence: January 2021 Session

Sara Maria Pani gratefully acknowledges Sardinian Regional Government for the financial support of her PhD scholarship (P.O.R. Sardegna F.S.E. - Operational Programme of the Autonomous Region of Sardinia, European Social Fund 2014-2020 - Axis III Education and training, Thematic goal 10, Investment Priority 10ii), Specific goal 10.5.

TABLE OF CONTENTS

Acknowledgments

I would like to thank Monica Pulighedu for going with my idea of a project about functional brain networks, and the freedom given to me to develop something out of the comfort zone.

I wholeheartedly thank Matteo Fraschini, my mentor from my student days at the medical school, that still represents my go-to person, and without which there wouldn't have been this research project. Thanks for encouraging me to apply to the PhD program in Neuroscience, for being always supportive both from the professional and human side, during the course and the experience abroad.

I would like to express my gratitude also to Prof. Alex Fornito and the Brain, Mind and Society Research Hub' team of the Monash University, who welcomed me in their research group, allowing me to carry out a study included in the present thesis. The experience at Monash University it's been highly educational and I'm glad to have spent nine months in such an inclusive, friendly and supportive professional environment.

Thanks to all the colleagues and staff of the Sleep Center, the Forensic Science Unit and the Electrical and Electronic Engineering Department of the University of Cagliari for the help and collaboration.

Thanks to all my extended beloved family, pets, and to my friends, but especially to my husband Gigi and my daughter Isabella, who always stood by my side during this three years-long adventure, facing with me victories and defeats, intercontinental travels, and the perils and pleasures of our beautiful daily life. Thanks for being always supportive and caring. To them I want to dedicate my work.

Finally I'm grateful for the gift of curiosity and passion for science, without which I'd have never agreed to study, study and more studying!

Author's publications

1. Fraschini, M**., Pani, S.M**., Didaci, L., Marcialis, G.L., 2019. Robustness of functional connectivity metrics for EEG-based personal identification over task-induced intra-class and inter-class variations. Pattern Recognit. Lett. https://doi.org/10.1016/j.patrec.2019.03.025

2. Demuru, M., La Cava, S.M.**, Pani, S.M**., Fraschini, M., 2020. A comparison between power spectral density and network metrics: An EEG study. Biomed. Signal Process. Control. https://doi.org/10.1016/j.bspc.2019.101760

3. **Pani, S.M**., Ciuffi, M., Demuro, M., La Cava, S.M., Bazzano, G., D'Aloja, E., Fraschini, M., 2020. Subject, session and task effects on power, connectivity and network centrality: A source-based EEG study. Biomed. Signal Process. Control. https://doi.org/10.1016/j.bspc.2020.101891

4. **Pani, S.M.**, Sabaroedin, K., Tiego, J., Bellgrove, M.A., Fornito, A., 2020. A multivariate analysis of the association between corticostriatal functional connectivity and psychosis-like experiences in the general community. Psychiatry Research: Neuroimaging. https://doi.org/10.1016/j.pscychresns.2020.111202

Abbreviations

AEC: amplitude envelope correlation
AECc: corrected version of aec
BCT: brain connectivity toolbox
CC: correlation coefficient
CST: corticostriatal
DC: dorsal causate
DCP/dcPT: dorso-caudal putamen
DRP/drPT: dorso-rostral putamen
EC: Eigenvector Centrality
EEG: electroencephalography
EER: equal error rate
FC: functional connectivity
fMRI: functional magnetic resonance imaging
FOV: field of view
ICA: independent component analysis
LV: latent variable
MEG: magnetoencephalography
NREMp: non-rem parasomnias
PCA: principal component analysis
PFC: prefrontal cortex
PLEs: psychosis-like experiences
PLI: phase log index
PLS: partial least square
PLV: phase locking value
PSD: power spectral density
ROI: region of interest
SHE: sleep-related hypermotor epilepsy
TE: echo time
TR: repetition time
VRP/vrPT: ventro-rostral putamen
VSi: ventro-striatal inferior
VSs: ventro-striatal superior

PART I

GENERAL INTRODUCTION

CHAPTER 1

Summary and Aims

The projects of this thesis sits at the intersection between classical neuroscience and aspects related to engineering, signals' and neuroimaging processing. Each of the three years has been dedicated to specific projects carried out on distinct datasets, groups of individuals/patients and methods, putting great emphasis on multidisciplinarity and international mobility. The studies carried out in Cagliari were based on EEG (electroencephalography), and the one conducted abroad was developed on functional magnetic resonance imaging (fMRI) data.

The common thread of the project concerns variability and stability of individuals' features related primarily to functional connectivity and network, as well as to the periodic and aperiodic components of EEG power spectra, and their possible use for clinical purposes.

In the first study (Fraschini et al., 2019) we aimed to investigate the impact of some of the most commonly used metrics to estimate functional connectivity on the ability to unveil personal distinctive patterns of inter-channel interaction.

In the second study (Demuru et al., 2020) we performed a comparison between power spectral density and some widely used nodal network metrics, both at scalp and source level, with the aim of evaluating their possible association.

The first first-authored study (Pani et al., 2020)was dedicated to investigate how the variability due to subject, session and task affects electroencephalogram(EEG) power, connectivity and network features estimated using source-reconstructed EEG time-series of healthy subjects.

In the study carried out with the supervision of Prof. Fornito (https://doi.org/10.1016/j.pscychresns.2020.111202) during the experience at the Brain, Mind and Society Research Hub of Monash University, partial least square analysis has been applied on fMRI data of an healthy cohort to evaluate how different specific aspects of psychosis-like experiences related to functional connectivity.

Due to the pandemic of Sars-Cov-2 it was impossible to continue recording the patients affected by neurological diseases (Parkinson's, Diskynesia) involved in the study we planned for the third year, that should have replicated the design of the first first-authored one, with the aim of investigate how individual variability/stability of functional brain networks is affected by diseases. For the aforementioned reason, we carried out the last study on a dataset we finished to record in February 2020. The analysis has the aim of investigate whether it is possible by using 19 channels sleep scalp EEG to highlight differences in the brain of patients affected by non-rem parasomnias and sleep-related hypermotor epilepsy, when considering the periodic and aperiodic component of EEG power spectra.

CHAPTER 2

Functional Connectivity

Human brain is often considered the most interesting mystery of our times. A small complex object of 1,300-1,500 grams, made up of 100 billion neurons, each of which develops an average of 100 trillion connections with neighbouring cells, from which emerge our entire being in terms of emotions, feelings, thoughts and behaviours (Fornito et al., 2016). We can describe it as a network, with complex anatomical and functional characteristics, and the way in which its components communicate and are organized in normal condition and disease is one of the most important questions of modern neuroscience. The recent confluence of neuroscience and network science open up fresh possibilities for understanding the brain as a complex system of interacting units (Stam, 2014), improving our comprehension of normal brain-network organization and of how its architecture dismantles in neurological and psychiatric diseases. Network science is based on the concept that to understand complex systems we require not only knowledge of their elementary components but also of the ways in which these components interact, as well as the emergent properties of their interactions (Sporns 2010). Complex networks study had a spike over the last decades with applications in several fields: biology, physics, social sciences, economy etc.. Even if these areas seem to be very different from each other, all these complex systems can be defined in terms of characteristics and patterns that derive from defined selective interactions and coupling between the elements that compose them. The brain is no exception and its integrative nature is suitable to be investigated with a complex network approach, considering its multiscale arrangement from singular cells and synapsis to cognitive systems. Each level of the multiple spatial scale is important, shall work with the others and depends mutually from higher and lower levels, giving rise through integration to complex functions as cognition and behaviour.

Modern network science is a mix of different theories and methods including graph theory, statistical mechanics from physics, computer science and inferential modeling. The core concept about graph theory is to represent the considered network with a set of nodes and connections, that can respectively constitute any sort of entity and relationship, allowing us to generalize this idea to any kind of complex network (Stam, 2014). Two models introduced at the end of the twentieth century, namely the small-world network by Watts and Strogatz (Watts and Strogatz, 1998) and the scale-free network by Barabási (Barabási and Albert, 1999), set the stage for the interdisciplinary applications of network neuroscience. Since its inception the power of the network science was represented by the capacity to explain a wide variety of phenomena staying relative simple and suited to a deep mathematical understanding.

It is now largely recognized the peculiar architecture of the brain that guarantees an equilibrium between segregation and integration of information, optimizing the ratio between connection cost and processing efficiency (Bullmore and Sporns, 2012). Namely, physiological brain networks show small-world typical characteristics combining high clustering with short path length, and scale-free features, that imply the existence of a subset of highly connected hub nodes, sometimes referred as a "rich club", that manage most of the information flow in the network (Sporns, 2013). Physiological brain networks are organized following a hierarchical modular structure, with large-scale modules corresponding to major functional systems such as motor, sensory and association networks (Meunier et al., 2010). The optimal combination of healthy brain characteristics seem to emerge during development, to be regulated by genes and influenced by aging, and to be strongly related to cognitive function (Stam, 2014).

This knowledge about the healthy brain has laid the foundation for studies concentrated on one of the main open question that network neuroscience is trying to address: networks changes in neurological and psychiatric disease.

We can derive brain networks from anatomical observations resulting in structural networks, or from physiological observations that result in functional networks.
The anatomical connections that link a set of neural elements, namely white matter projections that link cortical and subcortical areas, are described by structural connectivity (Sporns, 2013). Functional connectivity, on the other hand, describes patterns of statistical dependence among neural element, and it's obtained from time series observations (Smith, 2012), that can be derived from various techniques: EEG, MEG, fMRI. Although the statistical relationship among two neural elements could be taken as a sign of functional coupling, the latter doesn't give us information about causality. It is the effective connectivity that focuses on the influence that a node exert over another using a network model of causal dynamics (Gao et al., 2011). Despite the effective connectivity is very promising most studies on brain networks are nowadays conducted on structural or functional connectivity.

Focusing on functional connectivity, the data recorded from the human brain must first be processed into a network, starting with the definition of the nodes and the edges of the latter. If the empirical data derive from EEG or MEG a node can be defined as a channel, a sensor or a source; in case of fMRI data a voxel or a group of voxels corresponds to a node. Links can be instead defined as a measure of synchronization between two EEG, MEG or fMRI signals. The data can be then represented as a connectivity matrix N-by-N, with N constituted by the number of nodes, and each cell of the matrix provides information about the presence and strength of any relation (Stam, 2014). Inconsistent or weak interactions can be removed subjecting connection matrices to averaging across imaging runs/individuals or to thresholding (Sporns, 2013).The result of this process it's a network that can be analysed with tools and methods of network neuroscience, as graph theory. We can define a graph as unweighted, when edges are simply present or absent, or as weighted if we assign a weight to each link; likewise a graph is defined as undirected, if links indicate symmetric relationships, or directed if links correspond to directed relationships. Basic concepts of graph theory include: node degree, the number of links connected to the node; degree

distribution, the probability that a randomly chosen node has k degree; clustering coefficient of a node, the probability that two neighbours of that node are themselves connected; motifs, small subnetworks in which graphs can be decomposed; path length (binary graph), the minimum number of edges as distance between two nodes; centrality, the importance of a node compared to other nodes of the same network, it can be measured by degree, closeness centrality, eigenvector centrality and betweenness centrality (Stam, 2014).

The application of these mathematical concepts and measures allowed the definition of a general pattern of the healthy brain, that is characterized by high clustering, short path length, hierarchical modularity, scale-free degree distribution and a rich club made by hub nodes. A general conclusion that can be drown from the multitude of studies about functional changes in diseases is that usually network organization of patients affected by neurological/psychiatric conditions reflects a deviation from the optimal pattern. Remains a challenge to identify the nature of this deviation for single pathology, coming up with clinical useful applications, such as the use of diagnostic measures or biomarkers in day-to-day medicine.

CHAPTER 3

Intra and Inter-subject variability

Each brain seems to possess a set of unique characteristics that make it distinguishable from the multitude of other brains, and at the same time a complex batch of common patterns shared with the latter. This concept is fascinating and the importance of unveil the subject-specific characteristics of human brains has been stressed out in the last few years. Individual variability may indeed play an important role in both neuroimaging/neurophysiological human brain studies and bio-engineering applications. One need only think to biometric systems, computer interfaces and to the clinical advantage to have biomarkers specific for diseases. Different areas of medicine, first among all psychiatry, lack of diagnostic criteria based on validated biomarkers (Finn and Todd Constable, 2016). Filling this gap could mean enable the identification of at-risk individuals for prevention and early intervention, or in case of full-blown illness, prediction of trajectory and definition of the best strategy for treatment. Therefore several studies, using fMRI, EEG and MEG, have been focusing on study human brain networks organization and its variability across individuals in resting conditions, specific tasks, behaviours and especially in subjects affected by neurological or neuropsychiatric (Agosta et al., 2013; Baggio et al., 2014; de Haan et al., 2012; Delbeuck et al., 2003; Fornito and Bullmore, 2015; Olde Dubbelink et al., 2014; Skidmore et al., 2011; Stam, 2010). A crucial point that has to be considered trying to define biomarkers is how much of the functional connectivity variance is state-related versus trait-related (Finn and Todd Constable, 2016; Gratton et al., 2018), because from this depends the validity of all measurements about variability. Several connectivity studies, carried out using fMRI and MEG, showed that functional familial and heritable traits seem to be stable over a long time interval (Demuru et al., 2017; Miranda-Dominguez et al., 2018). In addition, EEG time-frequency and connectivity-based features could be considered as subject-specific

fingerprints by which distinguish different individuals, but it's also true that connectivity-based biometric systems performance varies with the connectivity metric and the task, and that the permanence has to be evaluated. In other words although there is clear evidence of individual variations in functional brain networks, their stability over-time needs to be carefully evaluated to validate the implications of individual approaches to neurological and psychiatric illness (Arns, 2012; Finn and Todd Constable, 2016) and in developing brain (Horien et al., 2019). Different studies were conducted using both fMRI, MEG and EEG following this common tread, with the aim of investigate to what extent subject-specific features are stable over time and different states: Gratton et al (2018), using fMRI, detected stable individual characteristics of functional brain networks that are modestly influenced by task state and show minimal day-to-day variability; likewise Cox et al (2018) detected subject-specific and stable over-time network profiles, although should be taken into account that the approach used, in specific EEG scalp level analysis, is prone to volume conduction and signal leakage problems. It is therefore extremely important to evaluate supposed effects of disease on brain networks considering all sources of variance, namely the ones linked to the pathology and those related to individuality, avoiding results' misinterpretation. In light of these considerations we can say that the nature of functional networks makes them promising as biomarkers, but also that the clinical use for high-quality personalized medicine approaches depends on how much we are accurate studying each subject/patient. Finally we must face the needing of a large amount of artifact-free data, considering the variability linked to the sampling process.

The future of medicine seems to be a shift from the traditional patient-control comparison to subject-specific analysis, and each step towards the understanding of the impact of intra and inter-subject variability brings us closer to the use of functional connectivity biomarkers on day-to-day clinic decisions.

PART II

EEG: Intra and inter-subject variability

CHAPTER 4

Robustness of functional connectivity metrics for EEG-based personal identification over task-induced intra-class and inter-class variations.

Fraschini M..

Pani S.M..

Didaci L.

Marcialis G.L.

Pattern Recognition Letters, 125 (2019) 49-54.

Abstract

Growing interest is devoted to understanding in which situations and with what accuracy brain signals recorded from scalp electroencephalography (EEG) may represent unique fingerprints of individual neural activity. In this context, the present paper aims to investigate the impact of some of the most commonly used metrics to estimate functional connectivity on the ability to unveil personal distinctive patterns of inter-channel interactions. Different metrics were compared in terms of equal error rate. It is widely accepted that each connectivity metric carries specific information in respect to the underlying interactions. Experimental results on publicly available EEG recordings show that different connectivity metrics define peculiar subjective profile of connectivity and show different mechanisms to detect subject-specific patterns of inter-channel interactions. Moreover, these findings highlight that some measures are more accurate and more robust than others, regardless of the task performed by the user. Finally, it is important to consider that frequency content and spurious connectivity may still play a relevant role in determining subject-specific characteristics.

Introduction

The investigation of subject specific human characteristics that can be used to develop robust biometric systems still represents a big challenge. In this context, growing interest is devoted to understanding how brain signals recorded from scalp electroencephalography (EEG) may represent a unique fingerprint of individual neural activity. In the last few years a huge number of works have investigated the potential role of EEG signal characteristics as biometric system (about 300 new papers in the last 10 years). A detailed literature overview of the methods proposed so far is therefore quite challenging and in any case out of the scope of the present study. Nevertheless, some attempts to summarize the state of the art was previously proposed in [6,9,19]. In brief, it is possible to consider the approaches proposed up until now mainly organized into two fundamental categories: (i) task based and (ii) resting-state based EEG analysis. The first category is oriented on experimental setups that allow to investigate properties of the EEG signal that are strictly related to some specific stimulus. Motor (real and imagery) tasks [33], visual evoked potentials [2,8,27], auditory stimuli [24], imagined speech [4], eye blinking [1] and multiple functional brain systems [29] have been proposed so far in order to elicit individual unique responses. In contrast, the second category is mainly oriented to detect characteristic patterns of induced brain activity at rest both during eyes-closed and eyes-open. In line with the extensive use of tools from modern network science to understand brain complex organization [31], measures of functional connectivity [10,14,16,21] and network metrics have been recently proposed [7,12] as EEG-based biometric traits. Finally, multimodal approaches based on the fusion of EEG and Electrocardiography (ECG) features have been also proposed [3,28]. However, it seems still evident that there exists a gap between current investigations of EEG signal as neurophysiological marker

and its application in personal verification systems. In particular, it is widely accepted that different metrics used to assess functional connectivity carry specific information with respect to the underlying interactions network [20]. Nevertheless, it is still not clear if these metrics convey different subject specific information. Following what previously reported in [12,14], the present paper aims to investigate and compare the impact of some of the most commonly used techniques to estimate functional connectivity on the ability to detect personal unique distinctive features based on inter-channel interaction profiles. In order to answer this question, we focused our attention on measures based on different properties of the original signals. In particular, the following measures were included in the present study: (i) the Correlation Coefficient (CC), representing a sort of (spurious) connectivity baseline; (ii) the Phase Lag Index (PLI) [32], which quantifies the asymmetry of the distribution of phase differences between two signals; (iii) the uncorrected Amplitude Envelope Correlation (AEC) and (iv) the corrected AEC version (after performing the orthogonalisation of raw signals) [5,17], which provides functional coupling estimate without coherence or phase coherence; (v) the Phase Locking Value (PLV) [22], which detects frequency-specific transient phase locking independently from amplitude. Each of the proposed metric has different properties and capture different characteristics of the EEG signals interaction which will be discussed in this paper. We hypothesized that the choice of the metric may have a great impact in unveil subject specific pattern of functional interactions, and that advantages and disadvantages of each technique should be correctly taken into account when interpreting the corresponding results in terms of performance of a EEG based biometric system. Finally, although the aim of this study was to compare different connectivity metrics without focusing on absolute performance of the system, considering that the so called single-run approach (within-task design, where the system is tested on a single run) still represents the more important limitation of EEG based biometric systems,

we replicated our study using a multi-runs approach (between-task design, where the system is tested on multiple and different runs). Despite a within-task approach would have been adequate to test differences between the different connectivity metrics, a between-tasks approach allowed to have a more clear idea on the actual performance of the biometric system on possible real life applications.

Material and methods

EEG dataset

The analysis was performed using a widely used and freely available EEG dataset containing 64 channels scalp EEG recordings from 109 subjects including fourteen different runs. The full dataset was created and contributed to PhysioNet [15] by the developers of the BCI2000 instrumentation system. A detailed description of the original system can be found in [30] and the access to the raw EEG recordings is possible at the following website: https://www.physionet.org/pn4/eegmmidb/. For the purpose of the present study our analysis was applied to all the fourteen different runs, using 105 out of the 109 subjects, since four of them were excluded for differences in EEG acquisition parameters. The fourteen runs are organized as follows: 1st and 2nd runs contain eyes-open and eyes close resting-state, respectively. The remaining twelve runs consist of three different repetitions of four motor tasks: (i) open and close left or right fist; (ii) imagine opening and closing left or right fist; (iii) open and close both fists or both feet and (iv) imagine opening and closing both fists or both feet.

Preprocessing

As a first step, original raw data undergo a fully automatic algorithm based on Independent Component Analysis (ICA) using ADJUST (version 1.1.1) [25] which is optimized to detect and remove artifacts as blinks, eye movements, and generic discontinuities. Later, artifact-free EEG signals were band-pass filtered in the common frequency bands: delta (1–4 Hz), theta (4–8 Hz), alpha (8–13 Hz), beta (13–30 Hz) and gamma (30–45 Hz). Finally, each single EEG recording was organized into five different epochs (without overlap) of 12 seconds which guarantee to have a correct estimate of the connectivity profiles [11]. As a consequence, our analysis refers to one minute EEG signal for each subject and each run, so obtaining an overall of 24.5 hours of EEG recordings. Fig. 1 shows a schematic representation of the different steps involved in the analysis.

Connectivity metrics

From the preprocessed EEG signals, separately for each subject, each epoch and each frequency band, a connectivity matrix was computed. Each single entry of the connectivity matrix, which represents the weight of the functional interaction, was computed by using a connectivity metric *fc* following the Algorithm 1.

Algorithm 1: Build the connectivity matrix.

Input:
- A matrix TS of size *channels x samples*;
- A connectivity metric $fc(\cdot, \cdot)$

Output: A matrix *CONN* of size *channels x channels*

```
CONN = zeros(channels, channels);
for i ← 1 to channels do
    for j ← 1 to channels do
        if i < j then
            CONN(i, j) ← fc(TS(i), TS(j));
        end
    end
end
return CONN;
```

Correlation

The Correlation Coefficient (CC) represents the simpler method to estimate statistical relationship between two random variables and it is widely used in fMRI studies [13]. However, since scalp EEG signals contain electric fields derived from common current sources, CC does not represent the optimal metric to estimate functional interactions in this context. In this study, CC was mainly applied in order to quantify the possible effect of spurious patterns of connectivity on the definition of subject specific EEG traits.

Phase lag index

The phase lag index (PLI) [31] is a technique that quantify the asymmetry of the distribution of phase differences between two signals and removes the effect of amplitude information. Furthermore, PLI is less affected by the influence of common sources and thus defines more reliable interactions between the underlying signals. The PLI is computed as the asymmetry of the distribution of instantaneous phase differences between two signals *i*, *j*:

$$\mathrm{PLI}(i, j) = | \langle sign[\Delta\phi_{(i, j)}(t_k)] \rangle | \quad (1)$$

where $\Delta\phi_{(i,j)}$ is the difference between instantaneous phases of the signals *i* and *j*, t_k are discrete steps and $\langle\ \rangle$ denotes the average over the time *t*.

Amplitude envelope correlation

Band limited amplitude envelop correlation (AEC) [5,17], using Hilbert transform, was also used in this study. In particular, the envelope is obtained by measuring the magnitude of the analytic signal and successively the

Pearson's correlation between envelopes is computed as a metric of functional connectivity.

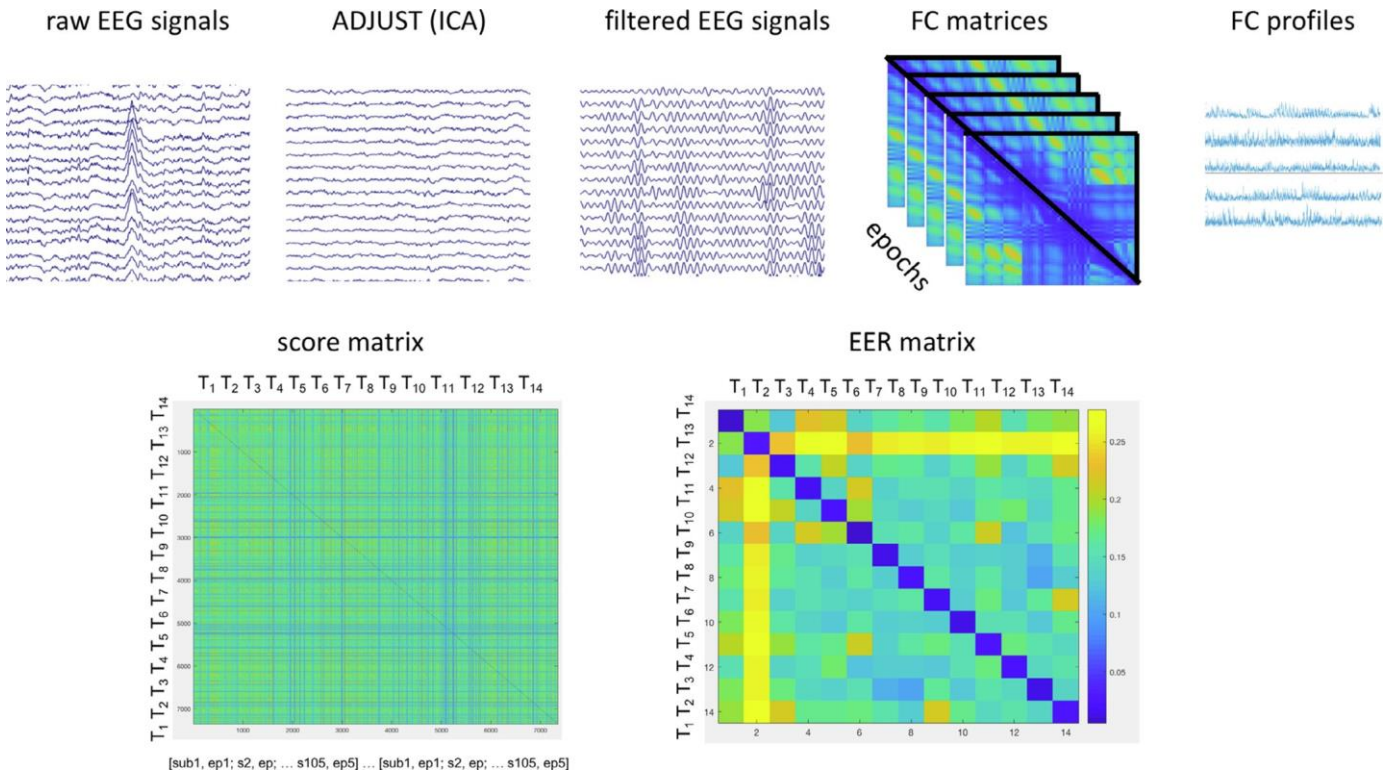

Fig. 1. A schematic representation of the different steps involved in the analysis. From upper-left to bottom-right the panels represent: original raw EEG signals, artifact-free EEG traces, band-pass filtered signals, FC connectivity matrices for each epoch, FC profiles extracted from each matrix, score matrix derived from Euclidian distance between FC profiles from all the 14 runs / 105 subjects / 5 epochs and EER matrix reporting the performance for each combination of the 14 different runs.

Amplitude envelope correlation, corrected version

It is well known that signal components that pick up the same source at different sites (i.e., EEG channels) have an identical phase. In this work, to overcome this possible limitation, we used an orthogonalisation procedure performed in the spatial domain (by removing the linear regression) before to compute the AEC values. In the present paper, the corrected version of AEC is reported as AECc.

Phase locking value

The phase locking value (PLV), introduced by [22], allows to detect transient phase locking values which are independent of the signal amplitude. The PLV therefore represents the absolute value of the mean phase difference between the two signals *i, j*:

$$PLV_{(i,j)} = \left| \frac{1}{T} \sum e^{j[\Delta\phi_{(i,j)}(t_k)]} \right|$$

where $\Delta\phi(i,j)$ is the difference between instantaneous phases of the signals *i* and *j*, t_k are discrete steps and *T* is the number of trials.

Features extraction and performance evaluation

The performance obtained by applying the different connectivity metrics have been reported in terms of Equal Error Rate (EER). The EER refers to the rate at which both acceptance error (that occurs when the system accepts an impostor) and rejection error (that occurs when the system rejects a genuine match) are equal. It represents a quick and efficient way to compare the accuracy of different systems and it is widely used in evaluating the performance of biometric fingerprints. In short, the EER is the point where false identification and false rejection rates are equal, thus the lower the EER, the better the performance of the system. As previously proposed [12], the system performance is based on the computation of genuine and impostor matching scores. The scores, computed separately for each frequency band, represent the Euclidean distance (d) between each pair of feature vectors.

The feature vectors are represented by the individual connectivity profiles extracted from the upper (or lower) triangular (symmetrical) connectivity matrix obtained by using the different metrics. Therefore, each feature vector

contains (number of channels)× (number of channels - 1) / 2 elements, where each element represents the corresponding connectivity value between a pair of EEG channels. Finally, from the matching scores, the similarity scores was computed as $1/(1 + d)$, where d represents the Euclidean distance. All these steps lead to a square (symmetrical) score matrix with a number of rows and columns equal to 7350 (14 runs × 105 subjects × 5 epochs). Finally, a 14 × 14 square matrix, containing the EER values for each combination of runs is obtained: in-diagonal values represent between-task performance; out-diagonal values represent between-task performance. Fig.1 shows a schematic representation of the different steps involved in the analysis.

Results

As a first step, in order to highlight the inherent dissimilarities between the different metrics, Fig. 2 shows the global averaged (over epochs and subjects) connectivity matrices and corresponding subject's variance (expressed as standard deviation) for the eyes-closed resting-state condition. In other words, Fig. 2 shows that, despite the fact that different connectivity metrics promise to catch the real underlying connectivity, they define peculiar subjective profile of connectivity and show different mechanisms to detect subject-specific patterns of inter-channel interactions. Successively, a summary of the results (in terms of EER) obtained from the whole analysis, for each frequency band and each connectivity metric separately, are summarized in Fig. 3. The remaining of the results are organized into two main sub-sections. In the first sub-section, we reported the results derived from the within-task approach, the second sub-section contains the results from the between-tasks comparison.

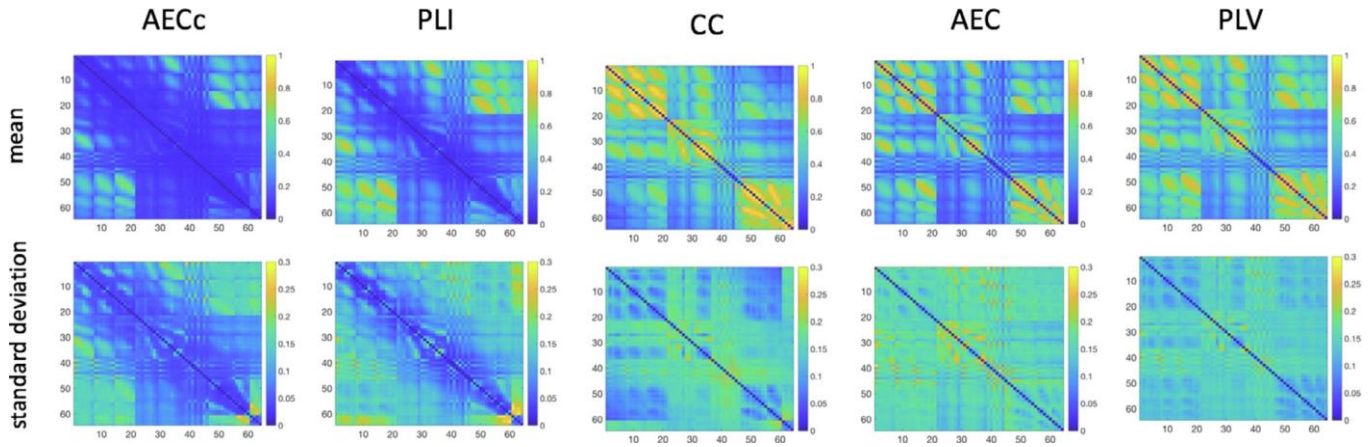

Fig. 2. Connectivity patterns for each metric and corresponding between subjects variation expressed as standard deviation for eyes-closed resting-state run. Each entry represents the global average over epochs and subjects.

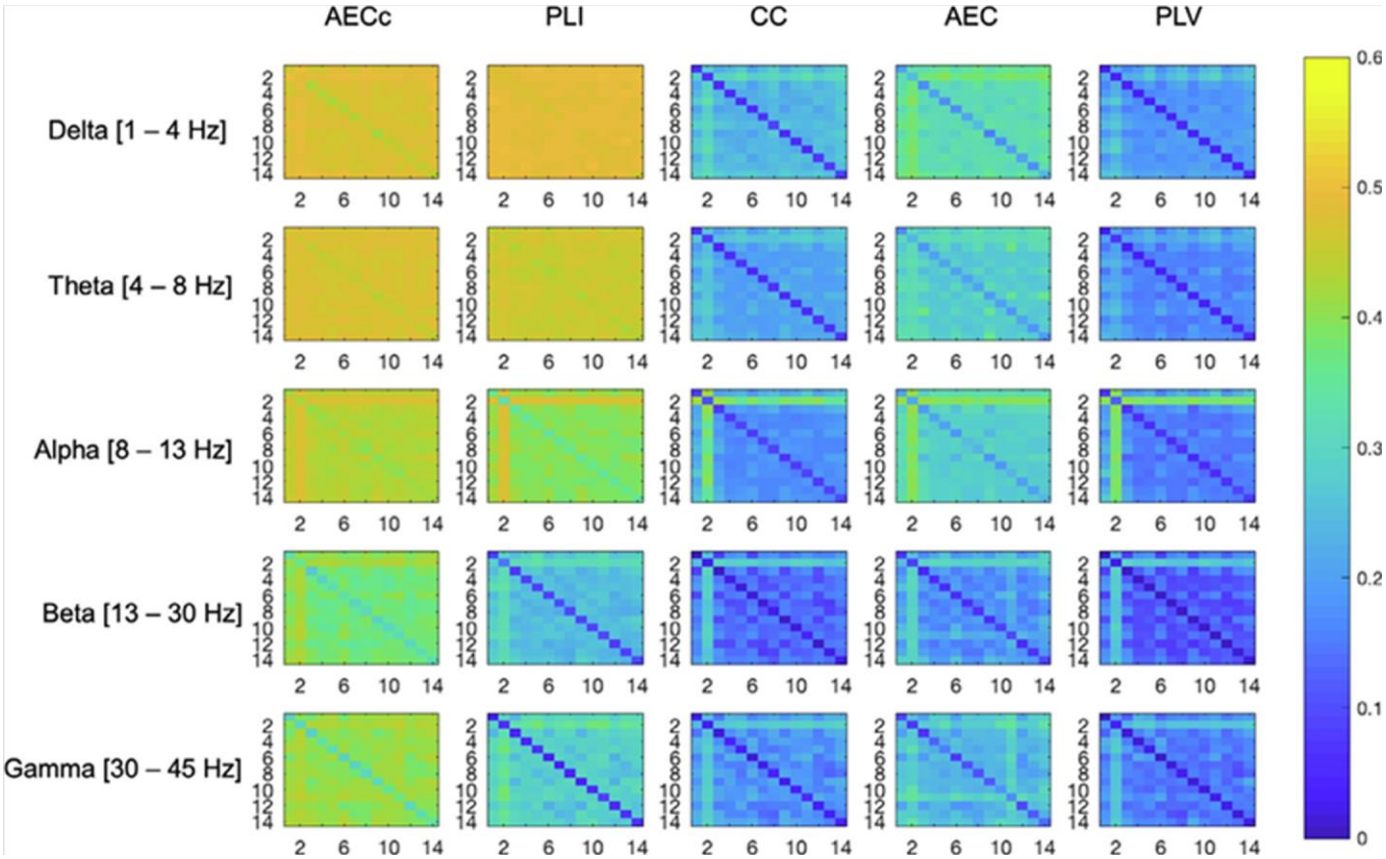

Fig. 3. Results in terms of EER obtained from the whole analysis, for each frequency band (rows) and each connectivity metric (columns). In-diagonal values represent within-task performance; out-diagonal values represent between-tasks performance.

Within task

The results from within-task analysis, which represents the best and more trivial situation where the performance are evaluated within the same task, show the absolute higher performance in the beta band with an EER = 0.09% for the PLV connectivity metric. A graphical representation of the results is reported in Fig. 3, see in-diagonal values from each single EER matrix. The other connectivity metrics performed worse, with the best EER ranging from 26.9% for AECc (beta band) to 0.57% for CC (beta band). PLI and AEC best performance were respectively equal to 3.65% (gamma band) and 4.94% (beta band). PLV and CC performed well for all the frequency bands with range from 5.37% (alpha band) to 0.09% (beta band) for PLV and from 7.03% (alpha band) to 0.57% (beta band) for CC, AECc showed the worst absolute results, with range from 41.9% (delta band) to 26.9% (beta band). For PLI, CC and PLV the results were consistent across tasks since the within task analysis that showed the lower performance were still acceptable. In details, the corresponding EER were: 8.52% for PLI (gamma band), 3.78% for CC (beta band) and 2.37% for PLV (beta band). A summary of the performance over the different within-task are included in the Table 1.

Table 1

Worst (left) and best (right) within-task performance for the different connectivity metrics expressed as EER for each frequency band. EER values lower than 10% were marked as bold.

	AECc	PLI	CC	AEC	PLV
Delta	48.29–41.89	48.90–46.06	**9.27–5.91**	25.30–15.32	**5.65–3.30**
Theta	46.22–43.33	45.25–42.98	**8.20–5.01**	23.97–17.54	**7.34–3.19**
Alpha	42.79–39.38	36.58–33.43	10.17–**7.03**	24.78–18.67	12.67–**5.37**
Beta	36.34–26.86	14.06–**8.37**	**3.78–0.57**	10.28–**4.94**	**2.37–0.09**
Gamma	36.71–28.64	**8.52–3.65**	**5.76–1.55**	17.90–**7.44**	**2.90–0.58**

Between tasks

The results from between-tasks analysis, which represents the more realistic and challenging situation where the performance are evaluated between (all the) different tasks, show the absolute higher performance in the beta band with an EER = 7.38% for the PLV connectivity metric. Fig. 3 shows the corresponding pairwise performance in the out-diagonal entries of each single EER matrix. The other connectivity metrics performed worse, with the best EER ranging from 35.03% for AECc (beta band) to 8.14% for CC (beta band). PLI and AEC best performance were respectively equal to 21.89% (beta band) and 14.23% (beta band). PLV and CC performed well for all the frequency bands with range from 15.00% (delta band) to 7.38% (beta band) for PLV and from 19.74% (delta band) to 8.14% (beta band) for CC, AECc showed the worst absolute results, with range from 46.05% (delta band) to 35.03% (beta band). A summary of the performance over all the different between-tasks are included in the Table 2.

Table 2

Worst (left) and best (right) between-tasks performance for the different connectivity metrics expressed as EER for each frequency band. EER values lower than 10% were marked as bold. In brackets EER values when between-tasks comparison including eyes- closed resting-state conditions were excluded from the analysis.

	AECc	PLI	CC	AEC	PLV
Delta	49.92 (49.48)–46.05	49.88 (49.82)–47.90	32.90 (28.83)–19.74	39.82 (37.22)–29.51	29.12 (25.99)–15.00
Theta	48.73–45.80	47.11 (46.63)–44.42	28.76 (26.98)–17.88	36.68–25.31	25.90 (24.19)–13.57
Alpha	47.84 (45.77)–41.67	47.92 (42.86)–37.55	41.88 (26.49)–15.67	41.04 (33.63)–23.60	40.24 (27.58)–12.56
Beta	43.59 (41.78)–35.03	34.01 (32.13)–21.89	29.96 (19.84)–**8.14**	30.46 (28.24)–14.23	29.09 (18.69)–**7.38**
Gamma	44.40 (44.00)–37.86	37.81 (32.27)–22.53	29.47 (24.30)–12.40	34.93 (32.64)–18.09	27.78 (22.66)–10.29

Discussion

The present paper aimed to investigate and compare the impact of common metrics used to estimate functional connectivity on their capacity to detect personal distinctive fingerprints. In summary, the results of this study show that, as expected, different connectivity metrics, each characterized by different mechanisms of functional interaction, define a peculiar subjective profile of connectivity. In particular, PLV and CC show excellent performance for the within-task approach, PLI and AEC show slightly lower performance which is however dependent on the frequency content. AECc, which underwent to the orthogonalization procedure to limit signal leakage, shows the worst overall performance even in the more favorable situation (single-run approach). Furthermore, despite the inherent complexity which characterize a multi-runs approach, where the performance are assessed between different tasks, PLV and CC still show interesting (although reduced) performance with peak accuracy of 7.38% and 8.14% respectively, for the beta band. This last result represents probably the more interesting finding of the present study, which shows the robustness of some connectivity metrics, namely PLV and CC, to detect individual fingerprints even in the more challenging experimental design. The absolute worst performance in the case of between-tasks approach, as can be visually seen from the Fig. 3 (second row/column) and as reported in Table 2 in brackets, are particularly influenced by the eyes-closed resting-state task, which represents the only run where the subjects were required to close their eyes during the EEG recording. However, in our opinion, two relevant points deserve particular attention. The first important point is related to a marked association between the frequency content and the ability to discriminate among different subjects at least for the metrics which are more robust to volume conduction and signal leakage problems. Indeed, for both the

experimental designs (within and between-tasks approaches) the best performance (lower EER) were obtained for the higher frequency bands (beta and gamma). It is interesting to note that this finding represents a confirmation of previously reported results using different approaches [7,12]. In this context, it is not possible to rule out the hypothesis that muscle artifacts, particularly evident at high frequencies [26], may play a key role in the definition of distinctive characteristics. The second point is related to the different performance obtained using the different class of connectivity estimators. It is evident that some of connectivity metrics, namely AECc and PLI, give the lower performance even for the higher frequency bands (especially evident for the between-tasks approach). This event may be, at least in part, due to the inherent common properties of these two approaches that try to limit the signal leakage problem, which probably go to the detriment of individual characteristics regressing out subject specific features. The other way around, it should be noted that PLV is a connectivity metric that is deeply influenced by mechanisms of volume conduction, signal spread and common sources. Therefore, caution should be used when interpreting the reported results. In particular, it is still possible that the distinctive patterns of connectivity, as highlighted by PLV (and CC), may be strongly influenced by spurious connectivity values generated by the previously cited sources of noise (i.e., volume conduction, signal spread and common sources). Despite these limitations, it is surprising that even in the worst scenario, when the subjects are matched during different activities, for some connectivity metrics (i.e., CC and PLV) and specific tasks it is still possible to observe very interesting performance. Future works should investigate if the results reported so far at scalp level still hold when the EEG signals are reconstructed (by resolving the inverse problem) at source level where the effects due to spurious connections are, at least in part, attenuated [23]. Finally, it is important to highlight that, as recently reported [18], EEG based biometric systems should be designed also keeping into account their

dependence to multiple factors as age, sex, pathology and, more importantly, in a multi-sessions scenario, where the variability over-time may play a fundamental role.

Conclusions

To sum up, this work suggests that different functional connectivity metrics have different mechanism to detect subject specific patterns of inter-channel interactions, that it is important to consider the effect of the frequency content and that spurious connectivity values may play an important role in this context.

References

[1] M. Abo-Zahhad, S.M. Ahmed, S.N. Abbas, A new multi-level approach to eeg based human authentication using eye blinking, Pattern Recognit. Lett. 82 (2016) 216–225.

[2] B.C. Armstrong, M.V. Ruiz-Blondet, N. Khalifian, K.J. Kurtz, Z. Jin, S. Laszlo, Brainprint: assessing the uniqueness, collectability, and permanence of a novel method for erp biometrics, Neurocomputing 166 (2015) 59–67.

[3] S. Barra, A. Casanova, M. Fraschini, M. Nappi, Fusion of physiological mea- sures for multimodal biometric systems, Multimedia Tools Appl. 76 (4) (2017) 4835–4847.

[4] K. Brigham, B.V. Kumar, Subject identification from electroencephalogram (eeg) signals during imagined speech, in: Biometrics: Theory Applications and Systems (BTAS), 2010 Fourth IEEE International Conference on, IEEE, 2010, pp. 1–8.

[5] M.J. Brookes, J.R. Hale, J.M. Zumer, C.M. Stevenson, S.T. Francis, G.R. Barnes,

J.P. Owen, P.G. Morris, S.S. Nagarajan, Measuring functional connectivity us- ing meg: methodology and comparison with fcmri, Neuroimage 56 (3) (2011) 1082–1104.

[6] P. Campisi, D. La Rocca, Brain waves for automatic biometric-based user recog- nition, IEEE Trans. Inf. Forensics Secur. 9 (5) (2014) 782–800.

[7] A. Crobe, M. Demuru, L. Didaci, G.L. Marcialis, M. Fraschini, Minimum span- ning tree and k-core decomposition as measure of subject-specific eeg traits, Biomed. Phys. Eng. Express 2 (1) (2016) 017001.

[8] R. Das, E. Maiorana, D. La Rocca, P. Campisi, Eeg biometrics for user recognition using visually evoked potentials, in: Biometrics Special Interest Group (BIOSIG), 2015 International Conference of the, IEEE, 2015, pp. 1–8.

[9] M. Del Pozo-Banos, J.B. Alonso, J.R. Ticay-Rivas, C.M. Travieso, Electroen- cephalogram subject identification: a review, Expert Syst. Appl. 41 (15) (2014) 6537–6554.

[10] M. DelPozo-Banos, C.M. Travieso, C.T. Weidemann, J.B. Alonso, Eeg biometric identification: a thorough exploration of the time-frequency domain, J. Neural Eng. 12 (5) (2015) 056019.

[11] M. Fraschini, M. Demuru, A. Crobe, F. Marrosu, C.J. Stam, A. Hillebrand, The effect of epoch length on estimated eeg functional connectivity and brain net- work organisation, J. Neural Eng. 13 (3) (2016) 036015.

[12] M. Fraschini, A. Hillebrand, M. Demuru, L. Didaci, G.L. Marcialis, An eeg-based biometric system using eigenvector centrality in resting state brain networks, IEEE Signal Process. Lett. 22 (6) (2015) 666–670.

[13] K.J. Friston, K.J. Worsley, R.S. Frackowiak, J.C. Mazziotta, A.C. Evans, Assess- ing the significance of focal activations using their spatial extent, Hum. Brain Mapp. 1 (3) (1994) 210–220.

[14] M. Garau, M. Fraschini, L. Didaci, G.L. Marcialis, Experimental results on mul- ti-modal fusion of eeg-based personal verification algorithms, in: Biometrics (ICB), 2016 International Conference on, IEEE, 2016, pp. 1–6.

[15] A.L. Goldberger, L.A. Amaral, L. Glass, J.M. Hausdorff, P.C. Ivanov, R.G. Mark,

J.E. Mietus, G.B. Moody, C.-K. Peng, H.E. Stanley, Physiobank, physiotoolkit, and physionet, Circulation 101 (23) (2000) e215–e220.

[16] C. Han, S. Kim, H. Yoon, W. Lee, C. Park, K. Kim, K. Park, Contrast between spectral and connectivity features for electroencephalography based authen- tication, in: World Congress on Medical Physics and Biomedical Engineering, June 7–12, 2015, Toronto, Canada, Springer, 2015, pp. 1224–1227.

[17] J.F. Hipp, D.J. Hawellek, M. Corbetta, M. Siegel, A.K. Engel, Large-scale cortical correlation structure of spontaneous oscillatory activity, Nat. Neurosci. 15 (6) (2012) 884.

[18] Y. Höller, A.C. Bathke, A. Uhl, Age, sex, and pathology effects on stability of electroencephalographic biometric features based on measures of interaction, IEEE Trans. Inf. Forensics Secur. 14 (2) (2019) 459–471.

[19] W. Khalifa, A. Salem, M. Roushdy, K. Revett, A survey of eeg based user authen- tication schemes, in: Informatics and Systems (INFOS), 2012 8th International Conference on, IEEE, 2012, pp. BIO–55.

[20] T. Kida, E. Tanaka, R. Kakigi, Multi-dimensional dynamics of human electro- magnetic brain activity, Front. Hum. Neurosci. 9 (2016) 713.

[21] D. La Rocca, P. Campisi, B. Vegso, P. Cserti, G. Kozmann, F. Babiloni, F.D.V. Fal- lani, Human brain distinctiveness based on eeg spectral coherence connectiv- ity, IEEE Trans. Biomed. Eng. 61 (9) (2014) 2406–2412.

[22] J.-P. Lachaux, E. Rodriguez, J. Martinerie, F.J. Varela, Measuring phase synchrony in brain signals, Hum. Brain Mapp. 8 (4) (1999) 194–208.

[23] M. Lai, M. Demuru, A. Hillebrand, M. Fraschini, A comparison between scalp-and source-reconstructed eeg networks, Sci. Rep. 8 (1) (2018) 12269.

[24] G.A. Light, L.E. Williams, F. Minow, J. Sprock, A. Rissling, R. Sharp, N.R. Swerd- low, D.L. Braff, Electroencephalography (eeg) and event-related potentials (erps) with human participants, Curr. protoc.Neurosci. (2010) 6–25.

[25] A. Mognon, J. Jovicich, L. Bruzzone, M. Buiatti, Adjust: an automatic eeg artifact detector based on the joint use of spatial and temporal features, Psychophysi- ology 48 (2) (2011) 229–240.

[26] S. Muthukumaraswamy, High-frequency brain activity and muscle artifacts in meg/eeg: a review and recommendations, Front. Hum. Neurosci. 7 (2013) 138.

[27] R. Palaniappan, D.P. Mandic, Eeg based biometric framework for automatic identity verification, J. VLSI Signal Process. Syst.Signal Image Video Technol. 49 (2) (2007) 243–250.

[28] A. Riera, S. Dunne, I. Cester, G. Ruffini, Starfast: a wireless wearable eeg/ecg biometric system based on the enobio sensor, in: Proceedings of the Interna- tional Workshop on Wearable Micro and Nanosystems for Personalised Health, 2008.

[29] M.V. Ruiz-Blondet, Z. Jin, S. Laszlo, Cerebre: a novel method for very high accu- racy event-related potential biometric identification, IEEE Trans. Inf. Forensics Secur. 11 (7) (2016) 1618–1629.

[30] G. Schalk, D.J. McFarland, T. Hinterberger, N. Birbaumer, J.R. Wolpaw, Bci2000: a general-purpose brain-computer interface (bci) system, IEEE Trans. Biomed. Eng. 51 (6) (2004) 1034–1043.

[31] C.J. Stam, Modern network science of neurological disorders, Nat. Rev. Neu- rosci. 15 (10) (2014) 683.

[32] C.J. Stam, G. Nolte, A. Daffertshofer, Phase lag index: assessment of functional connectivity from multi channel eeg and meg with diminished bias from com- mon sources, Hum. Brain Mapp. 28 (11) (2007) 1178–1193.

[33] S. Yang, F. Deravi, S. Hoque, Task sensitivity in eeg biometric recognition, Pat- tern Anal. Appl. 21 (1) (2018) 105–117.

CHAPTER 5

A comparison between power spectral density and network metrics: An EEG study.

Demuru M.

La Cava S.M.

Pani S.M.

Fraschini M.

Biomedical Signal Processing and Control, 57 (2020) 101760

Abstract

Power spectral density (PSD) and network analysis performed on functional correlation (FC) patterns represent two common approaches used to characterize Electroencephalographic (EEG) data. Despite the two approaches are widely used, their possible association may need more attention. To investigate this question, we performed a comparison between PSD and some widely used nodal network metrics (namely strength, clustering coefficient and betweenness centrality), using two different publicly available resting-state EEG datasets, both at scalp and source levels, employing four different FC methods (PLV, PLI, AEC and AEC$_C$). Here we show that the two approaches may provide similar information and that their correlation depends on the method used to estimate FC. In particular, our results show a strong correlation between PSD and nodal network metrics derived from FC methods (pick at 0.736 for PLV and 0.530 for AEC) that do not limit the effects of volume conduction/signal leakage. The correlations are less relevant for more conservative FC methods (pick at 0.224 for AEC$_C$). These findings suggest that the results derived from the two different approaches may be not independent and should not be treated as distinct analyses. We conclude that it may represent good practice to report the findings from the two approaches in conjunction to have a more comprehensive view of the results.

Introduction

Power spectral density (PSD) and network analysis performed on functional correlation (FC) patterns represent two common approaches used to characterize Electroencephalographic (EEG) and Magnetoencephalographic (MEG) time-series data [1]. The importance of the two different approaches for the EEG characterization, in terms of novel insights into neuronal mechanisms underlying cognitive processes and potential clinical relevance, has been extensively discussed [1,2]. Interestingly, it has been also reported that higher brain functions depend upon a balance between local specialization and global integration of brain processes [3] and that this hypothesis can be investigated by evaluating the correlations between signals of brain activity recorded from different areas [4]. In particular, as for the relative power of alpha band, it has been shown a strong correlation of this feature also with impaired cognition [5]. Despite these two approaches are widely used, the possible association between the results derived from their application is probably overlooked and may deserve more attention. It is important to stress that measures of statistical interdependence between M/EEG time-series and the derived network parameters represent a higher order analysis compared to the power spectral density and may provide a less straightforward interpretation of the underlying brain mechanisms. Although few attempts to characterize their association have been performed, investigating, for instance, the dependency between patterns of global synchrony (phase) and local synchrony (amplitude) [6] on synthetic data, usually the two approaches are not analyzed in conjunction and their association is generally neglected. Interestingly, more recently [7] it has been suggested that time–frequency spectrograms do not merely represent a description of local synchrony but also reflect fluctuations in long-range connectivity. In this study we aimed to answer the following research

questions: (i) is there any association between the features extracted using the PSD analysis and those derived by using FC from resting-state time- series EEG? (ii) to what extent the two different approaches differ?(iii) is it possible to interpret the related findings as completely separated and independent? (iv) how the association between the two approaches may depend on the specific FC methods? In order to investigate in more details their possible relationship, we performed a comparison between PSD analysis and some widely used nodal network metrics (namely strength, clustering coefficient and betweenness centrality), using two different publicly available resting-state EEG datasets. To assess potential limitations due to scalp-level analysis [8,9], the analysis was further replicated using a source level approach. In order to control the possible effects derived from the use of different FC methods, which may result from distinct neural mechanisms [10], we performed the analysis using four different techniques to estimate patterns of phase- and amplitude- based correlation: the Phase locking value (PLV) [11], the Phase lag index (PLI) [3], the Amplitude Envelope Correlation (AEC) [12] and a corrected version performing a time-domain orthogonalization procedure (AECC) [12]. Our analysis was focused on the alpha band since it has been previously shown to provide the largest signal to noise ratio and the more reliable estimate of FC networks [13].

The paper is organized as follows: (i) a Material and Methods section, where we have described both the EEG dataset and the techniques used to perform the analysis. Furthermore, this section also contains a description of the statistical analysis; (ii) a Discussion and results section, where we have highlighted the main findings and discussed the contribution of the study; (iii) a Conclusion section, where we have summarized the main message of the present work.

Material and methods

EEG datasets

Two different EEG datasets were used for the analysis. The first dataset (EEG_DS1) is the EEG motor movement/imaginary dataset [14,15] (https://www.physionet.org/pn4/eegmmidb/), a freely available set of 64 channels EEG recordings, consisting of several tasks including one-minute eyes-closed resting-state from 109 subjects acquired with a sample frequency equals to 160 Hz. The second dataset (EEG_DS2) is another freely available set of 64 channels EEG recordings [16,17], consisting of eyes-closed resting-state from 12 subjects acquired with an original sample frequency equals to 5 KHz and successively resampled to 256 Hz.

All the analysis was performed using five epochs of 12 s [18] for each subject extracted from one-minute of eyes-closed resting state condition and successively, ADJUST (version 1.1.1) [19], a fully automatic algorithm based on Independent Component Analysis (ICA), was used to detect and remove artifacts from the filtered signals. For the first dataset (EEG_DS1) the epoch selection was performed considering the whole one-minute recording and splitting the signal into five non-overlapping chunks of equal length (12 s). We performed the same approach for the second dataset (EEG_DS2), repeating the procedure (i.e., splitting the signal into five non-overlapping chunks of equal length) using the first one-minute block of the EEG recording. All the reported results refer to the investigation of the alpha frequency band (8–13 Hz). The band-pass EEG filtering procedure was accomplished using the eeg-filt function provided by the EEGLAB toolbox (version 13) [20]. In order to evaluate the consistency of our results between scalp and source analysis [8], we replicated the analysis at source-level using

source-reconstructed time-series obtained by using Brainstorm software (version 3.4) [21], using the protocol described by Lai and colleagues [8].

Features extraction

For each subject and each epoch, we have extracted a set of features from the EEG time-series. In particular, the relative alpha band power was computed for each channel (at scalp level) and for each ROI (at source level) as the ratio between the sum of the original PSD (computed using the Welch method in Matlab R2017b) over the frequency range in 8–13 Hz and the sum of the original PSD over the frequency range in 1–40 Hz (total power). Later, four different and common methods to estimate (alpha band) FC patterns were used: PLV [11], AEC [12], PLI [3] and AECC [12] (an orthogonalized version of AEC). Finally, using the BCT [22], a set nodal network metrics were computed from the FC patterns: strength (the sum of weights of links connected to the node), clustering coefficient (the fraction of triangles around a node) and betweenness centrality (the fraction of all shortest paths in the network that contain a given node). All the extracted nodal features were represented as feature vectors of 64 (at scalp level) or 68 (at source level) entries. For a comprehensive description of the investigated features refer to [23]. All the code used to perform the analysis is available at the following link: https://github.com/matteogithub/PSD_NET_comparison.

Statistical analysis

In order to estimate the relevance of the correlations between the extracted PSD-based and network-based features, the Spearman's rank correlation coefficient (rho) was computed (using the corr function in Matlab R2017b with the Spearman type as parameter) for each comparison at channel level, without performing average across subjects, epochs or channels. The

Spearman's rho is equivalent to Pearson's Linear Correlation Coefficient applied to the rankings of the selected values.

Results and discussion

The results show a clear association between the power analysis, namely the alpha relative power content, and the network analysis performed using the four different FC methods and computing the three different nodal metrics. The level of association varies depending on the specific FC method and on the computed nodal metrics, but it is persistent over the three tested scenarios: EEG_DS1, EEG_DS2 at scalp level and EEG_DS1 at source level. In particular, the association is more evident for the strength and the clustering coefficient, whereas it results lower for the betweenness centrality. As shown in Fig. 1, for the EEG_DS1, the association results in the range 0.698 – 0.224 for the strength, with a pick rho value for the PLV (rho = 0.698). The PLV based network metrics confirm a higher association with alpha relative power also for the clustering coefficient (rho = 0.736) and for the betweenness centrality (rho = -0.344).

Considering the relative high association between the two approaches, we have replicated the whole analysis using a different EEG dataset (EEG_DS2) comparable with the previous one (EEG_DS1) in terms of number of channels and experimental condition. Even the replication, although with different correlation values, show a clear association between the two approaches. As shown in Fig. 2, not only the results still show relative high correlation values, with highest magnitude of rho equals to 0.493 for the strength and 0.572 for the clustering coefficient, but even more importantly, the reported findings are consistent with the previous analysis in term of the effects due to the different FC methods. The lowest level of association was obtained when using the AECC methods to extract the FC patterns.

Finally, considering the problems related with the not straight- forward interpretation of results derived from an EEG scalp level analysis, we have further replicated the analysis with source-reconstructed time-series (derived from EEG_DS1) using the procedure as described in [8]. Even in this case, as shown in Fig. 3, the results are still in line with the previous analysis performed at scalp level. In this latter case, where the source-based FC patterns should be clearly less affected by volume conduction and signal leakage, the differences among the FC methods are even less evident. For both the strength and the clustering coefficient, the associations remain moderately high, respectively in the range 0.618 – 0.328 and 0.601 – 0.316. Despite for PLV the correlation with PSD is not surprising, as already reported in previous studies [24,25], the correlation between the power and the other FC methods, as for PLI [26], is less straightforward.

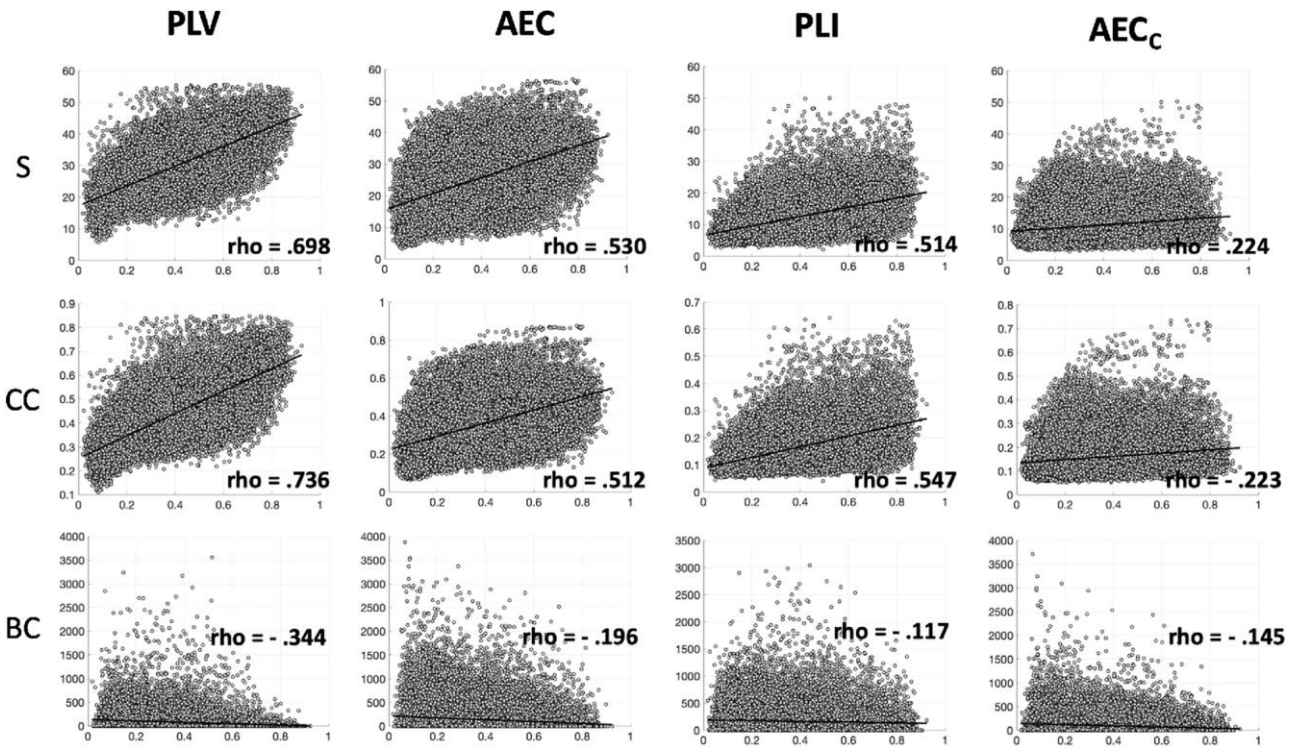

Fig. 1. Scatter plots and correlations between alpha relative power and nodal network metrics for all the FC methods using the EEG_DS1 at scalp level. The x axis represents the relative power in alpha band and the y axis represents the S, CC and BC respectively represent strength, clustering coefficient and betweenness centrality.

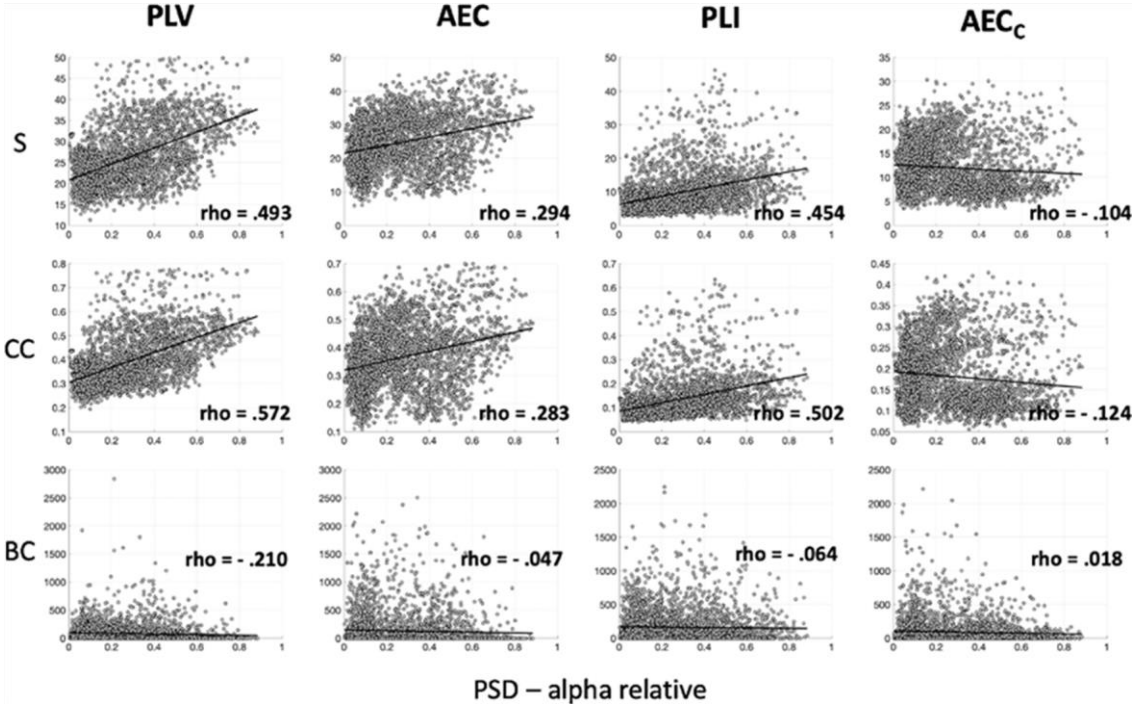

Fig. 2. Scatter plots and correlations between alpha relative power and nodal network metrics for all the FC methods using the EEG_DS2 at scalp level. The x axis represents the relative power in alpha band and the y axis represents the S, CC and BC respectively represent strength, clustering coefficient and betweenness centrality.

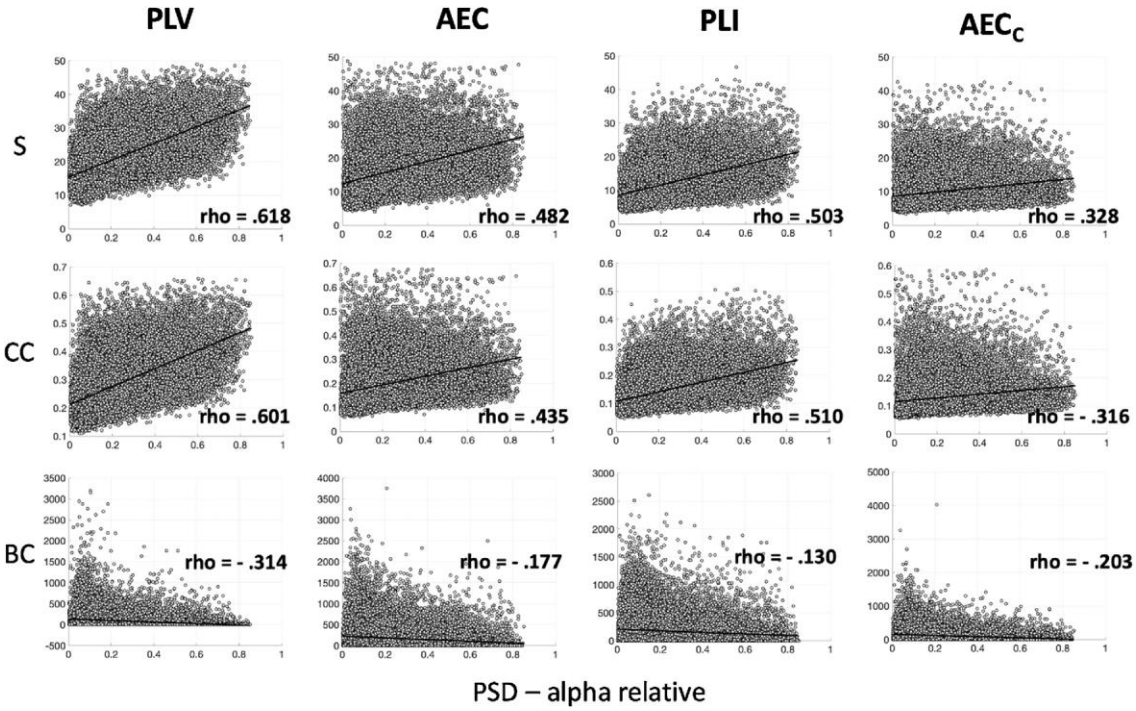

Fig. 3. Scatter plots and correlations between alpha relative power and nodal network metrics for all the FC methods using the EEG_DS1 at source level. The x axis represents the relative power in

alpha band and the y axis represents the S, CC and BC respectively represent strength, clustering coefficient and betweenness centrality.

In brief, the main findings of the present paper may be summarized as follows: (i) the results obtained using the two approaches, namely power spectral analysis and network analysis derived from the use of FC methods, show a clear and evident association between the approaches (ii) as highlighted by the statistical analysis this association is not to be negligible; (iii) as a consequence the two approaches should not be treated as completely independent; (iv) the strength of the association is not independent by the specific method used to evaluate the FC between EEG time-series. Although having found similar results on the two different datasets, despite the difference in the sampling frequency, represents a strength of the analysis, we also replicated part of the analysis (namely for the PLI metric) using a sample frequency of 160 Hz also for the EEG_DS02. As already reported in a previous work [18] the use of a different sample frequency has not shown an important impact on the reported findings.

Finally, the main contribution of this paper can be summarized as a clear warning to always assess and report the relationship between the two analyses. We suggest that this practice may avoid overestimating and to overinterpret their results when treated as separated approaches. More in general, despite network tools are easily accessible, widely used and provide appealing interpretations, findings derived from their application should be interpreted with caution and not translated as a direct consequence of functional brain mechanisms and/or alterations, as shown with simple simulations [27].

Conclusions

In conclusion, this study suggests that the results derived from the two different approaches, PSD and network analysis, may be strongly associated. The level of association may depend on the specific FC method used to

estimate the patterns of interactions and it is evident at both scalp and source level. As a consequence, we think that it would represent a good and necessary practice to report the results from the spectral analysis in conjunction with those obtained from network analysis.

References

[1] C.J. Stam, Modern network science of neurological disorders, Nat. Rev. Neurosci. 15 (2014) 683–695, http://dx.doi.org/10.1038/nrn3801.

[2] F. Lopes da Silva, EEG and MEG: relevance to neuroscience, Neuron 80 (2013) 1112–1128, http://dx.doi.org/10.1016/j.neuron.2013.10.017.

[3] C.J. Stam, G. Nolte, A. Daffertshofer, Phase lag index: assessment of functional connectivity from multi-channel EEG and MEG with diminished bias from common sources, Hum. Brain Mapp. 28 (2007) 1178–1193, http://dx.doi.org/ 10.1002/hbm.20346.

[4] C.J. Stam, B.F. Jones, G. Nolte, M. Breakspear, P. Scheltens, Small-world networks and functional connectivity in Alzheimer's disease, Cereb. Cortex 17 (2007) 92–99, http://dx.doi.org/10.1093/cercor/bhj127.

[5] D.N. Schoonhoven, M. Fraschini, P. Tewarie, B.M. Uitdehaag, A.J. Eijlers, J.J. Geurts, A. Hillebrand, M.M. Schoonheim, C.J. Stam, E.M. Strijbis, Resting-state MEG measurement of functional activation as a biomarker for cognitive decline in MS, Mult. Scler. J. (2018), 135245851881026, http://dx.doi.org/10. 1177/1352458518810260.

[6] A. Daffertshofer, B.C.M. van Wijk, On the influence of amplitude on the connectivity between phases, Front. Neuroinformat. 5 (2011), http://dx.doi. org/10.3389/fninf.2011.00006.

[7] P. Tewarie, B.A.E. Hunt, G.C. O'Neill, A. Byrne, K. Aquino, M. Bauer, K.J. Mullinger, S. Coombes, M.J. Brookes, Relationships between neuronal oscillatory amplitude and dynamic functional connectivity, Cereb. Cortex 29 (2019) 2668–2681, http://dx.doi.org/10.1093/cercor/bhy136.

[8] M. Lai, M. Demuru, A. Hillebrand, M. Fraschini, A comparison between scalp- and source-reconstructed EEG networks, Sci. Rep. 8 (2018) 12269, http://dx. doi.org/10.1038/s41598-018-30869-w.

[9] A. Anzolin, P. Presti, F. Van De Steen, L. Astolfi, S. Haufe, D. Marinazzo, Quantifying the effect of demixing approaches on directed connectivity estimated between reconstructed EEG sources, Brain Topogr. (2019), http:// dx.doi.org/10.1007/s10548-019-00705-z.

[10] M. Siems, M. Siegel, Dissociated cortical phase- and amplitude-coupling patterns in the human brain, BioRxiv (2018), 485599, http://dx.doi.org/10. 1101/485599.

[11] J.-P. Lachaux, E. Rodriguez, J. Martinerie, F.J. Varela, Measuring phase synchrony in brain signals, Hum. Brain Mapp. 8 (1999) 194–208, http://dx. doi.org/10.1002/(SICI)1097-0193(1999)8:4<194::AID-HBM4>3.0.CO;2-C.

[12] J.F. Hipp, D.J. Hawellek, M. Corbetta, M. Siegel, A.K. Engel, Large-scale cortical correlation structure of spontaneous oscillatory activity, Nat. Neurosci. 15 (2012) 884–890, http://dx.doi.org/10.1038/nn.3101.

[13] G.L. Colclough, M.W. Woolrich, P.K. Tewarie, M.J. Brookes, A.J. Quinn, S.M. Smith, How reliable are MEG resting-state connectivity metrics? Neuroimage 138 (2016) 284–293, http://dx.doi.org/10.1016/j.neuroimage.2016.05.070.

[14] G. Schalk, D.J. McFarland, T. Hinterberger, N. Birbaumer, J.R. Wolpaw, BCI2000: a general-purpose brain-computer interface (BCI) system, IEEE Trans. Biomed. Eng. 51 (2004) 1034–1043, http://dx.doi.org/10.1109/TBME.2004.827072.

[15] L. Goldberger Ary, A.N. Amaral Luis, Glass Leon, M. Hausdorff Jeffrey, Ch Ivanov Plamen, G. Mark Roger, E. Mietus Joseph, B. Moody George, Peng Chung-Kang, Stanley H. Eugene, PhysioBank, PhysioToolkit, and PhysioNet, Circulation 101 (2000) e215–e220, http://dx.doi.org/10.1161/01.CIR.101.23.e215.

[16] S. Sockeel, D. Schwartz, M. Pélégrini-Issac, H. Benali, Large-scale functional networks identified from resting-state EEG using spatial ICA, PLoS One 11 (2016), e0146845, http://dx.doi.org/10.1371/journal.pone.0146845.

[17] D.P. Schwartz, S. Sockeel, M. Pélégrini-Issac, H. Benali, Data from: Large-Scale Functional Networks Identified from Resting-State EEG Using Spatial ICA, 2016, http://dx.doi.org/10.5061/dryad.v9f16.

[18] M. Fraschini, M. Demuru, A. Crobe, F. Marrosu, C.J. Stam, A. Hillebrand, The effect of epoch length on estimated EEG functional connectivity and brain network organisation, J. Neural Eng. 13 (2016), 036015, http://dx.doi.org/10. 1088/1741-2560/13/3/036015.

[19] A. Mognon, J. Jovicich, L. Bruzzone, M. Buiatti, ADJUST: an automatic EEG artifact detector based on the joint use of spatial and temporal features, Psychophysiology 48 (2011) 229–240, http://dx.doi.org/10.1111/j.1469-8986. 2010.01061.x.

[20] A. Delorme, S. Makeig, EEGLAB: an open source toolbox for analysis of single-trial EEG dynamics including independent component analysis, J. Neurosci. Methods 134 (2004) 9–21, http://dx.doi.org/10.1016/j.jneumeth. 2003.10.009.

[21] Brainstorm: A User-Friendly Application for MEG/EEG Analysis, (n.d.). https:// www.hindawi.com/journals/cin/2011/879716/ (Accessed 17 April 2019).

[22] M. Rubinov, O. Sporns, Complex network measures of brain connectivity: uses and interpretations, NeuroImage 52 (2010) 1059–1069, http://dx.doi.org/10. 1016/j.neuroimage.2009.10.003.

[23] T. Kida, E. Tanaka, R. Kakigi, Multi-dimensional dynamics of human electromagnetic brain activity, Front. Hum. Neurosci. 9 (2016), http://dx.doi. org/10.3389/fnhum.2015.00713.

[24] L. Zhu, H. Bharadwaj, J. Xia, B. Shinn-Cunningham, A comparison of spectral magnitude and phase-locking value analyses of the frequency-following response to complex tones, J. Acoust. Soc. Am. 134 (2013) 384–395, http://dx. doi.org/10.1121/1.4807498.

[25] R. Brun˜a, F. Maestú, E. Pereda, Phase locking value revisited: teaching new tricks to an old dog, J. Neural Eng. 15 (2018), 056011, http://dx.doi.org/10. 1088/1741-2552/aacfe4.

[26] A. Hillebrand, G.R. Barnes, J.L. Bosboom, H.W. Berendse, C.J. Stam,

Frequency-dependent functional connectivity within resting-state networks: an atlas-based MEG beamformer solution, NeuroImage 59 (2012) 3909–3921, http://dx.doi.org/10.1016/j.neuroimage.2011.11.005.

[27] D. Marinazzo, Comment on "A Comparison between Power Spectral Density and Network Metrics: an EEG Study," Pubpeer, 2019 https://pubpeer.com/ publications/0732054EAAF1E3BC7C8248A8296CFC#

CHAPTER 6

Subject, session and task effects on power, connectivity and network centrality: A source-based EEG study

Pani S.M. - Ciuffi M.

Demuro M.

La Cava S.M.

Bazzano G.

D'Aloja E.

Fraschini M.

Biomedical Signal Processing and Control 59 (2020) 101891

Abstract

Inter-subjects' variability in functional brain networks has been extensively investigated in the last few years. In this context, unveiling subject-specific characteristics of EEG features may play an important role for both clinical (e.g., biomarkers) and bio-engineering purposes (e.g., biometric systems and brain computer interfaces). Nevertheless, the effects induced by multi-sessions and task-switching are not completely understood and considered. In this work, we aimed to investigate how the variability due to subject, session and task affects EEG power, connectivity and network features estimated using source-reconstructed EEG time-series. Our results point out a remarkable ability to identify stable subject features within a given task together with striking independence from the session. The results also show a relevant effect of task-switching, which is comparable to individual variability. This study suggests that power and connectivity EEG features may be adequate to detect stable (over-time) individual properties within predefined and controlled tasks and that these findings are consistent over a range of connectivity metrics, different epoch lengths and parcellation schemes.

Introduction

During the last few years it has been further recognized and stressed the importance to highlight that individual variability may play a relevant role in human neuroimaging studies [1,2]. The way in which each brain is unique and could be distinguished amidst a myriad of other brains is fascinating but unveiling the underlying subject-specific characteristics is crucial for both clinical (e.g., biomarkers) and bio-engineering purposes (e.g., biometric systems and brain computer interfaces). Recent studies have already highlighted the implications of individual variation for personalized approaches to mental illness [3], ADHD [4] and in the developing brain [5]. It has been also reported that these functional traits are familial, heritable and stable over a long time interval [6,7]. Electroencephalographic (EEG) time-frequency [8] and connectivity-based [9–12] features have shown subject-specific characteristics comparable in terms of performance to other more common fingerprints. Nevertheless, it has been recently shown that the performance of the connectivity-based biometric systems varies with the connectivity metric and with the specific task and is not yet investigated in terms of permanence (i.e., stability over-time) [13]. From this new perspective, with the clear evidence that functional brain networks vary across individuals, few studies investigated to what extent these subject-specific features are stable over time and over different states. Using functional Magnetic Resonance Imaging (fMRI), Gratton et al. [14] reported that functional net- works are suited to detect stable individual characteristics with a limited contribution from task-state and day-to-day variability, thus suggesting their possible utility in the personalized medicine approach. Similarly, Cox et al. [15], using EEG scalp level analysis, have reported that, despite a shared structure is still discernible across individuals, well-defined subject-specific and stable over-time network profiles were clearly detectable.

In this study we aim to investigate if these subject-specific features are still detectable, stable over time and consistent among different tasks using an EEG source level approach. This approach should provide a more accurate description of the underlying net- work [16] since the connectivity estimates should be less prone to volume conduction and signal leakage problems. In order to investigate this question we analysed source-reconstructed EEG time-series using three different and widely used analyses: Power Spectral Density (PSD), Phase Locking Value (PLV) [17] and nodal centrality network approaches, namely Eigenvector Centrality (EC). PSD has been shown to capture relevant subject-specific information [8] and represents a simple and easily interpretable EEG feature. PLV, in combination with weighted Minimum Norm Estimator (wMNE) [18], provides a good estimate of the functional brain organization in EEG [19] and, despite the PLV is not completely independent from the PSD [20], is known to be affected by volume conduction and signal leakage, it still performs better than other common connectivity metrics in terms of subject authentication [13]. Moreover, as previously stated, the PLV was recently used at scalp-level to investigate the variability and the stability of large- scale cortical oscillation patterns [15]. Finally, it was reported that the EC, which captures more information about the network topology then straightforward measure such as the degree, represents a promising measure to design of EEG-based biometric systems [9]. The analysis was performed on a novel EEG dataset consisting of eleven healthy subjects, recorded over two different sessions (after four weeks) and performing four different tasks. All the codes are freely available in a Github repository at the following link: https://github.com/matteogithub/individuality.

Material and methods

Dataset

Fifteen healthy volunteers (7 females, mean age 31.9 ± 3.1 years, range 28–38) were enrolled in the present study. Informed consent was obtained prior to the recordings and the study was approved by the local ethics committee. EEG signals were recorded using a 61 channels EEG system (Brain QuickSystem, Micromed, Italy) during four different tasks and repeated over two different sessions (the second acquired four weeks later from the first). Recordings were acquired in a sitting position in a normal daylight room; a dimly lit and sound attenuated room and supine position were avoided to prevent drowsiness. Signals were digitized with a sampling frequency of 1024 Hz with the reference electrode placed in close approximation of the electrode POz. The four tasks consisted of: (T1) five minutes eyes-closed resting-state, (T2) five minutes eyes-open resting-state, (T3) two minutes eyes-closed simple mathematical task and (T4) two minutes eyes-closed complex mathematical task. During the simple mathematical task, the subjects were asked to perform multiple subtractions, while during the complex mathematical task, subjects were asked to perform a series two digits multiplications. Three subjects were excluded from the analysis due to low quality of the EEG recordings and another one missed the second session.

EEG preprocessing

All the preprocessing steps were performed using the freely available toolbox EEGLAB (version 13_6_5b) [21]. The raw EEG signals were re-reference to common average reference and band-pass filtered (with fir1 filter type)

between 1 and 70 Hz and a notch filter set to 50 Hz was also applied. All the recordings were visually inspected and segments with clear artifacts were rejected and not further analysed.

Source reconstruction

In order to obtain the source-reconstructed time-series, the Brainstorm software (version 3.4) [22] was used to compute the head model with a symmetric boundary element method in Open-MEEG [23] based on the anatomy derived from the ICBM152 brain (with 15,002 vertices) [24]. It has been recently shown that the co-registration performed with a template provided consistent relative power, connectivity, and network estimates compared to the use of the native MRI [25]. EEG time-series at source level were reconstructed using whitened and depth-weighted linear L2 minimum norm estimate (wMNE) [18,26] and projected onto 68 regions of interest (ROIs) as defined by the Desikan-Killiany atlas [27]. For more details about the atlas visualization, please refer to the following link: https://surfer.nmr.mgh.harvard.edu/fswiki/ Cortical Parcellation.

In order to investigate the possible effect of brain parcellation, the analysis was replicated using the Schaefer atlas with 17 networks as reported in [28]. All the steps were performed using the software Brainstorm [22].

Features extraction

After the EEG time-series were reconstructed at source level, in order to increase the quality of the analysis, for each subject, each task and each session, we selected the best (less contaminated) 10 EEG epochs (segments of 5 s) ordering all the available epochs on the basis of the three-sigma rule (consequently discarding segments presenting values over than 3 standard

deviations from the mean) [29]. The analysis was also replicated using three different epoch length, respectively 6 s, 2 s and 1 s. Successively, for each selected epoch we have extracted three different features vectors, respectively for PSD, PLV and EC, representing the individual profiles or subject fingerprints. For the PSD analysis, the features vector, for each single epoch, was composed of the 272 entries representing the relative power (extracted using the Welch method) of alpha (8–13 Hz) and beta (13–30 Hz) frequency bands, separately for each of the 68 regions of interest. For the PLV analysis, the features vector, for each single epoch and for each frequency band, was composed of 2278 entries representing the connectivity profile upper triangular of the connectivity matrix, where each entry was computed as:

$$PLV_{xy} = \frac{1}{T}\left|\sum_{t=1}^{T} e^{-i(\varphi x(t)-\varphi y(t))}\right|$$

where T is the epoch length and φ is the instantaneous phase. Furthermore, we have replicated the analysis using two other connectivity metrics, the amplitude envelope correlation (AEC) approach [34] and the novel and revised version of PLV (icPLV) [35], which has been shown to be particularly valid to estimate synchronization in the presence of volume conduction or source leakage effects. For the network analysis, in order to keep a nodal resolution, we have computed the EC, a centrality measure based on the spectral decomposition of the weighted connectivity matrix [30]. The EC was computed using the Brain Connectivity Toolbox (brain-connectivity-toolbox.net) [31]. In this latter case the features vector, for each single epoch and separately for each frequency band, was composed of 68 entries, each representing the centrality value of the corresponding ROI. As a final step, in order to estimate the similarity among each pairs of possible observations

(between-epochs), we computed the Euclidian distance between features vectors (individual profiles) independently for PSD, PLV and EC analysis, thus obtaining, for each analysis, a square and symmetric matrix of distances, with the dimension equals to (number of subjects) * (number of sessions) * (number of tasks) * (number of epochs) as shown in Fig. 1. From this distances matrix, we have computed the average distances across epochs for each of the following six scenarios: (i) within-task, within-session and within-subject; (ii) between-tasks, within- session and within-subject; (iii) between-sessions, within-task and within-subject; (iv) between-sessions, between-tasks and within- subject; (v) within-task, within-session and between-subjects; (vi) all-between. All the code, developed in Matlab, reporting the extraction of the profiles and their comparison, is freely available at the following link in Github: https://github.com/matteogithub/ individuality.

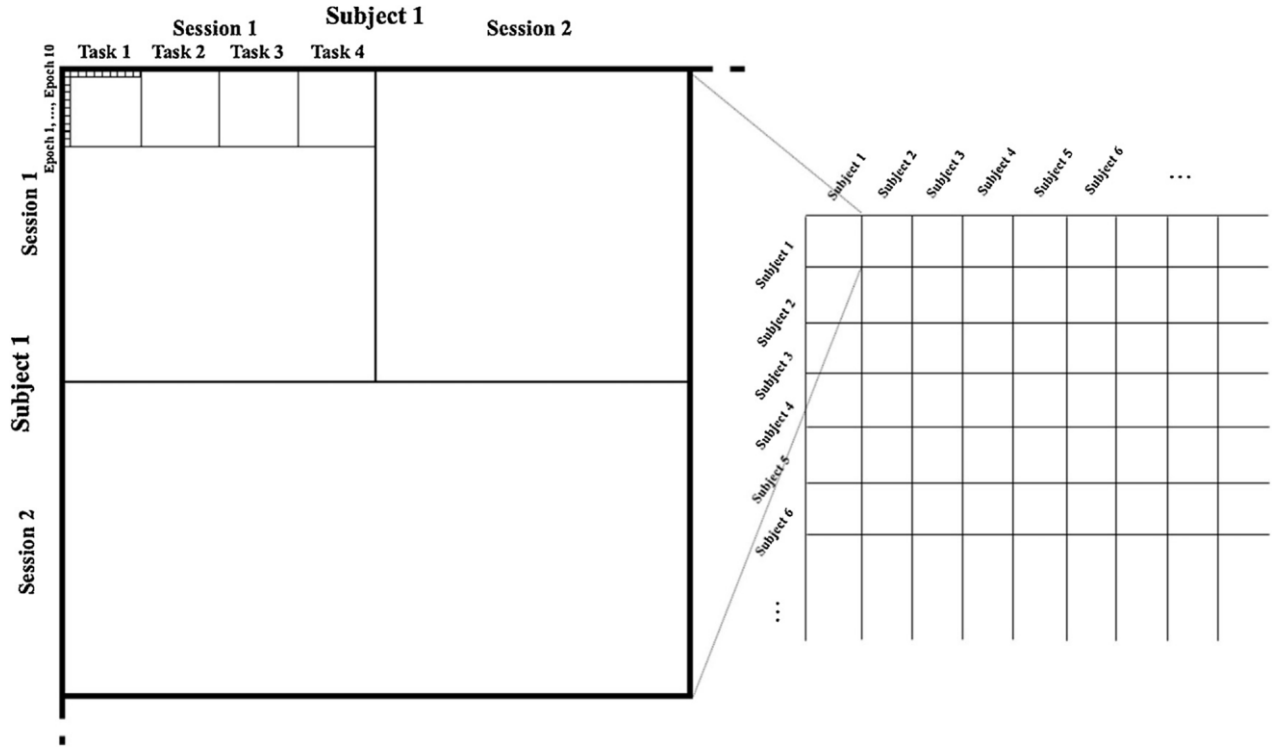

Fig. 1. A schematic representation of the first block (one subject) of the matrix containing the distances for all the possible investigated scenarios.

Statistical analysis

The statistical analysis was performed by using the non- parametric Kruskal-Wallis test [32] followed by two-stage linear step-up procedure of Benjamini, Krieger and Yekutieli [33] to account for the multiple comparison problem.

Results

PSD

Results derived from PSD analysis are shown in Fig. 2 and the corresponding statistics are summarized in Table 1. The lower distances were observed for the within-task, within-session, within-subject scenario (0.95 ± 0.34) and for the between-sessions, within-task, within-subject scenario (0.87 ± 0.30). The distances increased for the between-tasks scenarios, both for within-session (3.06 ± 1.20) and for between-sessions (3.09 ± 1.19). The distances further increased for the between-subjects' scenarios, both for within-session, within-task (3.23 ± 1.00) and for all between (3.59 ± 1.18). Values represent mean and standard deviation.

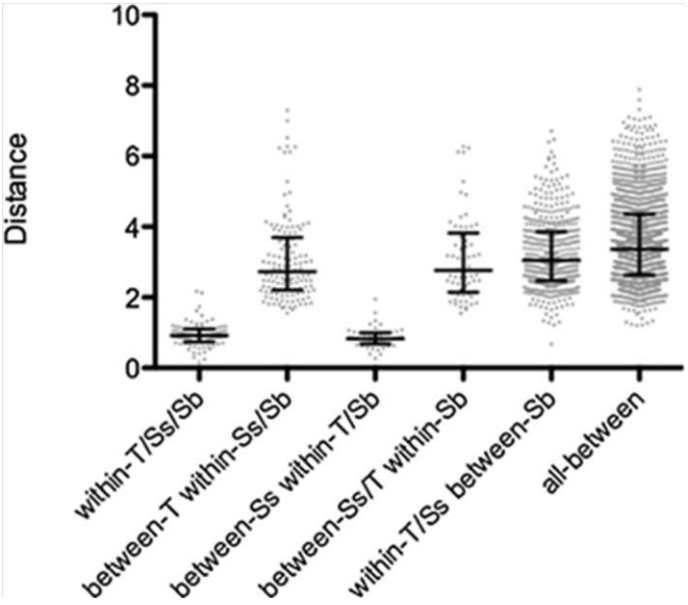

Fig. 2. Scatterplot of distances obtained by using the PSD approach. Bars represent median and interquartile range. T is for task, Ss for session and Sb for subject.

Table 1
Statistical results for PSD analysis

	Mean rank diff.	p-value
w-T/Ss/Sb vs. b-T w-Ss/Sb	−873.129	**<0.0001**
w-T/Ss/Sb vs. b-Ss w-T/Sb	146.023	0.9056
w-T/Ss/Sb vs. b-Ss/T w-Sb	−907.163	**<0.0001**
w-T/Ss/Sb vs. w-T/Ss b-Sb	−1033.61	**<0.0001**
w-T/Ss/Sb vs. all-b	−1209.25	**<0.0001**
b-T w-Ss/Sb vs. b-Ss w-T/Sb	887.731	**<0.0001**
b-T w-Ss/Sb vs. b-Ss/T w-Sb	−34.0341	0.7350
b-T w-Ss/Sb vs. w-T/Ss b-Sb	−160.484	0.0153
b-T w-Ss/Sb vs. all-b	−336.122	**<0.0001**
b-Ss w-T/Sb vs. b-Ss/T w-Sb	−921.765	**<0.0001**
b-Ss w-T/Sb vs. w-T/Ss b-Sb	−1048.21	**<0.0001**
b-Ss w-T/Sb vs. all-b	−1223.85	**<0.0001**
b-Ss/T w-Sb vs. w-T/Ss b-Sb	−126.450	0.1509
b-Ss/T w-Sb vs. all-b	−302.088	**0.0003**
w-T/Ss b-Sb vs. all-b	−175.638	**<0.0001**

Statistics refer to non-parametric multiple comparison tests (on mean rank) using the FDR correction approach, where w- and b- refer to within and between scenarios respectively. T, Ss and Sb refer to task, session and subject.

Connectivity

Results derived from PLV based analysis in the beta band are consistent with those obtained by PSD as shown in Fig. 3 and the corresponding statistics summarized in Table 2. Again, the lower distances were observed for the within-task, within-session, within-subject scenario (4.82 ± 0.33) and for the between-sessions, within-task, within-subject scenario (4.40 ± 0.34). The distances increased for the between-tasks scenarios, both for within-session (5.74 ± 0.85) and for between-sessions (5.85 ± 0.96). Finally, the distances further increased for the between-subjects' scenarios, both for within-session, within-task (7.07 ± 0.76) and for all between (7.25 ± 0.87).

The results show a similar pattern, still slightly less marked, also for the alpha band as shown in Fig. 4 and the corresponding statistics summarized in Table 3. In this case, again the lower distances were observed for the within-task, within-session, within-subject scenario (8.25 ± 0.86) and for the between-sessions, within-task, within-subject scenario (7.55 ± 0.83). The distances increased for between-tasks scenarios, both for within-session (9.21 ± 1.26) and for between-sessions (9.32 ± 1.27). Finally, the distances further increased for the between-subjects' scenarios, both for within-session, within-task (10.86 ± 2.11) and for all between (11.01 ± 2.16). In order to give a more detailed description of the connectivity patterns obtained during the different tasks and the different sessions, we have represented the corresponding average (the average was computed over epochs and subjects) matrices in Fig. 5.

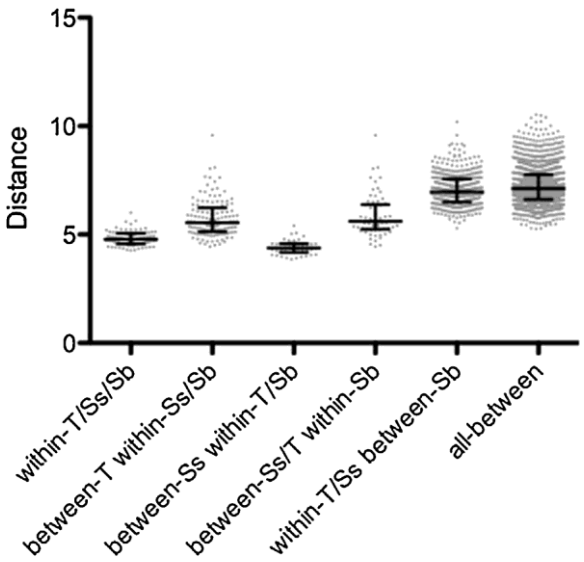

Fig. 3. Scatterplot of beta band distances obtained by using the PLV connectivity approach. Bars represent median and interquartile range. T is for task, Ss for session and Sb for subject.

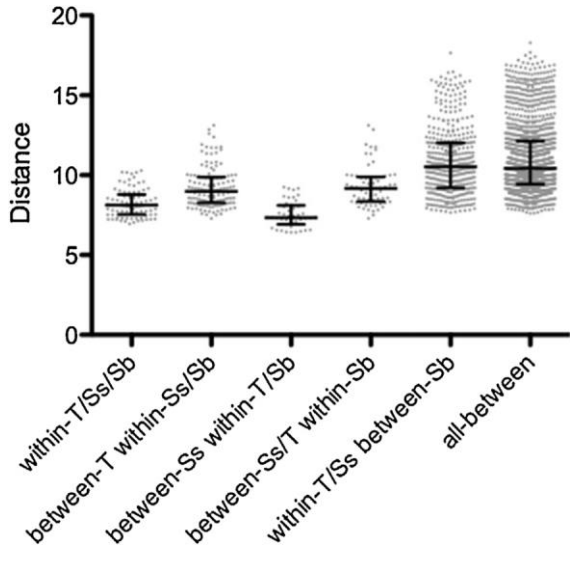

Fig. 4. Scatterplot of alpha band distances obtained by using the PLV connectivity approach. Bars represent median and interquartile range. T is for task, Ss for session and Sb for subject.

Table 2

Statistical results for PLV beta band.

	Mean rank diff.	p-value
w-T/Ss/Sb vs. b-T w-Ss/Sb	−317.8	**0.0005**
w-T/Ss/Sb vs. b-Ss w-T/Sb	61.03	0.6202
w-T/Ss/Sb vs. b-Ss/T w-Sb	−382.5	**0.0004**
w-T/Ss/Sb vs. w-T/Ss b-Sb	−1104	**<0.0001**
w-T/Ss/Sb vs. all-b	−1217	**<0.0001**
b-T w-Ss/Sb vs. b-Ss w-T/Sb	378.8	**0.0011**
b-T w-Ss/Sb vs. b-Ss/T w-Sb	−64.72	0.5198
b-T w-Ss/Sb vs. w-T/Ss b-Sb	−786.1	**<0.0001**
b-T w-Ss/Sb vs. all-b	−899.3	**<0.0001**
b-Ss w-T/Sb vs. b-Ss/T w-Sb	−443.6	**0.0006**
b-Ss w-T/Sb vs. w-T/Ss b-Sb	−1165	**<0.0001**
b-Ss w-T/Sb vs. all-b	−1278	**<0.0001**
b-Ss/T w-Sb vs. w-T/Ss b-Sb	−721.4	**<0.0001**
b-Ss/T w-Sb vs. all-b	−834.6	**<0.0001**
w-T/Ss b-Sb vs. all-b	−113.1	**0.0017**

Statistics refer to non-parametric multiple comparison tests (on mean rank) using the FDR correction approach, where w- and b- refers to within and between scenar- ios respectively. T, Ss and Sb refer to task, session and subject.

Table 3

Statistical results for PLV alpha band.

	Mean rank diff.	p-value
w-T/Ss/Sb vs. b-T w-Ss/Sb	−356.220	**0.0001**
w-T/Ss/Sb vs. b-Ss w-T/Sb	165.750	0.1783
w-T/Ss/Sb vs. b-Ss/T w-Sb	−402.515	**0.0002**
w-T/Ss/Sb vs. w-T/Ss b-Sb	−933.130	**<0.0001**
w-T/Ss/Sb vs. all-b	−974.344	**<0.0001**
b-T w-Ss/Sb vs. b-Ss w-T/Sb	521.970	**<0.0001**
b-T w-Ss/Sb vs. b-Ss/T w-Sb	−46.2955	0.6452
b-T w-Ss/Sb vs. w-T/Ss b-Sb	−576.910	**<0.0001**
b-T w-Ss/Sb vs. all-b	−618.124	**<0.0001**
b-Ss w-T/Sb vs. b-Ss/T w-Sb	−568.265	**<0.0001**
b-Ss w-T/Sb vs. w-T/Ss b-Sb	−1098.88	**<0.0001**
b-Ss w-T/Sb vs. all-b	−1140.09	**<0.0001**
b-Ss/T w-Sb vs. w-T/Ss b-Sb	−530.614	**<0.0001**
b-Ss/T w-Sb vs. all-b	−571.828	**<0.0001**
w-T/Ss b-Sb vs. all-b	−41.2140	0.2530

Statistics refer to non-parametric multiple comparison tests (on mean rank) using the FDR correction approach, where w- and b- refers to within and between scenar- ios respectively. T, Ss and Sb refer to task, session and subject.

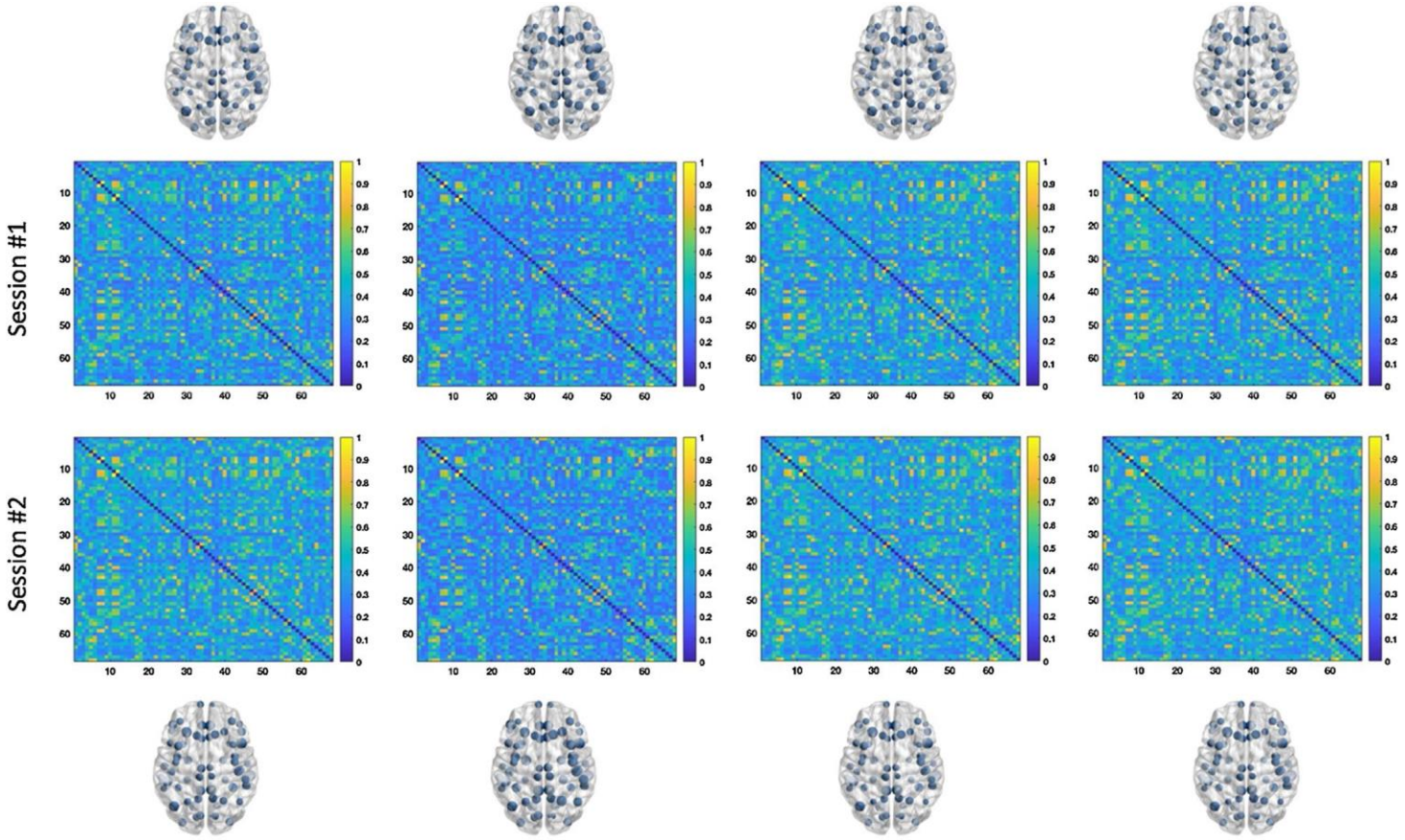

Fig. 5. Average connectivity matrices and glass brains visualization computed using PLV methods in alpha band for each task and for both sessions.

Network centrality

Results derived from the application of EC on PLV based analysis (in the beta band) are still consistent with the previous reports, as shown in Fig. 6 and the corresponding statistics summarized in Table 4. Again, the lower distances were observed for the within-task, within-session, within-subject scenario (0.12 ± 0.01) and for the between-sessions, within-task, within-subject scenario (0.11 ± 0.01). The distances increased for the between-tasks scenarios, both for within-session (0.14 ± 0.02) and for between-sessions (0.14 ± 0.02). Finally, the distances further increased for the between-subjects' scenarios, both for within-session, within-task (0.17 ± 0.03) and for all between (0.17 ±

0.03). In the Supplementary material we have also reported the results derived from the application of a very common technique used to threshold the connectivity matrix, namely the MST, on the EC based on PLV.

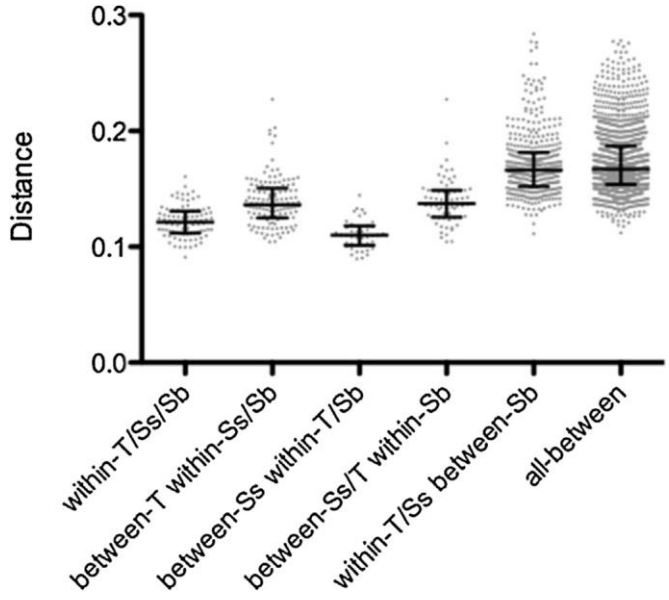

Fig. 6. Scatterplot of alpha band distances obtained by using the PLV connectivity approach and eigenvector centrality. Bars represent median and interquartile range. T is for task, Ss for session and Sb for subject.

Table 4

Statistical results for Eigenvector Centrality.

	Mean diff. Rank	p-value
w-T/Ss/Sb vs. b-T w-Ss/Sb	−309.489	**0.0007**
w-T/Ss/Sb vs. b-Ss w-T/Sb	935.795	0.4473
w-T/Ss/Sb vs. b-Ss/T w-Sb	−307.186	**0.0047**
w-T/Ss/Sb vs. w-T/Ss b-Sb	−1084.05	**<0.0001**
w-T/Ss/Sb vs. all-b	−1134.76	**<0.0001**
b-T w-Ss/Sb vs. b-Ss w-T/Sb	403.068	**0.0005**
b-T w-Ss/Sb vs. b-Ss/T w-Sb	230.303	0.9817
b-T w-Ss/Sb vs. w-T/Ss b-Sb	−774.561	**<0.0001**
b-T w-Ss/Sb vs. all-b	−825.269	**<0.0001**
b-Ss w-T/Sb vs. b-Ss/T w-Sb	−400.765	**0.0020**
b-Ss w-T/Sb vs. w-T/Ss b-Sb	−1177.63	**<0.0001**
b-Ss w-T/Sb vs. all-b	−1228.34	**<0.0001**
b-Ss/T w-Sb vs. w-T/Ss b-Sb	−776.864	**<0.0001**
b-Ss/T w-Sb vs. all-b	−827.573	**<0.0001**
w-T/Ss b-Sb vs. all-b	−50.7081	0.1596

Statistics refer to non-parametric multiple comparison tests (on mean rank) using the FDR correction approach, where w- and b- refers to within and between scenarios respectively. T, Ss and Sb refer to task, session and subject.

Between-tasks comparison

In order to understand if the reported between-tasks increase of distances comes from some specific task-switching (i.e., cognitive effort or eyes-closed/eyes-open) we further investigate this issue for both PSD and PLV beta band. For the PSD analysis, as shown in Fig. 7 the increase of distance in the between-tasks scenario mainly comes from the comparison of eyes-closed resting-state (T1) with the eyes-closed complex mathematical task (T4) and from the comparison of simple mathematical task (T3) with the eyes-closed complex mathematical task (T4). The main effect was tested using the Kruskall-Wallis approach obtaining a x^2 equals 27.2 to and p-value < .0001. For the PLV beta band analysis, as shown in Fig. 8 the increase of distance in the between-tasks scenario mainly comes from the comparison of eyes-open resting-state (T2) with the eyes- closed complex mathematical task (T4). The main effect was tested using the Kruskall-Wallis approach obtaining a x^2 equals 17.6 to and p-value equals to 0.004. All these analyses were performed in the within-session and within-subject scenario.

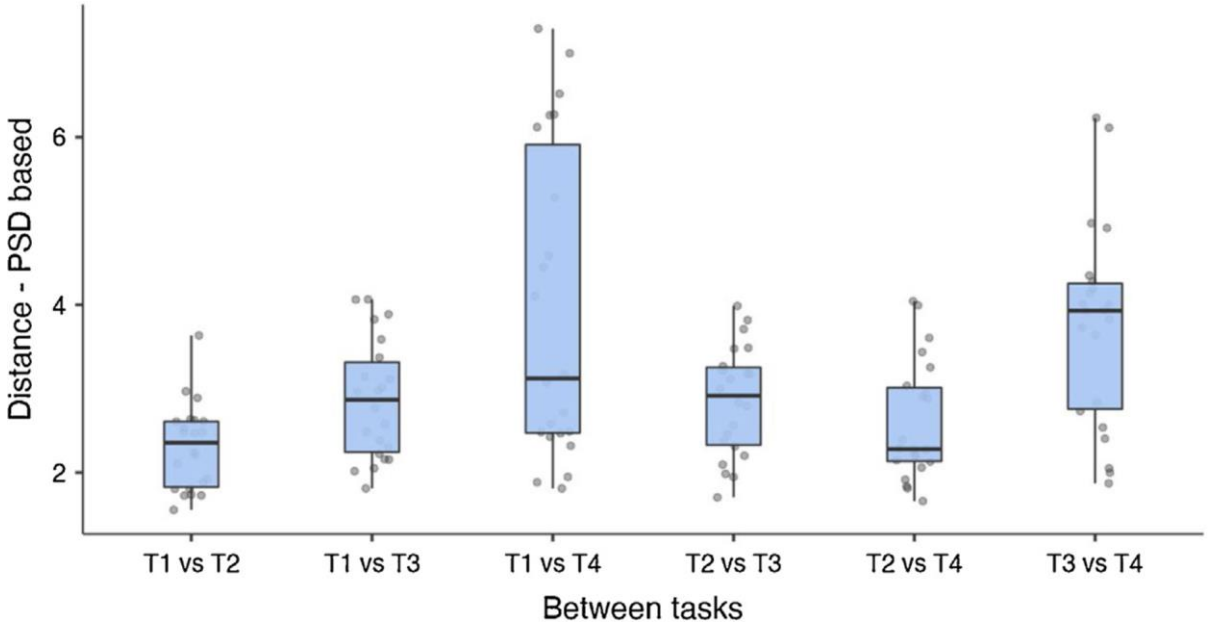

Fig. 7. Between task comparisons for PSD analysis. T1 refers to eyes-closed resting-state, T2 to eyes-open resting-state, T3 to eyes-closed simple mathematical task and T4 to eyes-closed complex mathematical task. Bars represent media and interquartile range.

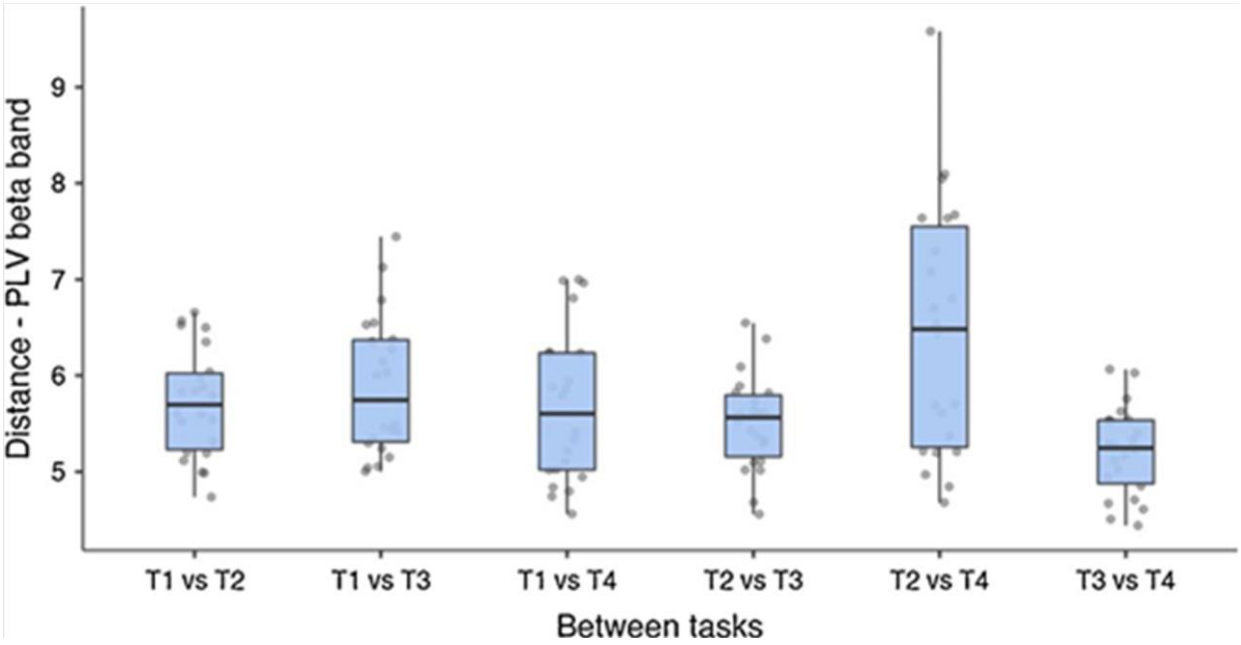

Fig. 8. Between task comparisons for PLV beta band analysis. T1 refers to eyes-closed resting-state, T2 to eyes-open resting-state, T3 to eyes-closed simple mathematical task and T4 to eyes-closed complex mathematical task. Bars represent media and interquartile range.

The effect of the connectivity metric

Although a comprehensive and detailed comparison among different connectivity metrics is out of the scope of the present study, in order to investigate the effect of the arbitrary choice of connectivity metric we have replicated part of the analysis to understand if the reported results still hold when a different method to estimate the connectivity is applied. In this context, here we report the results obtained using the amplitude envelope correlation (AEC) approach [34] and the novel and revised version of PLV (icPLV) [35], which has been shown to be particularly valid to estimate synchronization in the presence of volume conduction or source leakage effects. The results obtained by using these two different approaches are reported in Figs. 9 and 10 respectively for the AEC and icPLV approaches.

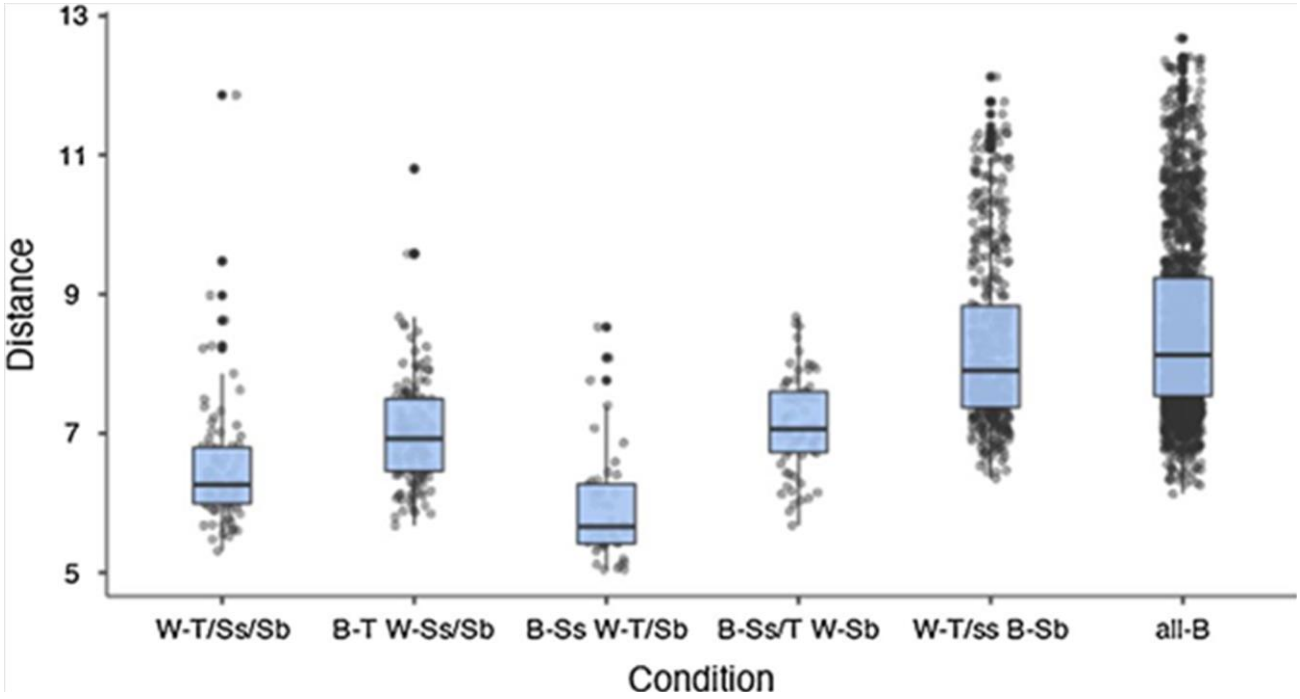

Fig. 9. Scatterplot of beta band distances obtained by using the AEC connectivity approach. Bars represent median and interquartile range.

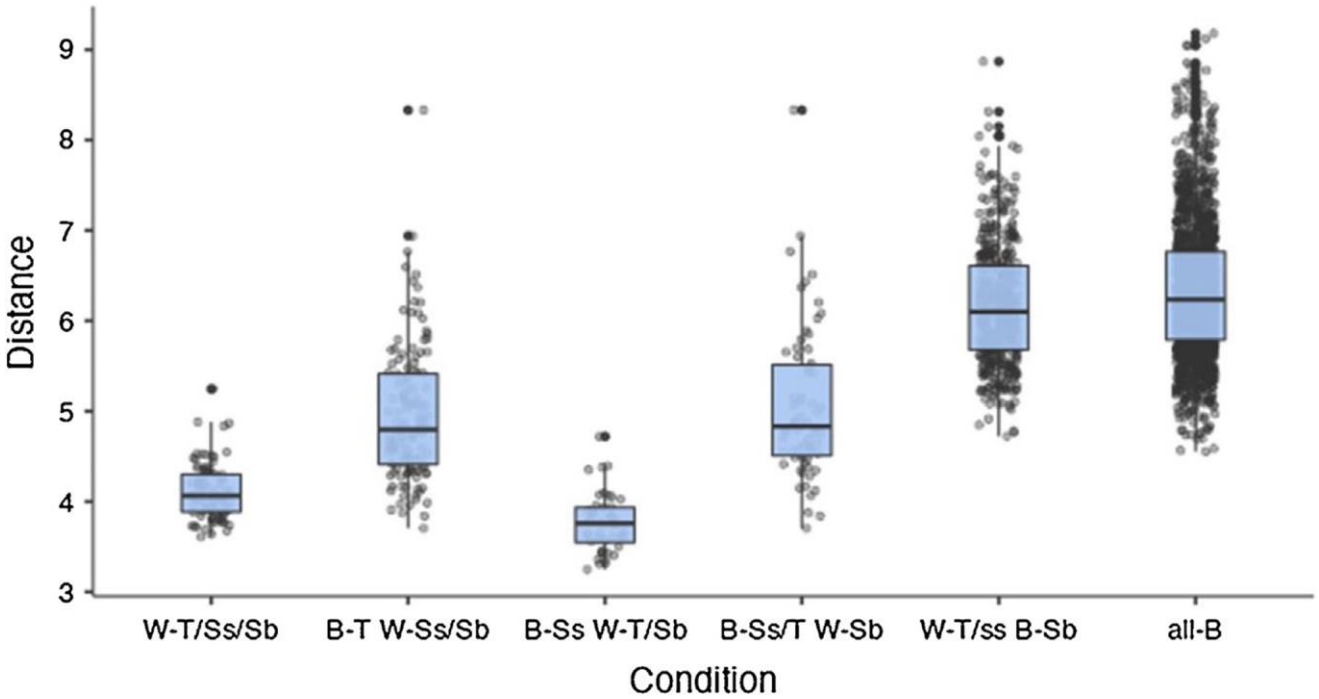

Fig. 10. Scatterplot of beta band distances obtained by using the icPLV connectivity approach. Bars represent median and interquartile range.

The effect of different atlas

In this section we report the results obtained using a different atlas, namely Schaefer atlas with 17 networks as described in [28], for the PSD (see Fig. 11), PLV (see Fig. 12) and EC PLV-based metrics (see Fig. 13). For all the three different analyses, the corresponding findings are in line with those obtained using the Desikan-Killiany atlas.

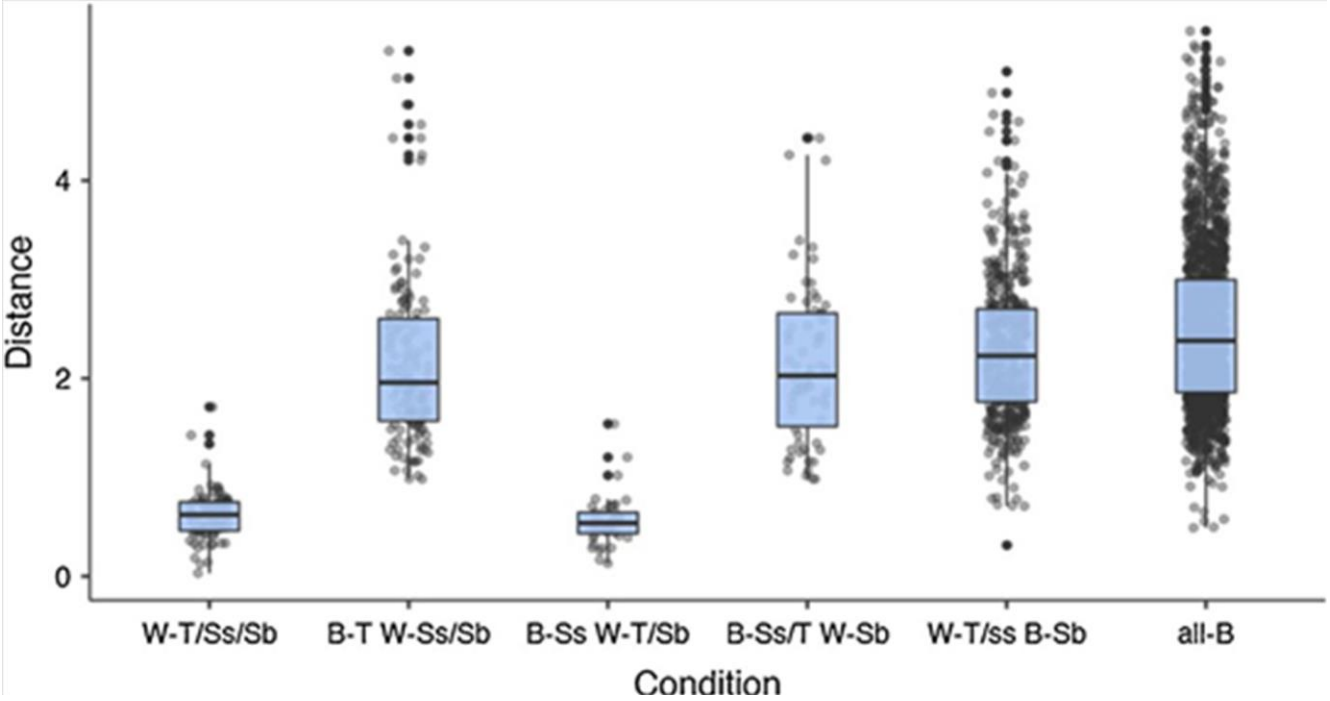

Fig. 11. Scatterplot of distances obtained by using the PSD approach with the Schaefer atlas. Bars represent median and interquartile range. T is for task, Ss for session and Sb for subject.

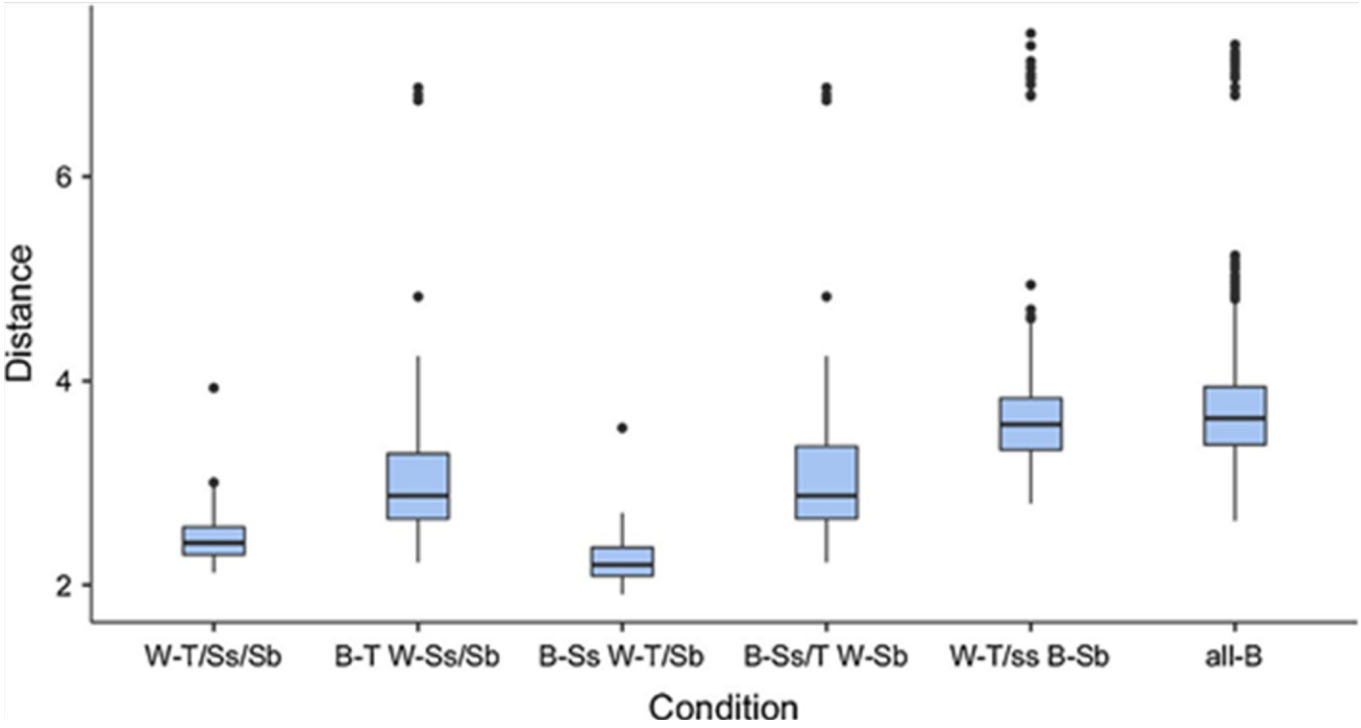

Fig. 12. Scatterplot of distances obtained by using the PLV approach with the Schaefer atlas in beta band. Bars represent median and interquartile range. T is for task, Ss for session and Sb for subject.

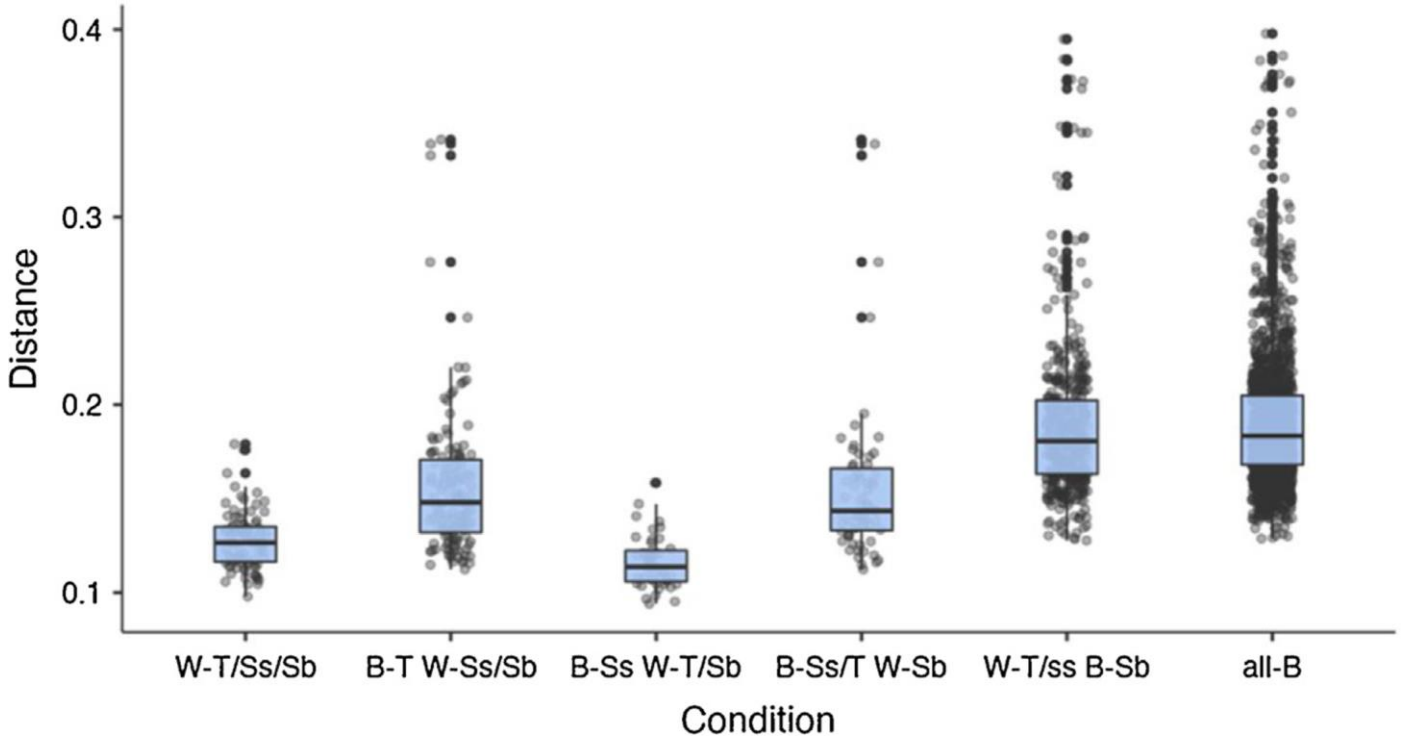

Fig. 13. Scatterplot of distances obtained by using the EC PLV-based approach with the Schaefer atlas in beta band. Bars represent median and interquartile range. T is for task, Ss for session and Sb for subject.

The effect of time window

Although the original epoch length was defined accordingly to a previous work which evaluated the effect of epoch length on connectivity and network metrics, in this section we report the results obtained using different time windows on beta band PLV connectivity profiles. In particular, in Fig. 14 it is represented the variability of the reported effects on three different epoch length, respectively 6 s (as the main finding), 2 s and 1 s. Although the main effects are still visible the intra task condition variability (see interquartile ranges) looks to increase as the epoch length decrease.

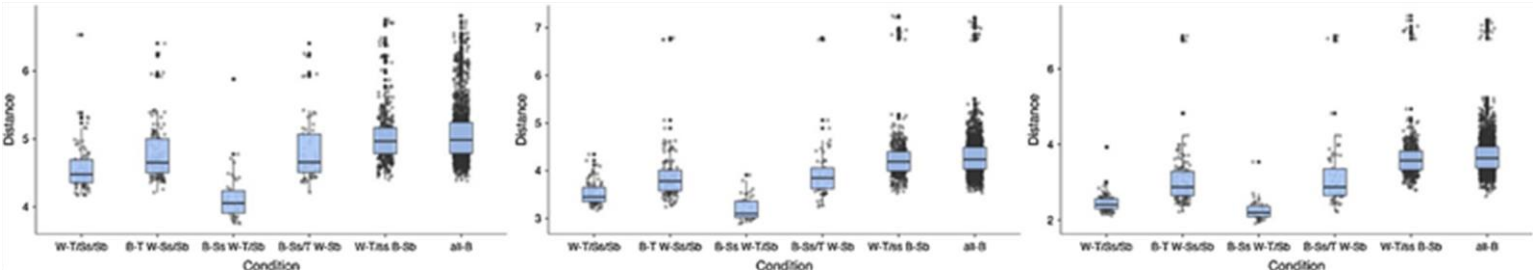

Fig. 14. Scatterplot of distances obtained by using the PLV approach with three different epoch lengths: 1 s (left panel), 2 s (middle panel) and 6 s (right panel). Bars represent median and interquartile range. T is for task, Ss for session and Sb for subject.

Discussion and conclusions

In summary, in this work we aimed to investigate how the variability due to subject, session and task affects EEG power, connectivity and network features estimated using source- reconstructed EEG time-series. Although this question was extensively investigated using fMRI [2,6,14], high density EEG, which still represents a very important and useful clinical tool, has received less attention in this context. Although, numerous studies have investigated the possibility to use EEG signals to develop biometric systems,

only recently more attention was devoted to the study of subject variability and stability over-time and states [15].

The results of this study show three main relevant points. First, as expected, for all the different analyses, PSD, PLV and EC based approaches, the lower distances were observed in the scenario corresponding to a simple between epochs scheme, within the same subject, the same session and the same task. It should be highlighted that this also represents the more common scenario in which studies do not consider the variance induced by subject-specific features, multi-sessions and/or by multi-tasks setup. Second, probably the more interesting finding, the distances obtained using the between-sessions, within-task, within-subject scenario are comparable with the previous one (namely, within-session scenario) for all the performed analyses. This finding suggests that the variance due to the session may be considered negligible, but we need to highlight that the task design is not considering the possible effects due to learning process or memory recall/consolidation processes. Third, conversely, the effect due to the task (task-switching) is substantial, as also highlighted by the statistics and consistent for all the different analyses (i.e., PSD, PLV in beta and alpha bands and EC analysis). Finally, as expected, the distances strongly increase in the between-subjects scenario, showing a clear effect due to specific subject, thus confirming the importance to address the issue related with the variance within a group.

The reported results support, as recently reported using a scalp-level EEG analysis [15], the existence of well-defined subject- specific profiles and that these features may be considered stable over a defined and limited time range. These results are also in line with the fact that task-invariant subject-specific features are stronger than task-dependent group profiles. Moreover, as reported in the between-tasks effect, it seems that the reported increase of distance in this scenario is not merely due to eyes-closed and eyes-open

switching. It is interesting to highlight, that the present findings, derived from source-reconstructed EEG time-series, are also in line with previous outcomes derived from fMRI network analysis. In particular, recently Finn et al. [3] have reported that brain functional organization varies between individuals, that this variability is robust and reliable and that can be used to identify subjects from a large group. Moreover, the authors also report that identification is successful across scan sessions and even between task and rest conditions. Later, Gratton et al. [14] have reported that functional networks, as measured by fMRI, are dominated by common organizational principles and stable individual features, with more modest contributions from task-state and day-to-day variability. We also would like to highlight that our results are based on a very limited set of tasks and therefore are not easily generalizable. We are aware that the reported findings would need to be replicated in set of EEG recordings that include a large number of subjects and tasks.

Although it is not possible to directly compare the absolute distances derived from the different features to understand if any approach outperforms the others, it is worth to highlight that the PSD analysis seems to be the most sensitive approach to inter-condition variability as marked by the larger mean rank differences for all the different scenarios investigated. This latest finding may suggest using this very simple and easily interpretable approach to check for the stability over session and task of the EEG signals.

Finally, the reported findings (derived from source level analysis) are in line with the results previously reported at scalp level [10,13]. On the other hand, these results also confirm what is generally observable by designing a brain computer interface system. In fact, even though it is still remarkable a strong effect of task-switching, it is still evident that the individual properties may strongly hinder the generalization of the approach (failing to keep a good performance across different subjects). It is also of relevance to notice that the

results reported using the PLV approach have been confirmed when the analysis was replicated using two other connectivity metrics, namely AEC and icPLV. In particular, the findings related to this last metric (icPLV), which has been shown to be particularly valid to estimate synchronization in the presence of volume conduction or source leakage effects [35], suggest that the reported effects are not a consequence of possible bias in estimating EEG connectivity. As reported, the results obtained on PSD, PLV and EC still hold when a different parcellation scheme [28] was used for the analysis.

In light of what we have shown up to this point, in our opinion, future studies should investigate how connectivity and network similarity across multiple tasks and sessions varies between different clinical conditions and, in particular it would be of relevance to evaluate its association with behavior.

In conclusion, we have shown that source-level EEG analysis confirms that PSD, PLV and PLV derived functional brain network, as measured by nodal centrality (namely, eigenvector centrality), are stable over-time, dominated by individual properties but largely dependent from the specific task. These findings may have important implications for both clinical (e.g., biomarkers) and bio-engineering applications (e.g., biometric systems and brain computer interfaces).

Appendix A. Supplementary data

Supplementary material related to this article can be found, in the online version, at https://doi.org/10.1016/j.bspc.2020.101891.

References

[1] O. Miranda-Dominguez, et al., Connectotyping: model based fingerprinting of the functional connectome, PLoS One 9 (November (11)) (2014) e111048, http://dx.doi.org/10.1371/journal.pone.0111048.

[2] E.S. Finn, et al., Functional connectome fingerprinting: identifying individuals using patterns of brain connectivity, Nat. Neurosci. 18 (November (11)) (2015) 1664–1671, http://dx.doi.org/10.1038/nn.4135.

[3] E.S. Finn, R. Todd Constable, Individual variation in functional brain connectivity: implications for personalized approaches to psychiatric disease, Dialogues Clin. Neurosci. 18 (September (3)) (2016) 277–287.

[4] M. Arns, EEG-based personalized medicine in ADHD: individual alpha peak frequency as an endophenotype associated with nonresponse, J. Neurother. 16 (April (2)) (2012) 123–141, http://dx.doi.org/10.1080/10874208.2012. 677664.

[5] C. Horien, X. Shen, D. Scheinost, R.T. Constable, The individual functional connectome is unique and stable over months to years, NeuroImage 189 (2019) 676–687, http://dx.doi.org/10.1016/j.neuroimage.2019.02.002, April.

[6] O. Miranda-Dominguez, E. Feczko, D.S. Grayson, H. Walum, J.T. Nigg, D.A. Fair, Heritability of the human connectome: a connectotyping study, Netw. Neurosci. (November (2)) (2017) 175–199, http://dx.doi.org/10.1162/netn a 00029.

[7] M. Demuru, et al., Functional and effective whole brain connectivity using magnetoencephalography to identify monozygotic twin pairs, Sci. Rep. 7 (August (1)) (2017) 9685, http://dx.doi.org/10.1038/s41598-017-10235-y.

[8] M. DelPozo-Banos, C.M. Travieso, C.T. Weidemann, J.B. Alonso, EEG biometric identification: a thorough exploration of the time-frequency domain, J. Neural Eng. 12 (October (5)) (2015) 056019, http://dx.doi.org/10.1088/1741-2560/ 12/5/056019.

[9] M. Fraschini, A. Hillebrand, M. Demuru, L. Didaci, G.L. Marcialis, An EEG-based biometric system using eigenvector centrality in resting state brain networks, IEEE Signal Process. Lett. 22 (June (6)) (2015) 666–670, http://dx.doi.org/10. 1109/LSP.2014.2367091.

[10] D.L. Rocca, et al., Human brain distinctiveness based on EEG spectral coherence connectivity, IEEE Trans. Biomed. Eng. 61 (September (9)) (2014) 2406–2412, http://dx.doi.org/10.1109/TBME.2014.2317881.

[11] A. Crobe, M. Demuru, L. Didaci, G.L. Marcialis, M. Fraschini, Minimum spanning tree andk-core decomposition as measure of subject-specific EEG traits, Biomed. Phys. Eng. Express 2 (January (1)) (2016) 017001, http://dx.doi. org/10.1088/2057-1976/2/1/017001.

[12] S. Barra, A. Casanova, M. Fraschini, M. Nappi, Fusion of physiological measures for multimodal biometric systems, Multimed. Tools Appl. 76 (February (4)) (2017) 4835–4847, http://dx.doi.org/10.1007/s11042-016-3796-1.

[13] M. Fraschini, S.M. Pani, L. Didaci, G.L. Marcialis, Robustness of functional connectivity metrics for EEG-based personal identification over task-induced intra-class and inter-class variations, Pattern Recognit. Lett. 125 (2019) 49–54, http://dx.doi.org/10.1016/j.patrec.2019.03.025, July.

[14] C. Gratton, et al., Functional brain networks are dominated by stable group and individual factors, not cognitive or daily variation, Neuron 98 (April (2)) (2018) 439–452.e5, http://dx.doi.org/10.1016/j.neuron.2018.03.035.

[15] R. Cox, A.C. Schapiro, R. Stickgold, Variability and stability of large-scale cortical oscillation patterns, Netw. Neurosci. 2 (February (4)) (2018) 481–512, http://dx.doi.org/10.1162/netn a 00046.

[16] M. Lai, M. Demuru, A. Hillebrand, M. Fraschini, A comparison between scalp- and source-reconstructed EEG networks, Sci. Rep. 8 (August (1)) (2018) 12269, http://dx.doi.org/10.1038/s41598-018-30869-w.

[17] J.-P. Lachaux, E. Rodriguez, J. Martinerie, F.J. Varela, Measuring phase synchrony in brain signals, Hum. Brain Mapp. 8 (January (4)) (1999) 194–208, http://dx.doi.org/10.1002/(SICI)1097-0193(1999)8:4<194::AID-HBM4>3.0. CO;2-C.

[18] M.S. Hämäläinen, R.J. Ilmoniemi, Interpreting magnetic fields of the brain: minimum norm estimates, Med. Biol. Eng. Comput. 32 (January (1)) (1994) 35–42, http://dx.doi.org/10.1007/BF02512476.

[19] M. Hassan, O. Dufor, I. Merlet, C. Berrou, F. Wendling, EEG source connectivity analysis: from dense array recordings to brain networks, PLoS One 9 (August (8)) (2014), http://dx.doi.org/10.1371/journal.pone.0105041.

[20] M. Demuru, S.M.L. Cava, S.M. Pani, M. Fraschini, A Comparison Between Power Spectral Density and Network Metrics: an EEG Study, April, 2019.

[21] A. Delorme, S. Makeig, EEGLAB: an open source toolbox for analysis of single-trial EEG dynamics including independent component analysis, J.

Neurosci. Methods 134 (March (1)) (2004) 9–21, http://dx.doi.org/10.1016/j. jneumeth.2003.10.009.

[22] F. Tadel, S. Baillet, J.C. Mosher, D. Pantazis, R.M. Leahy, Brainstorm: a user-friendly application for MEG/EEG analysis, Comput. Intell. Neurosci. 2011 (2011) 879716, http://dx.doi.org/10.1155/2011/879716.

[23] A. Gramfort, T. Papadopoulo, E. Olivi, M. Clerc, OpenMEEG: opensource software for quasistatic bioelectromagnetics, Biomed. Eng. Online 9 (2010) 45, http://dx.doi.org/10.1186/1475-925X-9-45, September.

[24] S. Cutini, P. Scatturin, M. Zorzi, A new method based on ICBM152 head surface for probe placement in multichannel fNIRS, NeuroImage 54 (January (2)) (2011) 919–927, http://dx.doi.org/10.1016/j.neuroimage.2010.09.030.

[25] L. Douw, D. Nieboer, C.J. Stam, P. Tewarie, A. Hillebrand, Consistency of magnetoencephalographic functional connectivity and network reconstruction using a template versus native MRI for co-registration, Hum. Brain Mapp. 39 (January (1)) (2018) 104–119, http://dx.doi.org/10.1002/hbm. 23827.

[26] F.-H. Lin, T. Witzel, S.P. Ahlfors, S.M. Stufflebeam, J.W. Belliveau, M.S. Hämäläinen, Assessing and improving the spatial accuracy in MEG source localization by depth-weighted minimum-norm estimates, NeuroImage 31 (May (1)) (2006) 160–171, http://dx.doi.org/10.1016/j.neuroimage.2005.11. 054.

[27] R.S. Desikan, et al., An automated labeling system for subdividing the human cerebral cortex on MRI scans into gyral based regions of interest, NeuroImage 31 (July (3)) (2006) 968–980, http://dx.doi.org/10.1016/j.neuroimage.2006. 01.021.

[28] A. Schaefer, et al., Local-global parcellation of the human cerebral cortex from intrinsic functional connectivity MRI, Cereb. Cortex 28 (9) (2018) 3095–3114, http://dx.doi.org/10.1093/cercor/bhx179.

[29] M. Fraschini, M. Demuru, A. Crobe, F. Marrosu, C.J. Stam, A. Hillebrand, The effect of epoch length on estimated EEG functional connectivity and brain network organisation, J. Neural Eng. 13 (3) (2016) 036015, http://dx.doi.org/ 10.1088/1741-2560/13/3/036015.

[30] B. Ruhnau, Eigenvector-centrality — a node-centrality? Soc. Networks 22 (October (4)) (2000) 357–365, http://dx.doi.org/10.1016/S0378- 8733(00)00031-9.

[31] M. Rubinov, O. Sporns, Complex network measures of brain connectivity: uses and interpretations, NeuroImage 52 (September (3)) (2010) 1059–1069, http://dx.doi.org/10.1016/j.neuroimage.2009.10.003.

[32] W.H. Kruskal, W.A. Wallis, Use of ranks in one-criterion variance analysis, J. Am. Stat. Assoc. 47 (December (260)) (1952) 583–621, http://dx.doi.org/10. 1080/01621459.1952.10483441.

[33] Y. Benjamini, A.M. Krieger, D. Yekutieli, Adaptive linear step-up procedures that control the false discovery rate, Biometrika 93 (September (3)) (2006) 491–507, http://dx.doi.org/10.1093/biomet/93.3.491.

[34] J.F. Hipp, D.J. Hawellek, M. Corbetta, M. Siegel, A.K. Engel, Large-scale cortical correlation structure of spontaneous oscillatory activity, Nat. Neurosci. 15 (June (6)) (2012) 884–890, http://dx.doi.org/10.1038/nn.

3101.

[35] R. Brun˜a, F. Maestú, E. Pereda, Phase locking value revisited: teaching new tricks to an old dog, J. Neural Eng. 15 (October (5)) (2018) 056011, http://dx. doi.org/10.1088/1741-2552/aacfe4.

PART III

fMRI: Risk phenotypes for psychotic disorders

CHAPTER 7

A multivariate analysis of the association between corticostriatal functional connectivity and psychosis-like experiences in the general community

Pani S.M.

Sabaroedin K.

Tiego J.

Bellgrove M.A.

Fornito A.

Psychiatry Research: Neuroimaging, 2020.

Corrected proof available online from 10 Oct 2020.

Abstract

Dysfunction of dorsal corticostriatal (CST) circuitry is thought to play an important role in psychosis. Here, we use multivariate analysis to characterize covariance between CST functional connectivity and psychosis-like experiences (PLEs) in non-clinical individuals. In 353 healthy adults (155 males), we use partial least squares (PLS) to identify latent variables (LV) describing covariance between seven PLE questionnaire measures and functional connectivity estimated between each of six striatal seed regions and the rest of the brain using multiband resting-state fMRI. Hypothesis-driven PLS of the dorsal caudate (DC) seed identified one significant LV, accounting for 23.88% of covariance, with loadings from nearly all PLE subscales. Cortical regions implicated in this LV comprise anterior cingulate and left dorsolateral prefrontal cortex. Lower connectivity between these cortical areas and the DC seed was associated with more severe PLEs. Using multivariate modeling, we identified an association between dorsal CST connectivity and PLEs in the general community that implicates similar brain regions to those identified in patient groups. Our results highlight that the severity of both positive/negative symptom-like PLEs is related with functional coupling between the DC and dorsolateral PFC (prefrontal cortex), suggesting this neural circuit may play a role in mediating risk for general psychosis-related psychopathology.

Introduction

Psychotic symptoms can vary in severity along a continuum that extends from isolated unusual experiences to clinical disorders such as schizophrenia (Grant et al., 2018; Kelleher and Cannon, 2011; Poulton et al., 2000; Van Os et al., 1999). In the subclinical range, psychosis-like experiences (PLEs) (Unterrassner et al., 2017) are thought to represent attenuated forms of typical positive symptoms, such as hallucinations and delusions, but they can also include negative-like symptoms (Stefanis et al., 2002; Verdoux and van Os, 2002). PLEs are quite common in the general population, with a prevalence of up to 8% (Van Os et al., 2009). People reporting higher levels of PLEs are at increased risk of schizophrenia-spectrum disorders, suggesting that PLE severity may relate to one's vulnerability to clinical disorder (Kelleher and Cannon,2011). The potential for PLEs to index liability for psychosis has driven a growing interest in understanding subclinical symptoms in the general community (Ettinger et al., 2014; Grant et al., 2018; Tandon et al., 2012). Indeed, the continuum model is supported by behavioral, genetic, cognitive, and neuroimaging evidence of continuities between clinical and subclinical phenomena (Cannon et al., 2002; Ettinger et al., 2012; Lee et al., 2012; Poulton et al., 2000; Sabaroedin et al., 2019; Van Os et al., 2009). PLE severity in non-clinical samples correlates with variations in the structure and function of brain systems implicated in psychotic disorders (e.g., frontotemporal, default mode, cingulo-opercular systems)(Ettinger et al., 2012; Garrity et al., 2007; Satterthwaite et al., 2015; Sheffield et al., 2016), and with measures of the integrity of their interconnecting white matter pathways (Jacobson et al., 2010; Skudlarski et al., 2013).

Corticostriatal (CST) circuits have been identified as playing an important role in the emergence of psychotic symptoms. These circuits comprise topographic connections from prefrontal cortex to striatum, with feedback

loops passing through the pallidum and thalamus (Haber, 2016; Simpson et al., 2010). Two circuits implicated in psychosis include a ventral limbic system, which connects orbitofrontal cortex, medial prefrontal cortex, and limbic structures with the ventral striatum, and a dorsal associative system, which connects the dorsolateral prefrontal cortex with the dorsal striatum (Dandash et al., 2017; Draganski et al., 2008; Grace, 2016; Haber, 2016). The function of the striatum is heavily modulated by dopamine, and a series of reports indicate that this neurotransmitter is most strongly elevated in the dorsal striatum of patients with schizophrenia, their unaffected relatives, and individuals with an at-risk mental state (ARMS) for psychosis (Howes et al., 2009; Huttunen et al., 2008; Fusar-Poli, 2010). Studies of striatal functional connectivity have also found decreased functional coupling between the dorsolateral prefrontal cortex (PFC) and dorsal striatum in first-episode psychosis-patients, their unaffected first-degree relatives, and individuals with ARMS (Dandash et al., 2014; Fornito et al., 2013), as well as in first-episode mania patients with psychotic symptoms (Dandash et al., 2018). These lines of evidence suggest that dorsal CST connectivity may play a critical role in the emergence of psychotic symptoms across traditional diagnostic categories. Additionally, reduced dorsal CST coupling is correlated with the severity of positive and negative symptoms in ARMS individuals when the thalamus, rather than striatum, is used as a seed for connectivity analysis (Anticevic et al., 2015; Dandash et al., 2014; Fornito et al., 2013).

Complimenting findings in clinical samples, we recently reported evidence that functional connectivity of dorsal CST circuits correlated with the severity of PLEs in a non-clinical sample of healthy individuals living in the general community (Sabaroedin et al., 2019). PLEs were quantified using 12 subscales taken from 7 different questionnaires, and principal component analysis (PCA) was used to summarize the data, wherein two components described

shared variance between measures of (1) PLEs related to positive symptoms; and (2) PLEs related to negative symptoms. The analysis revealed that higher levels of positive PLEs were associated with lower functional connectivity between dorsal caudate and anterior cingulate cortex, and between dorsorostral putamen and dorsolateral prefrontal cortex. Although our findings in the non-clinical sample support a general involvement of dorsal CST circuitry across the psychosis spectrum, the spatial topography of the circuits correlating with PLEs diverged from the areas implicated in studies of clinical and high-risk groups (Dandash et al., 2017; Fornito et al., 2013; see also Figure 3 in Sabaroedin et al., 2019). More specifically, where dysconnectivity between the dorsal caudate and dorsolateral PFC has been consistently implicated in clinical samples (Dandash et al., 2017, 2014; Fornito et al., 2013), positive PLEs in the non-clinical sample were associated with functional connectivity between the dorsal caudate and anterior cingulate cortex. One potential reason for this discrepancy is that the dimension reduction of PLE subscales via PCA in the non-clinical group emphasized only common modes of shared variance across measures and may have masked correlations between functional connectivity and specific aspects of PLEs.

Here, we apply partial least squares (PLS) analysis to the same cohortstudied in Sabaroedin et al. (2019) to uncover latent dimensions describing covariance between corticostriatal functional connectivity and the 12 subscales used to measure PLEs. This analysis allows a fine-grained examination of the covariation between functional connectivity and PLE scores, thus providing a more complete picture of the relation between the two. We hypothesized that this approach would reveal an association between positive PLE severity and functional connectivity between the dorsal caudate and dorsolateral prefrontal cortex, thus mapping an association between brain and behavior that more closely aligns with the circuit implicated in clinical samples.

Materials and methods

Participants

Data were collected as a part of a larger genetics study that required participants to have all four grandparents of European descent. The 672 participants recruited (274 males; age range = 18–50 years old, mean [SD] age = 23.2 [4.89]) from the general community completed an online battery of PLEs measures. All participants had no personal history of psychiatric or neurological illness, no significant drug use and were right-handed. Each participant voluntarily confirmed his/her willingness to participate, providing written informed consent after having been informed of all aspects of the study. The study was conducted in accordance with the Monash University Human Research Ethics Committee (reference number 2,012,001,562). A total of 379 participants with complete PLEs measures underwent our resting-state fMRI protocol, with data for 353 participants (155 males; mean [SD] = 23.4 [5.16]) being retained for final analysis following exclusions for imaging artifacts, poor scan quality, and excessive head motion (see Sabaroedin et al., 2019 for details). Here, we present analyses of this final sample.

Measures of psychosis-like experiences

Seven psychometrically validated self-report measures of sub- threshold psychotic symptoms were used, allowing us to sample a wide range of variation in PLEs. The scales included the Community Assessment of Psychotic Experience (CAPE)(Mossaheb et al., 2012), four Chapman Scales (Chapman and Chapman, 1980) measuring magical ideation (Eckblad and Chapman, 1983), perceptual aberration (Chapman et al., 1978), and social and physical anhedonia (Chapman et al., 1976), the short-form Oxford Liverpool Inventory of Feelings and Experiences (sO-LIFE) (Fonseca-Pedrero et al., 2015) and the Peters Delusion Inventory (PDI-21)(Peters et al., 2004) (a complete description of the above measures can be found in the Supplemental Information). The battery produced a total of 272 items spanning 12 subscales. These subscales, the questionnaires from which they were derived, and descriptive statistics (n = 353) are listed in Table 1.

Neuroimaging data acquisition and pre-processing

For each participant we acquired multiband resting-state echo-planar images (EPI; 620 vol, 754 milliseconds repetition time, 3 mm isotropic voxels) and anatomical T1-weighted scans (1 mm isotropic voxels) using 3T Siemens Skyra MRI scanner equipped with a 32-channel head coil, located at the Monash Biomedical Imaging Facility, Melbourne, Australia.

A total of 620 functional volumes, each with 42 slices, were acquired per subject using an interleaved acquisition with the following parameters: repetition time (TR) of 754 milliseconds, echo time (TE) of 21 milliseconds, flip angle of 50°, multiband acceleration factor of 3, field of view (FOV) of 190 mm, slice thickness of 3 mm, and 3 mm isotropic voxels. For each subject were also acquired anatomical T1-weighted images using a 3-dimensional magnetic-prepared rapid gradient echo sequence. For each subject's T1-

weighted images, we acquired a total of 192 slices using an ascending acquisition with the following parameters: TR of 2300 milliseconds, TE of 2.07 milliseconds, flip angle of 9°, FOV of 256 mm, and voxel size of $1mm^3$.

Table 1.

PLE subscales and descriptive statistics (*n* = 353).

PLEs Subscales	Mean	SD
CAPE		
Positive	25.72	4.72
Negative	23.99	5.84
Depressive	13.84	2.97
Chapman		
Magical Ideation	6.11	4.61
Physical Anhedonia	11.81	7.19
Perceptual Aberration	5.12	5.17
Revised Social Anhedonia	9.64	6.78
sO-LIFE		
Unusual Experiences	2.89	2.65
Cognitive Disorganization	4.67	2.92
Introvertive Anhedonia	1.69	1.8
Impulsive Non-conformity	3.18	2.1
PDI Total Score	5.32	3.44
AGE		
	23.4	5.16
SEX	F	M
	198	155

CAPE: Community assessment of psychotic experiences; Chapman Scales; sO- LIFE: Oxford-Liverpool inventory of feelings and experiences short form; PDI: Peters delusion inventory.

The EPI images were processed using the following steps. First, we performed basic pre-processing in FSL FEAT (Woolrich et al., 2001), which includes removal of the first four volumes, rigid-body head motion correction, 3 mm spatial smoothing, and a highpass temporal filter (75 s cut-off). Second, artefactual and other noise components were removed from the data using FSL-FIX (Griffanti et al., 2014; Salimi-Khorshidi et al., 2014), which was trained using an independent dataset of 25 individuals scanned with identical imaging parameters. This independent component analysis-based denoising approach uses the training data to automatically classify noise components (signal contributions from head motion, sources of scanner and physiological noise, white matter, cerebrospinal fluid signals) for removal from the data. As nuisance regressors, we used i) the time courses of the components labelled as noise, ii) 6 standard head motion parameters (3 rotation, 3 translation) in addition to their squares and derivatives, iii) the averaged signal taken from a mask of the entire brain (i.e., a "global" signal) along with the first derivatives and squares of each. The denoised data were then spatially normalized to the MNI152 template via ANTs (version 2.2.0)(Avants et al., 2011) following a three-step method that comprised the registration of the mean realigned functional scan to the skull-stripped high resolution anatomical scan via rigid-body registration; spatial normalization of the anatomical scan to the MNI template via a nonlinear registration; and normalization of the functional scan to the MNI template using a single transformation matrix that concatenates the transforms generated from the precedent steps. The spatially normalized functional images were subsequently spatially smoothed with a 6 mm full-width half maximum Gaussian kernel using AFNI (version 16). In line with past work (Parkes et al., 2018), the data were subjected to rigorous quality control for motion artefacts after pre-processing, and residual motion contamination was minimal. Full details can be found in Sabaroedin et al. (2019).

Definition of seed regions of interest

As per past work (Dandash et al., 2014; Fornito et al., 2013; Sabar- oedin et al., 2019) we seeded six striatal regions-of-interest (ROI)(figure SF8) in each hemisphere using a 3.5 mm radius spheres, following the method proposed by Di Martino et al. (2008). Three ROIs were seeded along a dorsoventral axis for the caudate, comprising the dorsal caudate (DC; x = ± 13, y = 15, z = 9), the superior ventral caudate (x = ± 10, y = 15, z = 0), and the inferior ventral caudate/nucleus accumbens (x = ± 9, y = 9, z = - 8). For the putamen, we seeded three ROIs along a similar axis, incorporating the dorso-caudal putamen (DCP; x = ± 28, y= 1, z = 3), the dorso-rostral putamen (DRP; x = ± 25, y = 8, z = 6), and the ventro-rostral putamen (VRP; x = ± 20, y = 12, z = - 3). The dorsal CST seeds incorporate DC, DRP, and DCP. The ventral CST seeds encompass the inferior ventral caudate/nucleus accumbens, superior ventral caudate, and VRP. We used the mean time series of each region to generate seed-related functional connectivity maps.

Functional connectivity analysis

As described in past work (Dandash et al., 2014; Sabaroedin et al., 2019), subject specific first-level analysis was performed using SPM8. For each subject, whole-brain functional connectivity maps of each striatal ROI were estimated by entering the time series from the six striatal ROIs into a general linear model. Left and right hemispheres were modelled separately, yielding a pair of functional connectivity maps for each striatal ROI. The unthresholded contrast images for both hemispheres were then entered into a PLS analysis.

PLS analysis

PLS is a multivariate statistical technique that combines PCA-style dimensionality reduction with linear regression. First introduced to functional neuroimaging by McIntosh et al. (1996), it is well-suited to uncovering multivariate associations between brain imaging and behavioral measures (Krishnan et al., 2011). The analysis examines the covariation among two or more "blocks" of variables (McIntosh et al.,1996). In our case, the blocks represent seed-related functional connectivity and PLEs scores, and the final aim is to obtain a new set of variates that represent linear combinations of each block's variables that maximally covary with each other.

In this study we used the Regular Behavior PLS analysis implemented in PLS toolbox (McIntosh et al., 1996) written in Matlab (The Math- Works, Inc., Natick, Massachusetts, US), to analyze the relationship between the 12 PLEs subscales, age and sex, and striatal functional connectivity. We ran a separate PLS analysis for each seed region, including the maps for left and right seed-related FC (functional connectivity) as different conditions (left: condition 1, right: condition 2). The PLS approach we used here is outlined in detail in (Krishnan et al., 2011; McIntosh et al., 1996). We started with two sets of variables, represented respectively by: (i) seed-to-brain functional connectivity maps; and (ii) PLE subscale scores, with the nuisance covariates age and sex. The sets of variables were organized in two different matrices: X for the brain activity and Y for behavioral and demographic data (age and sex). The matrix X consists of i observations and j voxels, where each voxel encodes functional connectivity with a given seed region. Voxels are ordered such that all left hemisphere voxels are listed first, followed by all right hemisphere voxels, representing two conditions in the PLS. The matrix Y consists of i observations and k behavioural measures and (optionally)

nuisance covariates. The two matrices were centered and normalized within each condition, and a matrix of correlations was computed separately for each condition. The two condition matrices of correlations were combined into a single matrix referred as the cross-block correlation matrix R, which contains the correlation of each of the *j* voxels in X with each of the *k* behavioural/demographic measures in Y, within each of the conditions.

The cross-block correlation matrix R was subjected to a singular value decomposition (SVD), which produced a set of independent (orthogonal) latent variables (LV) / singular vector pairs. Each pair is associated with a singular value that reflects the covariance between the paired LVs (i.e., the functional connectivity LV, comprising brain scores, and the PLE, or behavioral LV), ranked by the proportion of squared cross-block covariance explained. Each LV constitutes a distinct weighted pattern of functional connections and PLE subscale scores that covary, in an ideal manner, with each other. One member of an LV pair is composed of saliences/weights corresponding to each measure in the functional connectivity block, and the other member is composed of saliences for each measure in the behavioral measures block. Thus, saliences quantify how specific voxels/variables load on a given LV. The statistical significance of each LV is determined using permutation tests (Krishnan et al., 2011). The resulting p-values quantify the fraction of times the permuted singular values exceeded the observed singular values. In our study, we used 5000 permutations, performed by randomly reordering the rows of the original data matrix X. As our primary hypothesis concerned the dorsal caudate, LVs in this analysis were declared statistically significant at $p < 0.05$. All other results were declared significant if they survived Bonferroni-correction over the six seeds ($p < 0.008$).

We also assessed the reliability of brain saliences (voxel weights on the brain LV) via bootstrapping (Krishnan et al., 2011). A total of 1000 bootstrap samples were obtained by randomly resampling with replacement the X

matrix within each condition. The SVD was then performed on the resampled data matrices to generate new saliences (weights) which were projected into the space of the original analysis and used to estimate the standard error of each weight, representing a measure of stability. For each voxel, we then calculate a bootstrap ratio (BSR) by dividing the weight from the singular vector by its bootstrap-estimated standard error. The BSR ratio is considered equivalent to a z-score when the bootstrap distribution is approximately normal (Efron & Tibshirani, 1986), and if the ratio of a salience value to its standard error is greater than 2, the salience is considered reliable. The BSR ratio results are thresholded, by default, at values corresponding to the 95% confidence interval. The resulting voxelwise BSR maps may thus reveal voxels in which functional connectivity with the seed region contributed strongly and reliably to the multivariate pattern identified in a given LV. Permutation testing and bootstrapping ensured robustness and avoided over-fitting.

Results

We applied PLS to explain the covariance between left and right striatal seed-related FC and 14 behavioral/demographic measures, comprising 12 PLEs subscales, age, and sex. A separate PLS was run for each of the six seeds, with hemisphere included as a condition within each analysis (left, condition 1; right, condition 2).

Associations between dorsal caudate functional connectivity and PLEs

Our hypothesis-driven PLS analysis of the DC seed identified LV1 as statistically significant, accounting for 23.88% of cross-block covariance, with

a singular value of 56.94 and p = .019 (see Supplemental SF1). Fig. 1a shows that this LV pair was characterized by uniform loadings across nearly all PLE subscales on both left and right DC-related FC, with minimal contributions from age and sex. There was some evidence for lower contributions from negative PLE scales; namely, the CAPE negative and Chapman social and physical anhedonia scales, and sO-LIFE introvertive anhedonia. However, the 95% confidence intervals of the correlations between these scales and brain scores on LV1 did not cross zero, suggesting that they still make a significant contribution. Thus, this LV describes an association between DC-related FC and general PLE severity. Across all PLE scales, more severe experiences were associated with lower brain scores. Example scatterplots for two representative positive and negative PLE scales are shown in Supplemental Figure SF2. Fig. 1b shows the bootstrap image obtained from the PLS analysis, which maps voxels that reliably contribute to the significant LV (see ST1 for cluster sizes and peak coordinates for the maps in panel 1b). In other words, this map identifies voxels where functional connectivity with the DC seed is associated with the multivariate profile of PLE subscale scores shown in Fig. 1a.

The pattern is strongly expressed in the caudal and rostral anterior cingulate cortex, medial prefrontal cortex, left dorsolateral prefrontal cortex and dorsomedial thalamus, right pallidum, and posterior right cerebellum. These brain regions express a negative correlation between PLEs scores and DC-related FC; i.e., higher scores on PLE scales are associated with lower FC. This pattern is reversed in areas of bilateral occipital and parietal cortex, where higher PLEs scores are associated with higher DC-related FC (see Fig. 1, panel b).

Associations between PLEs and the functional connectivity of other striatal seed regions

No other LVs passed our Bonferroni-corrected threshold for significance (α= 0.008) when considering the remaining striatal seed regions (i.e., dcPT, drPT, vrPT, VSi, VSs). Three LVs, all involving the putamen, surpassed a p<.05, uncorrected threshold: two LVs were related to the dcPT seed and one LV was related to the vrPT seed.

The two dcPT-related seeds accounted for 59.5% and 46.7% of the cross-block covariance (p = .005 and p = .048, respectively; Figure SF3). The first LV shows comparable PLEs loadings across both hemispheres, with a behavioral profile characterized by similar loadings across most positive PLEs subscales, with attenuated loadings for anhedonia-related and CAPE negative scales (Figure SF4, panel a). The bootstrap ratio map revealed reliable contributions from dcPT-related FC in anterior and posterior cingulate cortices, dorsolateral prefrontal cortex, right superior parietal cortex, visual cortices, pallidum, and bilateral cerebellum (Figure SF4, panel b, ST2). LV2 for the dcPT seed described a profile in which negative PLEs scales consistently loaded on both left and right seed-related FC, whereas positive PLE scales showed smaller correlations which were negative in the left and positive in the right hemisphere (Figure SF5, panel a). The bootstrap ratio image identified reliable contributions from voxels in left medial prefrontal cortex, right orbitofrontal cortex, dorsal anterior and ventral posterior cingulate cortex, thalamus, sensorimotor cortex, right paracentral lobule, and right cerebellum (Figure SF5, panel b, ST3).

The vrPT-related LV accounted for 22.5% of the cross-block covariance (p = .043; Figure SF6). It was characterized by higher loadings from positive PLEs scales, particularly for right-hemisphere seed-related FC (Figure SF7, panel a). Voxels contributing reliably to this pattern were located in orbitofrontal right cortex, mid-cingulate cortex, medial prefrontal and dorsolateral

prefrontal cortices, inferior precentral sulcus and visual and somatosensory cortex (see SF7, panel b, ST4).

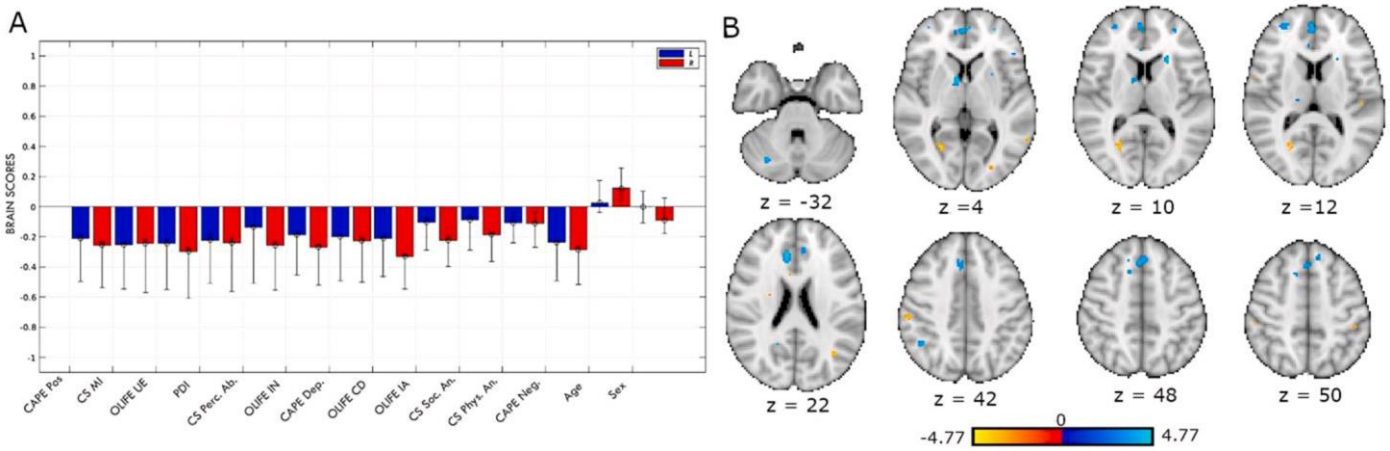

Fig. 1. Latent variable linking dorsal caudate functional connectivity and PLEs. A: Correlations between each PLE subscale, age, sex, and brain scores for LV1 in the PLS of dorsal caudate functional connectivity. Error bars represent 95% confidence intervals. The intervals do not cross zero for any PLEs scale; therefore, this LV contains significant loadings from all PLEs measures. Blue: left DC seed-related FC; Red: right DC seed-related FC. B: Axial slices through the bootstrap image showing regions reliably contributing to LV1. Cool colors identify regions where DC-related functional connectivity was associated with the multivariate profile depicted in panel A (i.e., higher functional connectivity was associated with lower scores); warm colors show the opposite. Left hemisphere is on the left. CAPE: community assessment of psychotic experience; sO-LIFE: Oxford-Liverpool Inventory of feelings and experiences short-form. PDI: Peters delusion inventory.

Discussion

Corticostriatal abnormalities are apparent from the earliest stages of psychosis, with patients, their unaffected-relatives, and ARMS individuals showing similar changes, suggesting that dorsal CST dysfunction may represent a risk phenotype for psychotic disorders (Dandash et al., 2017; Fornito et al., 2013). Dysconnectivity of dorsal CST circuitry also correlates with symptom severity in patient groups (Dandash et al., 2014; Fornito et al.,

2013) and subclinical variation in positive PLEs in a healthy community sample (Sabaroedin et al., 2019), although the specific regions implicated in the PLE analysis differed from those identified in clinical samples. Here, we applied PLS to identify multivariate associations between 12 PLE measures and CST FC in a non-clinical sample. We found that functional connectivity of the dorsal caudate was associated with PLE severity across both positive-like and negative-like symptom domains, with PLS identifying a significant LV with comparable loadings from all PLE subscales. Critically, the cortical regions implicated in this DC-related LV include regions of anterior cingulate cortex, as per the results of our prior univariate analysis in this sample (Sabaroedin et al., 2019), as well as areas of left dorsolateral PFC, which more closely align with areas implicated as dysfunctional in clinical samples. Paralleling the clinical findings, lower FC between these cortical areas and the DC seed was associated with more severe PLEs in the current study. A summary of the anatomical consistency of the circuits implicated in the current work and past studies of clinical cohorts is provided in Fig. 2.

These results suggest that dorsal circuit FC tracks symptom severity across a wide spectrum of clinical and subclinical severity, and that the spatial correspondence between the specific circuit elements involved is closer than suggested in Sabaroedin et al. (2019) analysis. Indeed, it seems that these earlier results, which did not implicate dorsolateral PFC, may have been driven by the different analysis method used, in which PLE scales were subjected to a PCA before being correlated with FC. In this way, the approach of Sabaroedin et al. mapped areas associated with common dimensions of variance specifically in positive PLE scores. The present findings indicate that DC-dorsolateral PFC FC is implicated when considering a dimension of variance common across all PLE scales, encompassing both positive-like and negative-like symptoms. It may thus be related to a more generalized component of schizophrenia risk. Consistent with this view, work in first

episode patients has reported that functional connectivity between the DC and left dorsolateral PFC is associated with the severity of both positive and negative symptoms (Fornito et al., 2013). Given that the LV identified in our analysis of DC-related functional connectivity included comparable loadings across all scales, it is possible that the multivariate FC profile identified in this analysis is associated with a more general psychopathology factor, sometimes referred to as the p-factor (Caspi and Moffitt, 2018). A more comprehensive investigation of non-psychosis-like symptoms would thus help to determine the specificity of our findings. We also found suggestive evidence for associations between the FC of other striatal seeds and PLE severity. Again, the dorsal circuit was pre- dominant, two LVs were identified for the dcPT and only one implicated the ventral system. The associations between dorsocaudal putamen FC and PLE severity involved areas that have been identified as dysfunctional in patients, such as orbitofrontal cortex and thalamus, pallidum, anterior cingulate cortex, and dorsal prefrontal cortex (Fornito et al., 2013, 2011, 2008; Haber and Knutson, 2010; Reid et al., 2010; White et al., 2010; Woodward and Heckers, 2016) as well as sensorimotor and visual cortices. The cortical regions implicated in the vrPT-related associations with PLE severity included regions of mid-cingulate cortex, the orbitofrontal cortex, medial and dorsolateral prefrontal cortex, and motor cortex, which have also been implicated in clinical reports (Abboud et al., 2017; Asemi et al., 2015; Walther and Strik, 2012). Lower functional connectivity between the vrPT and sensorimotor cortices was tied to greater severity of both positive and negative-like PLEs; the other areas expressed the opposite pattern, such that increased functional connectivity with vrPT was associate with higher PLE scores. We note however that these LVs did not survive correction for multiple comparisons and require replication.

Our findings are consistent with a continuum of risk for schizophrenia-like symptoms, in which symptom expression, across a broad spectrum of

severity, is related to dorsal CST function. Functional coupling between the DC and dorsolateral PFC was related to the severity of both positive symptom- and negative symptom-like PLEs, suggesting that this neural circuit may be tied to risk for general schizophrenia-like psychopathology.

Limitations

The majority of participants in our sample (~ 90%) had not yet completed the peak period of risk for schizophrenia at the time of testing. Given that psychotic experiences in early adulthood can predict later psychopathology (Rossler et al., 2007; Werbeloff et al., 2012), some of the subjects analyzed may develop a clinical disorder at a later time. Furthermore, our exclusion of individuals with a history of mental health treatment guaranteed that we were sampling the subclinical range of symptom expression, but it may neglect the more severe end of the PLE spectrum.

Due to our multivariate approach, we cannot draw inferences about single behaviors or voxels, because the optimization in PLS is conducted on the entire data matrix rather than individual behavior and voxels. As such, interpretation of associations between individual variables is restricted to the broader context of the multivariate pattern to which they belong.

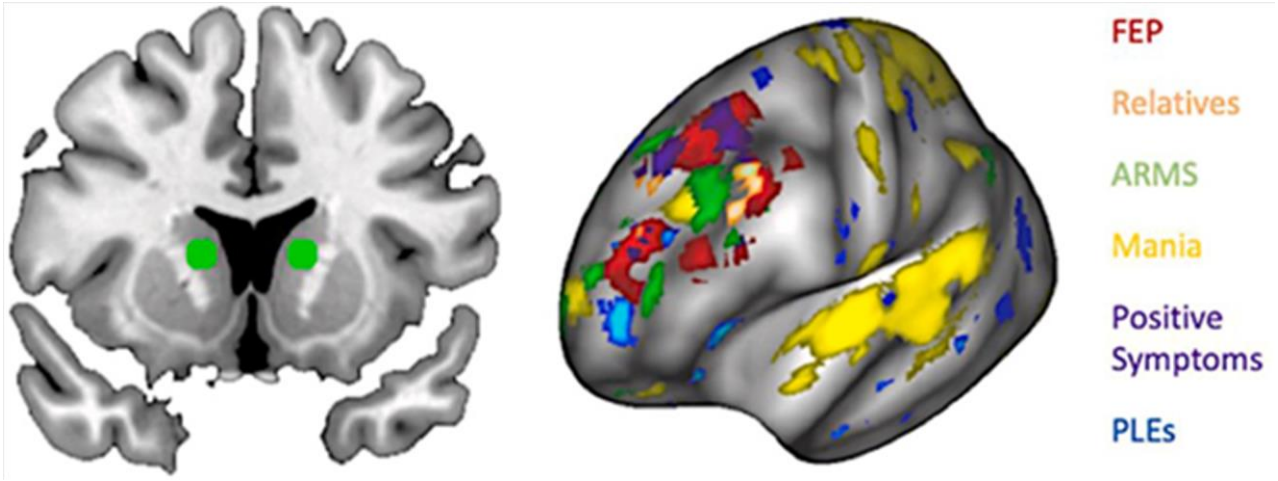

Fig. 2. Spatial consistency of dorsal corticostriatal circuit involvement across a broad spectrum of psychosis severity. The coronal slice on the left shows the location of the dorsal caudate (DC) seed region. The cortical surface map on the right depicts the area of dorsolateral prefrontal cortex where seed-related functional connectivity correlates with PLE severity in our community sample, together with prefrontal areas implicated in past work conducted in patients with first-episode psychosis and their first-degree relatives (Fornito et al., 2013), ARMS individuals (Dandash et al., 2014), first episode mania patients with psychosis (Dandash et al., 2018). The map of positive symptoms maps regions associated with positive symptom severity in first episode psychosis patients (Fornito et al., 2013).

Supplementary materials

Supplementary material associated with this article can be found, in the online version, at doi:10.1016/j.pscychresns.2020.111202.

References

Abboud, R., Noronha, C., Diwadkar, V.A., 2017. Motor system dysfunction in the schizophrenia diathesis: neural systems to neurotransmitters. Eur. Psychiatry. https://doi.org/10.1016/j.eurpsy.2017.04.004.

Anticevic, A., Haut, K., Murray, J.D., Repovs, G., Yang, G.J., Diehl, C., McEwen, S.C., Bearden, C.E., Addington, J., Goodyear, B., Cadenhead, K.S., Mirzakhanian, H., Cornblatt, B.A., Olvet, D., Mathalon, D.H., McGlashan, T.H., Perkins, D.O.,

Belger, A., Seidman, L.J., Tsuang, M.T., Van Erp, T.G.M., Walker, E.F., Hamann, S., Woods, S.W., Qiu, M., Cannon, T.D., 2015. Association of thalamic dysconnectivity and conversion to psychosis in youth and young adults at elevated clinical risk.

JAMA Psychiatry. https://doi.org/10.1001/jamapsychiatry.2015.0566.

Asemi, A., Ramaseshan, K., Burgess, A., Diwadkar, V.A., Bressler, S.L., 2015. Dorsal anterior cingulate cortex modulates supplementary motor area in coordinated unimanual motor behavior. Front. Hum. Neurosci. https://doi.org/10.3389/fnh um.2015.00309.

Avants, B.B., Tustison, N.J., Song, G., Cook, P.A., Klein, A., Gee, J.C., 2011.

A reproducible evaluation of ANTs similarity metric performance in brain image registration. Neuroimage. https://doi.org/10.1016/j.neuroimage.2010.09.025.

Cannon, T.D., Van Erp, T.G.M., Glahn, D.C., 2002. Elucidating continuities and discontinuities between schizotypy and schizophrenia in the nervous system. Schizophrenia Research. https://doi.org/10.1016/S0920-9964(01)00362-0.

Caspi, A., Moffitt, T.E., 2018. All for one and one for all: mental disorders in one dimension. Am. J. Psychiatry. https://doi.org/10.1176/appi.ajp.2018.17121383.

Chapman, L.J., Chapman, J.P., 1980. Scales for rating psychotic and psychotic-like experiences as continua. Schizophr. Bull. https://doi.org/10.1093/schbul/6.3.476.

Chapman, L.J., Chapman, J.P., Raulin, M.L., 1978. Body image aberration in schizophrenia. J. Abnorm. Psychol. 87, 399–407. https://doi.org/10.1037// 0021-843X.87.4.399.

Chapman, L.J., Chapman, J.P., Raulin, M.L., 1976. Scales for physical and social anhedonia. J. Abnorm. Psychol. https://doi.org/10.1037/0021-843X.85.4.374.

Dandash, O., Fornito, A., Lee, J., Keefe, R.S.E., Chee, M.W.L., Adcock, R.A., Pantelis, C., Wood, S.J., Harrison, B.J., 2014. Altered striatal functional connectivity in subjects with an at-risk mental state for psychosis. Schizophr. Bull. https://doi.org/10.1093/ schbul/sbt093.

Dandash, O., Pantelis, C., Fornito, A., 2017. Dopamine, fronto-striato-thalamic circuits and risk for psychosis. Schizophr. Res. https://doi.org/10.1016/j.schres.2016.08.0 20.

Dandash, O., Yücel, M., Daglas, R., Pantelis, C., McGorry, P., Berk, M., Fornito, A., 2018.

Differential effect of quetiapine and lithium on functional connectivity of the striatum in first episode mania. Transl. Psychiatry. https://doi.org/10.1038/s413 98-018-0108-8.

Di Martino, A., Scheres, A., Margulies, D.S., Kelly, A.M.C., Uddin, L.Q., Shehzad, Z., Biswal, B., Walters, J.R., Castellanos, F.X., Milham, M.P., 2008. Functional connectivity of human striatum: a resting state fMRI study. Cereb. Cortex. https:// doi.org/10.1093/cercor/bhn041.

Draganski, B., Kherif, F., Kloppel, S., Cook, P.A., Alexander, D.C., Parker, G.J.M., Deichmann, R., Ashburner, J., Frackowiak, R.S.J., 2008. Evidence for Segregated and Integrative Connectivity Patterns in the Human Basal Ganglia. J. Neurosci. https://doi.org/10.1523/jneurosci.1486-08.2008.

Eckblad, M., Chapman, L.J., 1983. Magical ideation as an indicator of schizotypy.J. Consult. Clin. Psychol. 51, 215–225. https://doi.org/10.1037/0022-006X.51.2.215.

Ettinger, U., Meyho¨fer, I., Steffens, M., Wagner, M., Koutsouleris, N., 2014. Genetics, cognition, and neurobiology of schizotypal personality: a review of the overlap with schizophrenia. Front. Psychiatry. https://doi.org/10.3389/fpsyt.2014.00018.

Ettinger, U., Williams, S.C.R., Meisenzahl, E.M., Mo¨ller, H.J., Kumari, V.,Koutsouleris, N., 2012. Association between brain structure and psychometric schizotypy in healthy individuals. World J. Biol. Psychiatry. https://doi.org/10.310 9/15622975.2011.559269.

Fonseca-Pedrero, E., Ortun˜o-Sierra, J., Mason, O.J., Mun˜iz, J., 2015. The Oxford-Liverpool Inventory of Feelings and Experiences short version: further validation. Pers. Individ. Dif. https://doi.org/10.1016/j.paid.2015.06.041.

Fornito, A., Harrison, B.J., Goodby, E., Dean, A., Ooi, C., Nathan, P.J., Lennox, B.R., Jones, P.B., Suckling, J., Bullmore, E.T., 2013. Functional dysconnectivity of corticostriatal circuitry as a risk phenotype for psychosis. JAMA Psychiatry. http s://doi.org/10.1001/jamapsychiatry.2013.1976.

Fornito, A., Radua, J., Walterfang, M., Seal, M., Wood, S.J., Yucel, M., Velakoulis, D., Pantelis, C., 2011. Neuroanatomical abnormalities in schizophrenia: a multimodal voxelwise meta-analysis and meta-regression analysis. Schizophr. Res.

Fornito, A., Yücel, M., Wood, S.J., Adamson, C., Velakoulis, D., Saling, M.M., McGorry, P. D., Pantelis, C., 2008. Surface-based morphometry of the anterior cingulate cortex in first episode schizophrenia. Hum. Brain Mapp. https://doi.org/10.1002/hbm.20412.

Fusar-Poli, P., et al., 2010. Abnormal frontostriatal interactions in people with prodromal signs of psychosis: a multimodal imaging study. Arch. Gen. Psychiatry. https://doi.org/10.1001/archgenpsychiatry.2010.77.

Garrity, A.G., Pearlson, G.D., McKiernan, K., Lloyd, D., Kiehl, K.A., Calhoun, V.D., 2007. Aberrant "default mode" functional connectivity in schizophrenia. Am. J. Psychiatry. https://doi.org/10.1176/ajp.2007.164.3.450.

Grace, A.A., 2016. Dysregulation of the dopamine system in the pathophysiology of schizophrenia and depression. Nat. Rev. Neurosci. https://doi.org/10.1038/nr n.2016.57.

Grant, P., Green, M.J., Mason, O.J., 2018. Models of Schizotypy: the Importance of Conceptual Clarity. Schizophr. Bull. https://doi.org/10.1093/schbul/sby012.

Griffanti, L., Salimi-Khorshidi, G., Beckmann, C.F., Auerbach, E.J., Douaud, G., Sexton, C. E., Zsoldos, E., Ebmeier, K.P., Filippini, N., Mackay, C.E., Moeller, S., Xu, J., Yacoub, E., Baselli, G., Ugurbil, K., Miller, K.L., Smith, S.M., 2014. ICA-based artefact removal and accelerated fMRI acquisition for improved resting state network imaging. Neuroimage. https://doi.org/10.1016/j.neuroimage.2014.03.034.

Haber, S.N., 2016. Corticostriatal circuitry. Neuroscience in the 21st Century: From Basic to Clinical, 2nd Edition. https://doi.org/10.1007/978-1-4939-3474-4_135.

Haber, S.N., Knutson, B., 2010. The reward circuit: linking primate anatomy and human imaging. Neuropsychopharmacology. https://doi.org/10.1038/npp.2009.129.

Howes, O.D., Montgomery, A.J., Asselin, M.C., Murray, R.M., Valli, I., Tabraham, P., Bramon-Bosch, E., Valmaggia, L., Johns, L., Broome, M., McGuire, P.K., Grasby, P. M., 2009. Elevated striatal dopamine function linked to prodromal signs of schizophenia. Arch. Gen. Psychiatry. https://doi.org/10.1001/archgenpsychiatry.2008.514.

Huttunen, J., Heinimaa, M., Svirskis, T., Nyman, M., Kajander, J., Forsback, S., Solin, O., Ilonen, T., Korkeila, J., Ristkari, T., McGlashan, T., Salokangas, R.K.R., Hietala, J., 2008. Striatal Dopamine Synthesis in First-degree Relatives of Patients with Schizophrenia. Biol. Psychiatry. https://doi.org/10.1016/j.biopsych.2007.04.017.

Jacobson, S., Kelleher, I., Harley, M., Murtagh, A., Clarke, M., Blanchard, M., Connolly, C., O'Hanlon, E., Garavan, H., Cannon, M., 2010. Structural and functionalbrain correlates of

subclinical psychotic symptoms in 11-13 year old schoolchildren. Neuroimage. https://doi.org/10.1016/j.neuroimage.2009.09.015.

Kelleher, I., Cannon, M., 2011. Psychotic-like experiences in the general population: characterizing a high-risk group for psychosis. Psychol. Med. https://doi.org/10.101 7/S0033291710001005.

Krishnan, A., Williams, L.J., McIntosh, A.R., Abdi, H., 2011. Partial Least Squares (PLS) methods for neuroimaging: a tutorial and review. Neuroimage. https://doi.org/10. 1016/j.neuroimage.2010.07.034.

Lee, S.H., Decandia, T.R., Ripke, S., Yang, J., Sullivan, P.F., Goddard, M.E., Keller, M.C., Visscher, P.M., Wray, N.R., 2012. Estimating the proportion of variation in susceptibility to schizophrenia captured by common SNPs. Nat. Genet. https://doi. org/10.1038/ng.1108.

McIntosh, A.R., Bookstein, F.L., Haxby, J.V., Grady, C.L., 1996. Spatial pattern analysis of functional brain images using partial least squares. Neuroimage. https://doi. org/10.1006/nimg.1996.0016.

Mossaheb, N., Becker, J., Schaefer, M.R., Klier, C.M., Schloegelhofer, M., Papageorgiou, K., Amminger, G.P., 2012. The Community Assessment of Psychic Experience (CAPE) questionnaire as a screening-instrument in the detection of individuals at ultra-high risk for psychosis. Schizophr. Res. https://doi.org/10.10 16/j.schres.2012.08.008.

Parkes, L., Fulcher, B., Yücel, M., Fornito, A., 2018. An evaluation of the efficacy, reliability, and sensitivity of motion correction strategies for resting-state functional MRI. Neuroimage. https://doi.org/10.1016/j.neuroimage.2017.12.073.

Peters, E., Joseph, S., Day, S., Garety, P., 2004. Measuring delusional ideation: the 21-Item Peters et al. Delusions Inventory. Schizophr. Bull. 30, 1005–1022. https://doi. org/10.1037/t03329-000.

Poulton, R., Caspi, A., Moffitt, T.E., Cannon, M., Murray, R., Harrington, H., 2000.Children's self-reported psychotic symptoms and adult schizophreniform disorder: a 15-year longitudinal study. Arch. Gen. Psychiatry.

Reid, M.A., Stoeckel, L.E., White, D.M., Avsar, K.B., Bolding, M.S., Akella, N.S., Knowlton, R.C., Den Hollander, J.A., Lahti, A.C., 2010. Assessments of function and biochemistry of the anterior cingulate cortex in schizophrenia. Biol. Psychiatry. https://doi.org/10.1016/j.biopsych.2010.04.013.

Ro¨ssler, W., Riecher-Ro¨ssler, A., Angst, J., Murray, R., Gamma, A., Eich, D., van Os, J.,Gross, V.A., 2007. Psychotic experiences in the general population: a twenty-year prospective community study. Schizophr. Res. https://doi.org/10.1016/j.schres.200 7.01.002.

Sabaroedin, K., Tiego, J., Parkes, L., Sforazzini, F., Finlay, A., Johnson, B., Pinar, A., Cropley, V., Harrison, B.J., Zalesky, A., Pantelis, C., Bellgrove, M., Fornito, A., 2019. Functional Connectivity of Corticostriatal Circuitry and Psychosis-Like Experiences in the General Community. Biol. Psychiatry. https://doi.org/10.1016/j.biopsych.2019.02.013.

Salimi-Khorshidi, G., Douaud, G., Beckmann, C.F., Glasser, M.F., Griffanti, L., Smith, S. M., 2014. Automatic denoising of functional MRI data: combining independent component analysis and hierarchical fusion of classifiers. Neuroimage. https://doi. org/10.1016/j.neuroimage.2013.11.046.

Satterthwaite, T.D., Vandekar, S.N., Wolf, D.H., Bassett, D.S., Ruparel, K., Shehzad, Z., Craddock, R.C., Shinohara, R.T., Moore, T.M., Gennatas, E.D., Jackson, C., Roalf, D. R., Milham, M.P., Calkins, M.E., Hakonarson, H., Gur, R.C., Gur, R.E., 2015.Connectome-wide network analysis of youth with Psychosis-Spectrum symptoms. Mol. Psychiatry. https://doi.org/10.1038/mp.2015.66.

Sheffield, J.M., Kandala, S., Burgess, G.C., Harms, M.P., Barch, D.M., 2016. Cingulo- opercular Network Efficiency Mediates the Association Between Psychotic-like Experiences and Cognitive Ability in the General Population. Biol. Psychiatry Cogn. Neurosci. Neuroimaging. https://doi.org/10.1016/j.bpsc.2016.03.009.

Simpson, E.H., Kellendonk, C., Kandel, E., 2010. A Possible Role for the Striatum in the Pathogenesis of the Cognitive Symptoms of Schizophrenia. Neuron. https://doi.org/10.1016/j.neuron.2010.02.014.

Skudlarski, P., Schretlen, D.J., Thaker, G.K., Stevens, M.C., Keshavan, M.S., Sweeney, J. A., Tamminga, C.A., Clementz, B.A., O'Neil, K., Pearlson, G.D., 2013. Diffusion tensor imaging white matter endophenotypes in patients with schizophrenia or psychotic bipolar disorder and their relatives. Am. J. Psychiatry. https://doi.org/1 0.1176/appi.ajp.2013.12111448.

Stefanis, N.C., Hanssen, M., Smirnis, N.K., Avramopoulos, D.A., Evdokimidis, I.K., Stefanis, C.N., Verdoux, H., Van Os, J., 2002. Evidence that three dimensions of psychosis have a distribution in the general population. Psychol. Med. https://doi. org/10.1017/S0033291701005141.

Tandon, N., Montrose, D., Shah, J., Rajarethinam, R.P., Diwadkar, V.A., Keshavan, M.S., 2012. Early prodromal symptoms can predict future psychosis in familial high-risk youth. J. Psychiatr. Res. https://doi.org/10.1016/j.jpsychires.2011.09.019.

Unterrassner, L., Wyss, T.A., Wotruba, D., Ajdacic-Gross, V., Haker, H., Ro¨ssler, W.,2017. Psychotic-like experiences at the healthy end of the psychosis continuum. Front. Psychol. https://doi.org/10.3389/fpsyg.2017.00775.

Van Os, J., Linscott, R.J., Myin-Germeys, I., Delespaul, P., Krabbendam, L., 2009.A systematic review and meta-analysis of the psychosis continuum: evidence for a psychosis proneness-

persistence-impairment model of psychotic disorder. Psychol. Med. https://doi.org/10.1017/S0033291708003814.

Van Os, J., Verdoux, H., Maurice-Tison, S., Gay, B., Liraud, F., Salamon, R., Bourgeois, M., 1999. Self-reported psychosis-like symptoms and the continuum of psychosis. Soc. Psychiatry Psychiatr. Epidemiol.

Verdoux, H., van Os, J., 2002. Psychotic symptoms in non-clinical populations and the continuum of psychosis. Schizophr. Res.

Walther, S., Strik, W., 2012. Motor symptoms and schizophrenia. Neuropsychobiology. https://doi.org/10.1159/000339456.

Werbeloff, N., Drukker, M., Dohrenwend, B.P., Levav, I., Yoffe, R., Van Os, J., Davidson, M., Weiser, M., 2012. Self-reported attenuated psychotic symptoms as forerunners of severe mental disorders later in life. Arch. Gen. Psychiatry. http s://doi.org/10.1001/archgenpsychiatry.2011.1580.

White, T.P., Joseph, V., Francis, S.T., Liddle, P.F., 2010. Aberrant salience network (bilateral insula and anterior cingulate cortex) connectivity during information processing in schizophrenia. Schizophr. Res. https://doi.org/10.1016/j.schres.2010.07.020.

Woodward, N.D., Heckers, S., 2016. Mapping Thalamocortical Functional Connectivity in Chronic and Early Stages of Psychotic Disorders. Biol. Psychiatry. https://doi. org/10.1016/j.biopsych.2015.06.026.

Woolrich, M.W., Ripley, B.D., Brady, M., Smith, S.M., 2001. Temporal autocorrelation in univariate linear modeling of FMRI data. Neuroimage. https://doi.org/10.1006/nimg.2001.0931.

PART IV

Periodic and aperiodic component of EEG power spectra: application on sleep-disorders.

CHAPTER 8

Sleep-related hypermotor epilepsy (SHE) and non-rapid eye movement (NREM) parasomnias: differences in the periodic and aperiodic component of the EEG power spectra.

Pani S.M.

Fraschini M.

Figorilli M.

Taburrino L.

Puligheddu M.

Abstract accepted for oral presentation at XXXIII AIMS (Italian Association of Sleep Medicine) National Conference, 25-27 October 2020.

Abstract

Over the last two decades our understanding of clinical and pathophysiological aspects of sleep-related epileptic and non-epileptic paroxysmal behaviours has improved considerably, although it is far from complete. Indeed, even though many of Sleep-Related Hypermotor Epilepsy (SHE) and of non-rapid eye movement (NREM) parasomnias core characteristics have been clarified, some crucial points remain controversial, and the overlap of the behavioral patterns among the disorders represents a diagnostic challenge. In this work we focused on nocturnal sleep (videolab-recording scalp EEG, 19 channels) free of clinical episodes from two groups of patients affected respectively by SHE (N = 15) and NREM parasomnias (N = 16). We examined N2 and N3 stages of the first part of the night (cycle 1 and 2), and investigated the existence of differences in the periodic and aperiodic component of the EEG power spectra between the two groups using the Fitting Oscillations &One Over f (FOOOF) toolbox. The results of this study show a significant difference in the gamma frequency band, with an increased basic high frequency component in SHE patients, in both N2 ($U = 34$, $p < 0.001$) and N3 stages ($U = 24$, $p < 0.001$) , and a significant higher slope for the NREM parasomnias compared with SHE, in N3 stage ($U = 57.0$, $p = 0.012$). We hypothesize that the slope extracted from the aperiodic component of the EEG signal may be helpful to distinguish characterize differences between subjects affected by NREM parasomnias and those affected by SHE.

Introduction

Non-rapid eye movement (NREM) parasomnias are sleep disorders with a peculiar association with slow wave sleep (SWS), arising typically from N3 sleep, and occasionally from N2 sleep. Common during both childhood and adulthood, NREM parasomnias are defined as abnormal behaviours and physiological events stemming outside of consciousness, and they encompass: confusional arousals, sleepwalking and night terrors, also called 'disorders of arousal', as well as lesser-known entities as sleep-related eating disorder, sexsomnia and sleep-related violence (Hrozanova et al., 2018; Medicine, 2014). Some basic features are shared by all types of NREM parasomnias: i) arising of the events in the first part of the night or sleep period, ii) unresponsiveness to the environment during the episodes, iii) post-episodic amnesia for events (full or partial), iv) EEG recordings showing simultaneously sleep-like and wake-like features, v) the presence of priming and precipitating factors. The dissociation between self-awareness and behaviour is a crucial feature of NREM parasomnias, and different studies demonstrated a dissociation among wakefulness and sleep in different brain regions (Januszko et al., 2016; Sarasso et al., 2014; Terzaghi et al., 2012, 2009). This key point makes NREM parasomnias particularly fascinating disorders, and explains the possibly negative after-effects of the episodes, as psychological distress, sleepiness, but especially the risk of injuries to themselves and to others, and their potential legal implications.

One of the most difficult challenges for sleep physicians and epileptologists is the differential diagnosis between NREM parasomnias and sleep-related hypermotor epilepsy (SHE). The latter, changed its face numerous times: mentioned for the first time in 1981 by Lugaresi and Cirignotta (1981) and misleadingly defined as Nocturnal Paroxysmal Dystonia (NPD), it was

subsequently renamed Nocturnal Frontal Lobe Epilepsy (NFLE) once proved the epileptic origin of the syndrome (Tinuper et al., 1990); until 2014, when a Consensus Conference helded in Bologna (Italy) renamed it conclusively sleep-related hypermotor epilepsy (SHE) (Tinuper et al., 2016; Tinuper and Bisulli, 2017). 2014 change of nomenclature was justified by three key points on which all experts were in agreement: i) the seizures occurrence in sleep, without a specific relationship with the night; ii) the potential onset of the seizures from extrafrontal areas; iii) the hyperkinetic nature of SHE seizures.

SHE seizures may arise in rather unconventional ways, as ambulations, complex automatisms or vocalizations, often mistaken for parasomnias; likewise some NREM parasomnias may have particularly violent clinical features that can be mistaken for SHE seizures (Derry et al., 2006). Moreover, classical sleep parameters seem to be broadly unchanged in both SHE and NREM parasomnias patients, in contrast with the presence of sleep instability, detectable by microstructure analysis, and arousal fluctuations (Zucconi and Ferini-Strambi, 2000). It's often impossible to find evidence of any ictal/interictal abnormalities during EEG investigations in SHE patients (e.g. when seizures originate from the deep-seated cortex), and even detectable epileptic discharge are frequently masked by muscular artefacts (Oldani et al., 1998; Provini et al., 1999; Tinuper et al., 2016; Tinuper and Bisulli, 2017). Several scalp sleep EEG studies, conducted on NREM parasomnia patients, highlighted increased sleep fragmentation and slow waves activity (SWA) abnormalities (Desjardins et al., 2017; Januszko et al., 2016); Castelnovo et al. (2016) demonstrated with an hdEEG study the persistence of local sleep differences in EEG SWA power during both NREM, REM sleep and wakefulness, even in nights without clinical episodes, and they source localized the local SWA decrease mainly to cingulate and motor regions supporting the theory that sees the local arousals in these brain areas as the source of the NREM parasomnias motor behaviours (Terzaghi et al.,

2012). The past findings seem to not make the process towards diagnosis and differential diagnosis easier or quicker, and the gold standard remains nocturnal video-polysomnography, an expensive, time consuming and operator-dependent procedure, in which the video component is essential and, in association with the clinical features, allows to formulate the diagnosis.

While the oscillatory component it's been investigated extensively, no attention was reserved to aperiodic component changes in patients affected by SHE or NREM parasomnias. The aperiodic 1/f component of neural power spectra represents a significant fraction of the spontaneous electrical fields potentials of the EEG recordings, and constitutes the arrhythmic and scale-free (no predominant temporal scale) brain activity (He et al., 2010). Although the aperiodic activity is the prevailing one when the oscillatory is absent (Schaworonkow and Voytek, 2020), most of the studies are conducted on an ex ante basis, defining canonical frequency bands to investigate and ignoring the arrhythmic "background" activity, failing to verify if the power changes detected are really driven by the oscillatory component, or are the result of the aperiodic signal/a combination of the two (Haller et al., 2018). The aperiodic signal may correspond both to neural noise and physiologically relevant signals with a functional significance (Haller et al., 2018), and its dynamism manifest itself with changes dependent on task demands (He et al., 2010), cognitive states (Podvalny et al., 2015), aging (Voytek et al., 2015), and diseases (Peterson et al., 2017). The 1/f signal of the power spectrum may be characterized in terms of slope, namely the exponential decrease of power in a spectrogram as a function of frequency, and offset of the broadband power of the signal.

Here we set out to investigate the classical EEG power spectral features regarding the periodic component, but also to extract the features of the aperiodic component slope and offset , and evaluate whether it's possible to

highlight significant differences between the two groups of patients, with a firm diagnosis respectively of NREM parasomnias or SHE, using 19 channels sleep scalp EEG.

Materials and methods

Patients

After have given written informed consent, according to the Declaration of Helsinki, a total of 15 patients with SHE (5 M, mean ages 32.8±15.3 years) and 16 patients with NREM parasomnia (8 M, mean ages 29.5±10.7 years) were enrolled at the Sleep Center and the Epilepsy Center of the University of Cagliari. The inclusion criteria were diagnosis of SHE or NREM parasomnia according to current diagnostic criteria (Tinuper et al., 2016)(Medicine, 2014), respectively for the SHE and NREMp group, age ≥18 years, while the exclusion criteria for overall populations were the presence of other sleep disorders, neurological disease and psychiatric comorbidities, according to the DSM V.

Demographic data, such as age, sex and current therapy were evaluated by neurologists experts in sleep medicine ad epilepsy.

All participants were free from psychotropic medications. The local ethic committee approved the study.

Polysomnographic analysis

All patients underwent a full-night attended video-polysomnography (vPSG) recording at sleep laboratory according to the American Academy of Sleep Medicine (AASM) recommendations (Berry et al., 2017) .

The following vPSG montage included electroencephalographic leads (10-20 international system), left and right electrooculography (EOG), chin and lower limbs (EMG) channels, electrocardiography, nasal airflow, thoracic and abdominal respiratory effort, pulse-oximeter and microphone. All participants were asked to sleep uncovered with allowance of a light sheet for comfort, in order to better observe any motor activity. All healthy subjects underwent a full-night home-based PSG recording.

The PSG recordings were scored according to the AASM criteria by neurologists experts in sleep medicine. The following sleep data were collected: total bedtime (TBT), total sleep time (TST), sleep efficiency (SE), wake after sleep onset (WASO), percentage of time in each sleep stage (N1, N2, N3, R), number of REM sleep episode, arousal index (AI), periodic limb movements index (PLMSi), Apnea-hypopnea index (AHI).

All video recordings were carefully analyzed by experts in epilepsy and sleep medicine in order to detect minor and major events. In SHE patients minor events were defined as nose scratching, dystonic posture of feet or hands, hyperextension of limbs, rigid posture of upper or lower limbs, myoclonus, trunk flexion/extension, paroxysmal arousal, nocturnal wanderings and automatisms according to current diagnostic criteria (Tinuper et al., 2016). While in NREMp patients simple arousal movements and rising arousal movements were identified as minor events according to the latest classification (Loddo et al., 2018). Major events were defined as complex hypermotor seizure were considered in the SHE group (Tinuper et al., 2016), and as complex arousal with motor behaviors and ambulatory movements while in the NREMp group (Loddo et al., 2018).

Preprocessing

Original raw data underwent multiple rounds of visual inspections by two operators, and 25 epochs of 10 seconds for each of the sleep stages considered

(N2-N3) were retained through a process of manual epoching that excluded artifacts and generic discontinuities, using the freely available toolbox EEGLAB (Delorme and Makeig, 2004). Our analysis refers therefore to 4 minutes and 10 seconds of EEG signal for each subject and each of the two sleep stages, N2 and N3 .

Features extraction

We extracted from the epoched signals the features characterizing i) the periodic component, namely the relative power of delta (0.5-4 Hz) , theta (4-8 Hz), alpha (8-12 Hz), sigma (12-16 Hz), beta (16-32 Hz) and gamma (32-45 Hz) frequency bands; ii) and the aperiodic component, namely the slope and the offset. The relative power for each of the five frequency bands was computed as the ratio between the absolute band-specific power and absolute total power (between 1 and 45 Hz) using the Power Spectral Density estimate through Welch's method using MATLAB (The MathWorks, Inc., Natick, Massachusetts,United States, version R2020). The Fitting Oscillations & One Over f (FOOOF) toolbox (Haller et al., 2018) were used to compute the slope and the offset (https://fooof-tools.github.io/fooof/index.html).

Statistical analysis

Based on the characteristics of our data, namely two groups of subjects that can be considered as two independent samples and the continuous nature of the variables examined, we chose to use the Mann-Whitney U test, often considered the non-parametric analogous of T-test, in order to estimate whether the two populations of subjects differ, and the actual divergence of their medians. In consideration of the small sample size of the groups of subjects, we also calculated the effect sizes by means of the biserial rank correlation. With this approach, an absolute r value of 0.10 is considered to represent a small effect, r = 0.30 represents a medium effect, and r = 0.50 represents a large effect (Conroy, 2012). The Mann Whitney U test was

computed for each frequency band using Jamovi (version 1.1.9.0) available from https://www.jamovi.org, after performing average across all channels and epochs.

We approached the multiple comparison problem lowering the critical value of p for significance with the Bonferroni-correction. For the comparison of the periodic component, the critical value for an individual test was found dividing the familywise error rate (0.05) by the number of the bands (six), the results were thus declared significant if they survived Bonferroni-correction over the six bands ($p = 0.0083$). For the comparison of the aperiodic component a critical p value of 0.025 was used, because we made only two comparisons (offset and slope), for each sleep stage.

Results

vPSG features.

SHE subjects showed significantly lower total sleep time, higher amount of stages W and N1 and longer REM sleep latency ($p=0.01$) compared to subjects with NREM-parasomnia. Table 1 summarizes the vPSG parameters of subjects with NREM parasomnia and of subjects with SHE.

Tab 1. Video-polysomnographic features of NREM-parasomnia patients and SHE patients.

	NREM Parasomnia (n=16)		**Sleep-related hypermotor epilepsy (n=15)**		**Mann-Whitney**	
	Median	*IQR*	*Median*	*IQR*	*U*	*p*
Age, years	30.6	22.9 - 37.7	25.9	21.7 - 52.1	111	0.741
Total sleep time, min	465.5	423.5 - 503	409	373 - 448	66.5	**0.034**
Sleep efficiency, %	89.7	81.1 - 95.7	80	70 - 85.9	74	0.070
Sleep latency, min	13.5	6.3 - 24-3	22.5	7 - 45	93	0.295
Arousal index	10.6	7.3 - 14.1	9.6	7.7 - 12.7	96.5	0.363
WASO	30	12.1 - 64.3	73.5	38 - 126.5	63-5	**0.025**
Stage N1, %	7.1	4.1 - 8.9	8.9	6.9 - 14.3	70	**0.048**
Stage N2, %	42.3	33.2 - 45.6	37.8	26.7 - 48.8	110.5	0.719
Stage N3, %	31.4	27.8 - 39.3	2.1	23.6 - 42.8	103.5	0.526
Stage R, %	18.6	16.5 - 21.9	14.9	6.8 - 22.5	79	0.108
REM sleep latency, min	87.8	71.1 - 124.4	184.5	92 - 264.5	48	**0.004**
REM sleep episodes, number	4	3 - 4.8	4	3-4	91	0.227
Apnea-hypopnea index	0	0	0	0	114	>0.999
Periodic leg movements during sleep index	5.1	1.4 - 10	0	0	84.5	0.153
Minor motor episodes, number	48.5	34.5 -57.8	40	29 - 64	103.5	0.526
IQR = interquartile range. Significant p values (without Bonferroni correction) are marked in bold.						

Periodic component

A significant difference between the groups was found for the gamma band relative power during N2, as well as during N3 (table 2). No other difference survived Bonferroni-correction. The relative power analysis of the gamma frequency band, respectively during N2 and N3 sleep stages, are graphically shown also in Fig. 1.

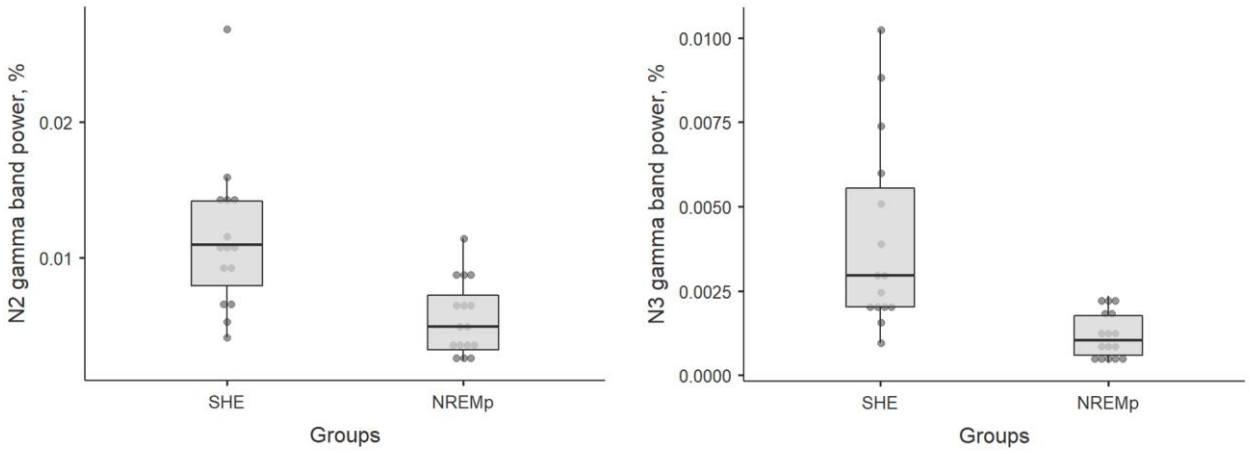

Fig.1 Scatterplot of the results for the gamma relative power during sleep stages N2 and N3.

Tab. 2. Results of the comparison of the relative power of the different EEG bands found in NREM Parasomnia and SHE, during sleep stages N2 and N3.

	NREM Parasomnia (n=16)		**Sleep-related hypermotor epilepsy (n=15)**		**Mann-Whitney**	**Effect size Biserial rank correlation**
	Median	*IQR*	*Median*	*IQR*	*p*	
N2 sleep stage						
Delta	0.654	0.576 – 0.676	0.616	0.518 – 0.681	0.379	0.192
Theta	0.178	0.165 – 0.208	0.209	0.162 – 0.254	0.520	0.142
Alpha	0.089	0.074 – 0.109	0.088	0.071 – 0.123	0.800	0.058
Sigma	0.054	0.041 – 0.084	0.050	0.045 – 0.076	0.984	0.008
Beta	0.033	0.021 – 0.050	0.040	0.028 – 0.060	0.379	0.192
Gamma	0.005	0.003 – 0.007	0.011	0.008 – 0.014	**<0.001**	**0.717**
N3 sleep stage						
Delta	0.860	0.762 – 0.900	0.792	0.749 – 0.854	0.105	0.308
Theta	0.087	0.080 – 0.116	0.117	0.099 – 0.158	0.093	0.358
Alpha	0.046	0.026 – 0.070	0.048	0.030 – 0.075	0.401	0.183
Sigma	0.018	0.011 – 0.026	0.020	0.015 – 0.034	0.281	0.233
Beta	0.005	0.004 – 0.009	0.009	0.007 – 0.013	0.024	0.475
Gamma	0.001	0.0006 – 0.002	0.003	0.002 – 0.005	**<0.001**	**0.800**

IQR = interquartile range. Significant p values (after Bonferroni correction) and "large" effect sizes (≥0.5) are marked in bold.

Aperiodic component

No significant differences between NREM parasomnias and SHE subjects were found in offset of the power spectrum, both during N2 and N3 stages, while a significant higher slope was found for the NREM parasomnias group in sleep stage N3 only; see Fig. 2 for a graphical representation of these results and table 3 for the corresponding statistics

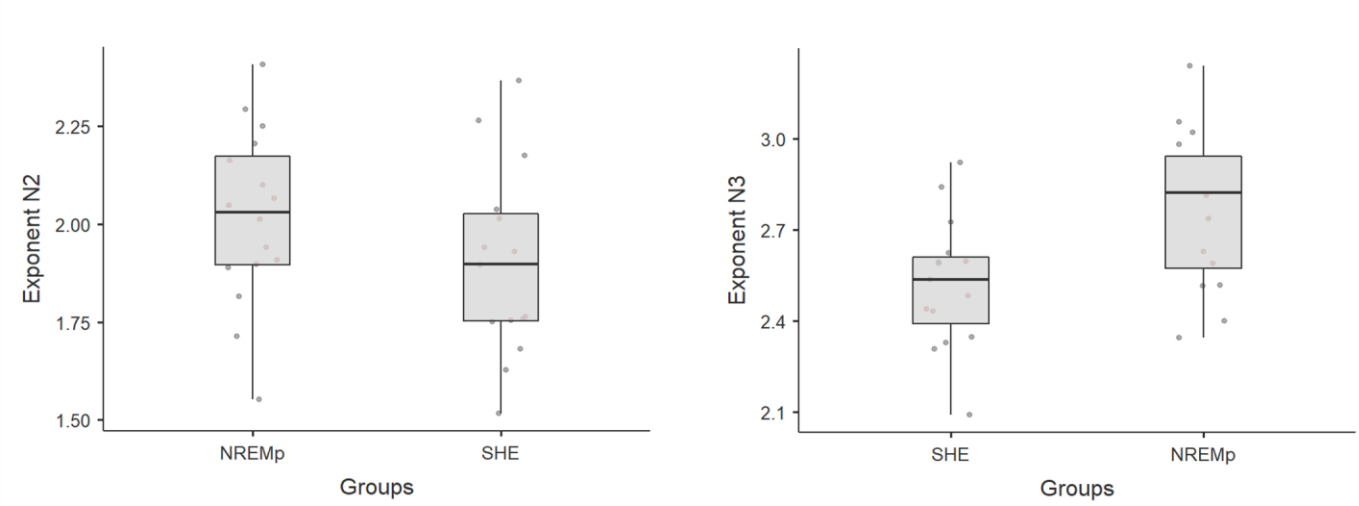

Fig.2 Scatterplot of the slope (exponent) of the aperiodic component during sleep stages N2 and N3.

Tab. 3 Results of the comparison of the offset and slope (exponent) of the EEG power spectrum in NREM Parasomnia and SHE, during sleep stages N2 and N3.

	NREM Parasomnia (n=16)		**Sleep-related hypermotor epilepsy (n=15)**		**Mann-Whitney**	**Effect size Biserial rank correlation**
	Median	*IQR*	*Median*	*IQR*	*p*	
N2 sleep stage						
Offset	1.91	1.82 – 2.07	1.89	1.57 – 2.07	0.495	0.150
Slope	2.03	1.90 – 2.17	1.90	1.75 – 2.03	0.163	0.300
N3 sleep stage						
Offset	2.74	2.55 – 2.86	2.56	2.38 – 2.72	0.101	0.350
Slope	2.82	2.57 – 2.94	2.54	2.39 – 2.61	**0.012**	**0.525**
IQR = interquartile range. Significant p values (after Bonferroni correction) and "large" effect sizes (≥0.5) are marked in bold.						

Discussion

Nocturnal video-polysomnography is indispensable for making a precise diagnosis on subjects affected by respectively SHE or NREM parasomnias. While EEG is in general a tool with optimal accessibility and cost-effectiveness, a full-night attended vPSG and the scoring process conducted by sleep medicine experts are very expensive and time-consuming procedures. Part of the research on SHE and NREM parasomnias focus on a potential solution to the problem represented by the differential diagnosis, with the goal to identify electrophysiological biomarkers specific for disease. As much of the studies conducted on clinical and cognitive neuroscience, sleep studies focus on the so-called periodic activity, namely the rhythmic or oscillatory activity, organized in distinct frequency bands. Therefore, band power differences across conditions result to be the most widely studied features of the EEG power spectrum, at the expense of the aperiodic component. However, in contrast with the traditional view, the 1/f component of neural power spectra seems to may represent both background noise and physiologically relevant signals, and taking into account that it incorporates the oscillatory component, it should be considered to avoid misinterpretation of band-limited power differences (Haller et al., 2018). Recent experimental findings confirm the dynamism of the aperiodic component, showing how its parameters change depending on age and aging (Schaworonkow and Voytek, 2020; Tran et al., 2020; Voytek et al., 2015), cognitive states (Podvalny et al., 2015) and diseases (Peterson et al., 2017; Robertson et al., 2019). Furthermore it was very recently demonstrated that the aperiodic component is characterized by strong subject-specific properties and its features may help to characterize and make inferences at single subject level, with a better performance than classical frequency bands (Demuru and Fraschini, 2020). Together this findings suggest the importance

to consider the aperiodic component of the EEG power spectra as partly independent from oscillations, with its own physiological significance and dynamicity, and also the interesting possible use of its features for both diagnostic purposes (biomarkers) and bio-engineering clinical applications of brain fingerprint. Robertson et al (Robertson et al., 2019) identified for the first time differences in the aperiodic components of the EEG power spectrum in children with ADHD, proving that the slope is a reliable index of an increase in low relative to high frequency power in ADHD. In the light of this approach, that emphasizes the clinical utility of quantifying in a more comprehensive way features of the EEG power spectrum, we realised the first report evaluating spectral slope and offset in subjects affected by SHE and NREM parasomnias, with the aim of detect and study the aperiodic features looking for possible biomarkers enabling to distinguish them in a systematic way. Our results show a significant lower slope in patients affected by sleep-related hypermotor epilepsy compared with patients affected by non-rem parasomnias, with an important difference between the two groups ($U = 57.0$, $p = 0.012$, Effect size = -1.05). This preliminary findings suggest that a feature extracted from the aperiodic component, namely the slope, seem to convey physiological information that might differ in the long term between the groups of patients affected respectively by SHE and NREM parasomnias, offering us an electrophysiological biomarker to help discriminate patients with an uncertain diagnosis.

Limitations of this preliminary study are represented by i) a low number of subjects enrolled, due to the difficulty of collect, in our catchment area, patients with a firm diagnosis and none of the exclusion criteria defined (including comorbidities and treatments); ii) the choice to compare two groups of patients focusing selectively on differences between the two groups, not between each group and healthy controls, searching for a feature that make more smooth the differential diagnosis.

Next steps include therefore enlarge the number of patients involved and extend the study to the healthy controls, already recorded, to evaluate matching or discrepancies with the groups of patients. Our hypothesis is that healthy controls may have a closer correspondence with non-rem parasomnias patients in terms of slope extracted from the aperiodic component of the EEG power spectra.

References

American Academy of Sleep Medicine. (2014). *The international classification of sleep disorders (ICSD-3). American Academy of Sleep Medicine*.

Berry, R. B., Brooks, R., Gamaldo, C., Harding, S. M., Lloyd, R. M., Quan, S. F., … Vaughn, B. V. (2017). AASM scoring manual updates for 2017 (version 2.4). *Journal of Clinical Sleep Medicine*. https://doi.org/10.5664/jcsm.6576

Castelnovo, A., Riedner, B. A., Smith, R. F., Tononi, G., Boly, M., & Benca, R. M. (2016). Scalp and Source Power Topography in Sleepwalking and Sleep Terrors: A High-Density EEG Study. *Sleep*. https://doi.org/10.5665/sleep.6162

Conroy, R. M. (2012). What hypotheses do "nonparametric" two-group tests actually test? *Stata Journal*. https://doi.org/10.1177/1536867x1201200202

Delorme, A., & Makeig, S. (2004). EEGLAB: An open source toolbox for analysis of single-trial EEG dynamics including independent component analysis. *Journal of Neuroscience Methods*. https://doi.org/10.1016/j.jneumeth.2003.10.009

Demuru, M., & Fraschini, M. (2020). EEG fingerprinting: Subject-specific signature based on the aperiodic component of power spectrum. *Computers in Biology and Medicine*. https://doi.org/10.1016/j.compbiomed.2020.103748

Derry, C. P., Davey, M., Johns, M., Kron, K., Glencross, D., Marini, C., … Berkovic, S. F. (2006). Distinguishing sleep disorders from seizures: Diagnosing bumps in the night. *Archives of Neurology*. https://doi.org/10.1001/archneur.63.5.705

Desjardins, M. È., Carrier, J., Lina, J. M., Fortin, M., Gosselin, N., Montplaisir, J., & Zadra, A. (2017). EEG functional connectivity prior to sleepwalking: Evidence of interplay between sleep and wakefulness. *Sleep*. https://doi.org/10.1093/sleep/zsx024

Haller, M., Donoghue, T., Peterson, E., Varma, P., Sebastian, P., Gao, R., … Voytek, B. (2018). Parameterizing neural power spectra. *BioRxiv*. https://doi.org/10.1101/299859

He, B. J., Zempel, J. M., Snyder, A. Z., & Raichle, M. E. (2010). The temporal structures and functional significance of scale-free brain activity. *Neuron*. https://doi.org/10.1016/j.neuron.2010.04.020

Hrozanova, M., Morrison, I., & Riha, R. (2018). Adult NREM Parasomnias: An Update. *Clocks & Sleep*. https://doi.org/10.3390/clockssleep1010009

Januszko, P., Niemcewicz, S., Gajda, T., Wołyńczyk-Gmaj, D., Piotrowska, A. J., Gmaj, B., … Szelenberger, W. (2016). Sleepwalking episodes are preceded by arousal-related activation in the cingulate motor area: EEG current density imaging. *Clinical Neurophysiology*. https://doi.org/10.1016/j.clinph.2015.01.014

Loddo, G., Sessagesimi, E., Mignani, F., Cirignotta, F., Mondini, S., Licchetta, L., … Provini, F. (2018). Specific motor patterns of arousal disorders in adults: a video-polysomnographic analysis of 184 episodes. *Sleep Medicine*. https://doi.org/10.1016/j.sleep.2017.08.019

Lugaresi, E., & Cirignotta, F. (1981). Hypnogenic paroxysmal dystonia: Epileptic seizure or a new syndrome? *Sleep*. https://doi.org/10.1093/sleep/4.2.129

Oldani, A., Zucconi, M., Asselta, R., Modugno, M., Bonati, M. T., Dalprà, L., … Ferini-Strambi, L. (1998). Autosomal dominant nocturnal frontal lobe epilepsy. A video-polysomnographic and genetic appraisal of 40 patients and delineation of the epileptic syndrome. *Brain*. https://doi.org/10.1093/brain/121.2.205

Peterson, E., Rosen, B., Campbell, A., Belger, A., & Voytek, B. (2017). 1/ f neural noise is a better predictor of schizophrenia than neural oscillations. *BioRxiv*. https://doi.org/10.1101/113449

Podvalny, E., Noy, N., Harel, M., Bickel, S., Chechik, G., Schroeder, C. E., … Malach, R. (2015). A unifying principle underlying the extracellular field potential spectral responses in the human cortex. *Journal of Neurophysiology*. https://doi.org/10.1152/jn.00943.2014

Provini, F., Plazzi, G., Tinuper, P., Vandi, S., Lugaresi, E., & Montagna, P. (1999). Nocturnal frontal lobe epilepsy: A clinical and polygraphic overview of 100 consecutive cases. *Brain*. https://doi.org/10.1093/brain/122.6.1017

Robertson, M. M., Furlong, S., Voytek, B., Donoghue, T., Boettiger, C. A., & Sheridan, M. A. (2019). EEG power spectral slope differs by ADHD status and stimulant medication exposure in early childhood. *Journal of Neurophysiology*. https://doi.org/10.1152/jn.00388.2019

Sarasso, S., Pigorini, A., Proserpio, P., Gibbs, S. A., Massimini, M., & Nobili, L. (2014). Fluid boundaries between wake and sleep: Experimental evidence from Stereo-EEG recordings. *Archives Italiennes de Biologie*. https://doi.org/10.12871/0002982920142311

Schaworonkow, N., & Voytek, B. (2020). Longitudinal changes in aperiodic and periodic activity in electrophysiological recordings in the first seven months of life. *BioRxiv*. https://doi.org/10.1101/2020.08.18.256016

Terzaghi, M., Sartori, I., Tassi, L., Didato, G., Rustioni, V., LoRusso, G., … Nobili, L. (2009). Evidence of dissociated arousal states during nrem parasomnia from an intracerebral neurophysiological study. *Sleep*. https://doi.org/10.1093/sleep/32.3.409

Terzaghi, M., Sartori, I., Tassi, L., Rustioni, V., Proserpio, P., Lorusso, G., … Nobili, L. (2012). Dissociated local arousal states underlying essential clinical features of non-rapid eye movement arousal parasomnia: An intracerebral stereo-electroencephalographic study. *Journal of Sleep Research*. https://doi.org/10.1111/j.1365-2869.2012.01003.x

Tinuper, P., & Bisulli, F. (2017). From nocturnal frontal lobe epilepsy to Sleep-Related Hypermotor Epilepsy: A 35-year diagnostic challenge. *Seizure*. https://doi.org/10.1016/j.seizure.2016.11.023

Tinuper, P., Bisulli, F., Cross, J. H., Hesdorffer, D., Kahane, P., Nobili, L., … Ottman, R. (2016). Definition and diagnostic criteria of sleep-related hypermotor epilepsy. *Neurology*. https://doi.org/10.1212/WNL.0000000000002666

Tinuper, P., Cerullo, A., Cirignotta, F., Cortelli, P., Lugaresi, E., & Montagna, P. (1990). Nocturnal Paroxysmal Dystonia with Short-Lasting Attacks: Three Cases with Evidence for an Epileptic Frontal Lobe Origin of Seizures. *Epilepsia*. https://doi.org/10.1111/j.1528-1157.1990.tb06105.x

Tran, T. T., Rolle, C. E., Gazzaley, A., & Voytek, B. (2020). Linked sources of neural noise contribute to age-related cognitive decline. *Journal of Cognitive Neuroscience*. https://doi.org/10.1162/jocn_a_01584

Voytek, B., Kramer, M. A., Case, J., Lepage, K. Q., Tempesta, Z. R., Knight, R. T., & Gazzaley, A. (2015). Age-related changes in 1/f neural electrophysiological noise. *Journal of Neuroscience*. https://doi.org/10.1523/JNEUROSCI.2332-14.2015

Zucconi, M., & Ferini-Strambi, L. (2000). NREM parasomnias: Arousal disorders and differentiation from nocturnal frontal lobe epilepsy. *Clinical Neurophysiology*. https://doi.org/10.1016/S1388-2457(00)00413-2

Conclusion and future directions

This multidisciplinary doctoral project has been developed combining engineering procedures and concepts about signals and neuroimaging processing with classical neurosciences, leading us to the final applications on clinical samples. Common denominator was represented by the concept of stability and variability of subject specific features related to functional connectivity, as well as to the periodic and aperiodic component of the EEG power spectra.

We aimed to investigate i) the impact of some of the most commonly used metrics to estimate functional connectivity on the ability to unveil personal distinctive patterns of inter-channel interaction; ii) the possible association between power spectral density and some widely used nodal networks metrics, both at scalp and source level; iii) how EEG power, connectivity and network features, estimated using source-reconstructed EEG time-series, are affected by the variability due to subject, session and task; iv) how different specific aspects of psychosis-like experiences related to functional connectivity; v) differences in the periodic and aperiodic component of the EEG power spectra of patients affected by sleep-related hypermotor epilepsy and non-rem parasomnias.

We demonstrated that different connectivity metrics have different performance detecting specific pattern of inter-channel interactions (Fraschini et al., 2019) and that power spectral density and network

analysis are not completely independent (Demuru et al., 2020). Our at source-level EEG report (Pani et al., 2020) confirmed the existence of well-defined specific profiles that are stable over-time, although dependent form the specific task. The findings from our fMRI study (https://doi.org/10.1016/j.pscychresns.2020.111202) also suggest that the neural circuit linking dorsal caudate to dorsolateral prefrontal cortex may be tied to risk for general schizophrenia-like psychopathology. Lastly, an evident electrophysiological difference was found between the two groups of patients affected by sleep disorders.

Here a summary of our findings:

- PLV and CC are the most robust connectivity metrics to detect individual fingerprints even in the more challenging experimental designs (scalp-level analysis).
- Power spectral density and network analysis show a clear association, and the level of the latter depends on the FC method used (both scalp- and source-level analysis).
- PSD, PLV and PLV derived functional brain networks (measured by nodal centrality) are stable over-time, dominated by individual properties but largely dependent from the specific task (source-level EEG analysis).
- Functional coupling between dorsal caudate and dorsolateral prefrontal cortex is related with the severity of psychosis like experiences (fMRI analysis).

- The slope of the aperiodic component of the EEG power spectra is significantly lower in patients affected by sleep-related hypermotor epilepsy compared with non-rem parasomnias patients.

Different considerations can be drown from this thesis project, first of all that procedures and methodological choices strongly influence the output of the analysis, and we need to proceed carefully starting with the preliminary design, till results rendering.

Although functional connectivity can be estimate dependably from scalp-level EEG the source-based network representation is a better approximation, and the higher the number of the EEG sensors the lower the error in electrical source estimation (Lai et al., 2018). That is why we decided to not perform the connectivity analysis in our last study on sleep disorders, because of the nature of the data: it is difficult to make inference on source using 19 channels scalp-EEG recordings.

Furthermore, the choice of the connectivity metric may influence the estimate of networks organization, both for the different mechanism to detect subject-specific patterns of inter-channel interactions, and for the important role that the frequency content and the spurious correlations have (Fraschini et al., 2019; Lai et al., 2018).

Also, ROI (regions of interest) selection can critically affect analysis results, causing missing of effects (to avoid inflating type I error rate) or detection of spurious effects (to avoid inflating type II error rate), and the right balance is often hard to find (Brooks et al., 2017; Krak et al., 2005).

Pre-processing is another crucial point, EEG data can indeed be altered by various factors and several steps are needed to make them ready to analysis. It's important to notice that the steps sequence and the order of pre-processing pipelines influences the output of the process and may have a large impact on particular portions of the signal (Robbins et al., 2020). Software packages coming with EEG systems or running on MATLAB/Phython/R platforms (freely available) or even custom-written, can be used, what is important is to describe step-by-step and in detail the workflow and, where possible, release publicly the code used, in order to enable other researchers to reproduce the analysis (Pernet et al., 2020). There are steps universally recognised to be valid after visual inspection, and it is possible to proceed both manually or using different semi/fully automated pre-processing pipelines, but the crucial point is the needing of chose a path that takes account of data characteristics and analysis nature, leading to more meaningful and reproducible results (Pernet et al., 2020).

Secondly, it is extremely important to consider all sources of variance of functional brain networks, included those related to

individuality, and the approach that considers subjects specific features could be in the future a useful tool to prevent misinterpretation of clinical studies results. Thinking to patient's follow-up, in a not too distant future, it could be demonstrated that monitoring the individual by considering the mean of subjects affected by the same pathology is a method not without flaws for the accurate evaluation of disease progression/regression, patients' response to the therapy and other clinical relevant factors. It is indeed becoming more and more important in a lot of medical branches to focus on the individual to guarantee a top-level standard of care and offer the best approach to the disease, improving treatment choice, quality of life and even survival (Krzyszczyk et al., 2018; Rossi et al., 2014).

We were supposed to verify part of this rationale in the clinical study we had planned, but were unable to realise due to the pandemic, on neurological patients; we would had evaluated how individual variability/stability of functional brain networks is affected by diseases, whether individual traits are still detectable in different phases of the disease and if they can be used to track the patient. Source-reconstructed EEG time-series could be used to study singular subjects in a group context and track their features over several session and tasks. We believe in the utility of EEG in clinical practice, being a powerful and low-cost tool, easy to use for trained personnel and practically free from discomfort for patients.

Once again is confirmed the importance to identify the deviation from the healthy brain connectivity pattern, specific for pathology, envisaging clinical useful applications that would enable the identification of at-risk individuals for prevention and early intervention (Stam, 2014).

Our results also corroborate the relevance of considering the aperiodic component when conducting analysis on the EEG power spectra, supporting the idea of its physiological significance, and the use of its features as electrophysiological biomarkers (Haller et al., 2018; He et al., 2010; Robertson et al., 2019).

Future steps should be to investigate how connectivity metrics and network similarity across tasks and sessions varies between clinical conditions, pushing the use of the individual connectivity EEG fingerprint beyond the bio-engineering applications towards clinical use in personalized medicine.

It would be also of interest to take advantage of the extremely high temporal resolution of the EEG to extend the traditional functional network analysis (static approach) to the dynamical functional connectivity, considering the additional dimension of time development (Hassan and Wendling, 2018, 2015; Mutlu et al., 2012). Especially regarding the studies that involved cognitive tasks it would be interesting to shift the focus on the evolution of neural activity, evaluating how the measures considered change over time, tracking sub-second reconfigurations of connectivity patterns (Hassan et al., 2015; Li et al., 2020). Furthermore, we think that the

interesting results of our study about sleep disorders will open new possibilities in this field. Future steps comprise the application of the study model, that investigate comprehensively the components of the EEG power spectra, to a variety of sleep disorders, searching for electrophysiological biomarkers that could change the clinical approach to differential diagnosis and hopefully to treatment, providing clinicians a tool to evaluate the efficacy of the adopted strategy.

References

Agosta, F., Sala, S., Valsasina, P., Meani, A., Canu, E., Magnani, G., Cappa, S.F., Scola, E., Quatto, P., Horsfield, M.A., Falini, A., Comi, G., Filippi, M., 2013. Brain network connectivity assessed using graph theory in frontotemporal dementia. Neurology. https://doi.org/10.1212/WNL.0b013e31829a33f8

Arns, M., 2012. EEG-Based Personalized Medicine in ADHD: Individual Alpha Peak Frequency as an Endophenotype Associated with Nonresponse. J. Neurother. https://doi.org/10.1080/10874208.2012.677664

Baggio, H.C., Sala-Llonch, R., Segura, B., Marti, M.J., Valldeoriola, F., Compta, Y., Tolosa, E., Junqué, C., 2014. Functional brain networks and cognitive deficits in Parkinson's disease. Hum. Brain Mapp. https://doi.org/10.1002/hbm.22499

Barabási, A.L., Albert, R., 1999. Emergence of scaling in random networks. Science (80-.). https://doi.org/10.1126/science.286.5439.509

Brooks, J.L., Zoumpoulaki, A., Bowman, H., 2017. Data-driven region-of-interest selection without inflating Type I error rate, in: Psychophysiology. https://doi.org/10.1111/psyp.12682

Bullmore, E., Sporns, O., 2012. The economy of brain network organization. Nat. Rev. Neurosci. https://doi.org/10.1038/nrn3214

Cox, R., Schapiro, A.C., Stickgold, R., 2018. Variability and stability of large-scale cortical oscillation patterns. Netw. Neurosci. https://doi.org/10.1162/netn_a_00046

de Haan, W., Van Der Flier, W.M., Wang, H., Van Mieghem, P.F.A., Scheltens, P., Stam, C.J., 2012. Disruption of Functional Brain Networks in Alzheimer's Disease: What Can We Learn from Graph Spectral Analysis of Resting-State Magnetoencephalography? Brain Connect. https://doi.org/10.1089/brain.2011.0043

Delbeuck, X., Van Der Linden, M., Collette, F., 2003. Alzheimer's Disease as a Disconnection Syndrome? Neuropsychol. Rev. https://doi.org/10.1023/A:1023832305702

Demuru, M., Fraschini, M., 2020. EEG fingerprinting: Subject-specific signature based on the aperiodic component of power spectrum. Comput. Biol. Med. https://doi.org/10.1016/j.compbiomed.2020.103748

Demuru, M., Gouw, A.A., Hillebrand, A., Stam, C.J., Van Dijk, B.W., Scheltens, P., Tijms, B.M., Konijnenberg, E., Ten Kate, M., Den Braber, A., Smit, D.J.A., Boomsma, D.I., Visser, P.J., 2017. Functional and effective whole brain connectivity using magnetoencephalography to identify monozygotic twin pairs. Sci. Rep. https://doi.org/10.1038/s41598-017-10235-y

Demuru, M., La Cava, S.M., Pani, S.M., Fraschini, M., 2020. A comparison between power spectral density and network metrics: An EEG study. Biomed. Signal Process. Control. https://doi.org/10.1016/j.bspc.2019.101760

Finn, E.S., Todd Constable, R., 2016. Individual variation in functional brain connectivity: Implications for personalized approaches to psychiatric disease. Dialogues Clin. Neurosci.

Fornito, A., Bullmore, E.T., 2015. Connectomics: A new paradigm for understanding brain disease. Eur. Neuropsychopharmacol. https://doi.org/10.1016/j.euroneuro.2014.02.011

Fraschini, M., Pani, S.M., Didaci, L., Marcialis, G.L., 2019. Robustness of functional connectivity metrics for EEG-based personal identification over task-induced intra-class and inter-class variations. Pattern Recognit. Lett. https://doi.org/10.1016/j.patrec.2019.03.025

Gao, Q., Duan, X., Chen, H., 2011. Evaluation of effective connectivity of motor areas during motor imagery and execution using conditional Granger causality. Neuroimage. https://doi.org/10.1016/j.neuroimage.2010.08.071

Gratton, C., Laumann, T.O., Nielsen, A.N., Greene, D.J., Gordon, E.M., Gilmore, A.W., Nelson, S.M., Coalson, R.S., Snyder, A.Z., Schlaggar, B.L., Dosenbach, N.U.F., Petersen, S.E., 2018. Functional Brain Networks Are Dominated by Stable Group and Individual Factors, Not Cognitive or Daily Variation. Neuron. https://doi.org/10.1016/j.neuron.2018.03.035

Haller, M., Donoghue, T., Peterson, E., Varma, P., Sebastian, P., Gao, R., Noto, T., Knight, R., Shestyuk, A., Voytek, B., 2018. Parameterizing neural power spectra. bioRxiv. https://doi.org/10.1101/299859

Hassan, M., Benquet, P., Biraben, A., Berrou, C., Dufor, O., Wendling, F., 2015. Dynamic reorganization of functional brain networks during picture naming. Cortex. https://doi.org/10.1016/j.cortex.2015.08.019

Hassan, M., Wendling, F., 2018. Electroencephalography source connectivity: Toward high time/space resolution brain networks. arXiv.

Hassan, M., Wendling, F., 2015. Tracking dynamics of functional brain networks using dense EEG. IRBM. https://doi.org/10.1016/j.irbm.2015.09.004

He, B.J., Zempel, J.M., Snyder, A.Z., Raichle, M.E., 2010. The temporal structures and functional significance of scale-free brain activity. Neuron. https://doi.org/10.1016/j.neuron.2010.04.020

Horien, C., Shen, X., Scheinost, D., Constable, R.T., 2019. The individual functional connectome is unique and stable over months to years. Neuroimage. https://doi.org/10.1016/j.neuroimage.2019.02.002

Krak, N.C., Boellaard, R., Hoekstra, O.S., Twisk, J.W.R., Hoekstra, C.J., Lammertsma, A.A., 2005. Effects of ROI definition and reconstruction method on quantitative outcome and applicability in a response monitoring trial. Eur. J. Nucl. Med. Mol. Imaging. https://doi.org/10.1007/s00259-004-1566-1

Krzyszczyk, P., Acevedo, A., Davidoff, E.J., Timmins, L.M., Marrero-Berrios, I., Patel, M., White, C., Lowe, C., Sherba, J.J., Hartmanshenn, C., O'Neill, K.M., Balter, M.L., Fritz, Z.R., Androulakis, I.P., Schloss, R.S., Yarmush,

M.L., 2018. The growing role of precision and personalized medicine for cancer treatment. TECHNOLOGY. https://doi.org/10.1142/s2339547818300020

Lai, M., Demuru, M., Hillebrand, A., Fraschini, M., 2018. A comparison between scalp- and source-reconstructed EEG networks. Sci. Rep. https://doi.org/10.1038/s41598-018-30869-w

Li, X., Mota, B., Kondo, T., Nasuto, S., Hayashi, Y., 2020. EEG dynamical network analysis method reveals the neural signature of visual-motor coordination. PLoS One. https://doi.org/10.1371/journal.pone.0231767

Meunier, D., Lambiotte, R., Bullmore, E.T., 2010. Modular and hierarchically modular organization of brain networks. Front. Neurosci. https://doi.org/10.3389/fnins.2010.00200

Miranda-Dominguez, O., Feczko, E., Grayson, D.S., Walum, H., Nigg, J.T., Fair, D.A., 2018. Heritability of the human connectome: A connectotyping study. Netw. Neurosci. https://doi.org/10.1162/netn_a_00029

Mutlu, A.Y., Bernat, E., Aviyente, S., 2012. A signal-processing-based approach to time-varying graph analysis for dynamic brain network identification. Comput. Math. Methods Med. https://doi.org/10.1155/2012/451516

Olde Dubbelink, K.T.E., Hillebrand, A., Stoffers, D., Deijen, J.B., Twisk, J.W.R., Stam, C.J., Berendse, H.W., 2014. Disrupted brain network topology in Parkinson's disease: A longitudinal magnetoencephalography study. Brain. https://doi.org/10.1093/brain/awt316

Pani, S.M., Ciuffi, M., Demuru, M., La Cava, S.M., Bazzano, G., D'Aloja, E., Fraschini, M., 2020. Subject, session and task effects on power, connectivity and network centrality: A source-based EEG study. Biomed. Signal Process. Control. https://doi.org/10.1016/j.bspc.2020.101891

Pernet, C., Garrido, M.I., Gramfort, A., Maurits, N., Michel, C.M., Pang, E., Salmelin, R., Schoffelen, J.M., Valdes-Sosa, P.A., Puce, A., 2020. Issues and

recommendations from the OHBM COBIDAS MEEG committee for reproducible EEG and MEG research. Nat. Neurosci. 23, 1473–1483. https://doi.org/10.1038/s41593-020-00709-0

Robbins, K.A., Touryan, J., Mullen, T., Kothe, C., Bigdely-Shamlo, N., 2020. How Sensitive Are EEG Results to Preprocessing Methods: A Benchmarking Study. IEEE Trans. Neural Syst. Rehabil. Eng. https://doi.org/10.1109/TNSRE.2020.2980223

Rossi, A., Torri, V., Garassino, M.C., Porcu, L., Galetta, D., 2014. The impact of personalized medicine on survival: Comparisons of results in metastatic breast, colorectal and non-small-cell lung cancers. Cancer Treat. Rev. https://doi.org/10.1016/j.ctrv.2013.09.012

Skidmore, F., Korenkevych, D., Liu, Y., He, G., Bullmore, E., Pardalos, P.M., 2011. Connectivity brain networks based on wavelet correlation analysis in Parkinson fMRI data. Neurosci. Lett. https://doi.org/10.1016/j.neulet.2011.05.030

Smith, S.M., 2012. The future of FMRI connectivity. Neuroimage. https://doi.org/10.1016/j.neuroimage.2012.01.022

Sporns, O., 2013. Structure and function of complex brain networks. Dialogues Clin. Neurosci.

Stam, C.J., 2014. Modern network science of neurological disorders. Nat. Rev. Neurosci. https://doi.org/10.1038/nrn3801

Stam, C.J., 2010. Use of magnetoencephalography (MEG) to study functional brain networks in neurodegenerative disorders. J. Neurol. Sci. https://doi.org/10.1016/j.jns.2009.08.028

Watts, D.J., Strogatz, S.H., 1998. Collective dynamics of 'small-world9 networks. Nature. https://doi.org/10.1038/30918